



Loughborough University

Plasma Device for Carbon Dioxide Conversion and Utilisation

A Doctoral Thesis

by

©Adriano André Randi

2019

Acknowledgments

I first would like to thank my family who is constantly encouraging me to overcome any challenge in this Ph.D., also to my friend Ed. Burcham and the professors from my undergraduate Dr. Demanboro and Dr. Fujimoto for their support when I applied to this Ph.D. I would like to thank Dr. Upul Wijayantha who was my first contact at Loughborough University when I was still living in the USA and told me not just once 'Don't give up'. I want to say a special thanks to Dr. Benjamin Buckley who stayed with me during the whole process of this Ph.D., giving tremendous support, enriching the discussions, approaches and helping me with my research plan. Dr. Felipe Iza who believed in me and gave me all the conditions to make it happen. I also would like to thank Volodymyr Tabas and Vanessa Silvestre for the support in my needs during all the time and last but not least, all the others Ph.D.s Masters and supervisors in Organic Laboratory, Renewable Energy Laboratory, and Electrical Engineering Department.

Abstract

The continuing increase in energy demands requires more fossil fuel consumption to feed our traditional means of energy generation. CO₂ is the main product of burning fossil fuel, and its increase in concentration in our atmosphere has led to global warming. This will result in the changing of the climate pattern, possibly resulting in numerous disasters and loss of human life. In order to reduce the CO₂ emissions and minimize its side effects, scientists around the world are developing techniques and methodologies such as carbon capture and storage to tackle this problem.

The process of capture, purification, and utilisation of CO₂ as a raw material in the synthesis of feedstocks is gaining much attention, however, the challenges of any method employed are to make it cost-effective, energetically efficient and environmentally friendly.

The use of electrochemical processes to incorporate CO₂ into organic compounds has been well explored. As a vital condition in electrochemistry, the use of a sacrificial electrode as an electron donor is essential which reflects as one of the main drawbacks in terms of cost and sustainability, the sacrificial electrode results in oxidized material requiring its replacement and a further purification process to remove the oxidized material from liquid, as a result, such technology has not yet fully been seen as an effective alternative to combat CO₂ reduction.

In this research thesis I introduced the development of a DC atmospheric-pressure plasma jet which in contact with liquid at room temperature containing organic compounds and CO₂ enable the synthesis of carboxylic acid, largely commercialized worldwide. The beauty of this method is the fact that there is no need for a sacrificial electrode or reducing agent to carry the reaction.

The investigation of plasma carboxylation of alkene and alkyne in the formation of its corresponding carboxylic acid were presented in chapter three with the highest conversion reported (68.1 %). This chapter also includes the investigation of greener solvents, electrolytic salt, current applied, designs of the plasma jet, the interaction of plasma channels in contact with liquids and nature of gas employed in plasma formation, all with NMR and GC-MS data provided.

Table of Contents

Acknowledgments	1
Abstract.....	2
Table of Contents.....	3
List of abbreviations	7
1.0 INTRODUCTION.....	10
1.1 Aims and Objective.....	10
1.2 Environmental Considerations	11
1.2.1 Greenhouse Gases (GHG).....	12
1.2.2 Global Warming.....	13
1.2.2.1 Positive Feedback	15
1.2.2.2 Arctic Sea	16
1.2.2.3 Permafrost	17
1.2.2.4 Sea Temperature	17
1.2.3 Petroleum Lifetime.....	18
1.2.4 Proposals to Minimize Climate Change While Reducing the Dependence of Petrochemical Products	19
1.2.4.1 Solar Shield and Aerosol	20
1.2.4.2 Ocean Iron Fertilization.....	20
1.2.4.3 CCS (Carbon Capture and Storage)	20
1.3 CDU (Carbon Dioxide Utilisation).....	21
1.3.1 Introduction	21
1.3.2 Applications of CDU	25
1.3.2.1 Mineral Carbonation.....	25
1.3.3 Biofuel from Microalgae	26
1.3.4 Carboxylation Reactions	26
1.3.5 Electrochemical Reactions	29
1.3.6 Electrocarboxylation	30
1.3.6.1 Use of Sacrificial Electrode in Electrocarboxylation.....	31
1.3.6.2 Electrocarboxylation of Alkynes.....	32
1.3.6.3 Electrocarboxylation of Unsaturated Hydrocarbons.....	34
1.3.6.4 Electroreduction of CO ₂ to Form Formic Acid.....	34
1.3.6.5 Electrocarboxylation of benzyl chlorides	35
1.3.6.6 Electrocarboxylation of Alkenes	35
1.4 Previous Buckley Group Findings	36

1.4.1	<i>Electrosynthesis of Cyclic Carbonates from Epoxides and Atmospheric Pressure Carbon Dioxide.</i>	36
1.4.2	<i>Electrocarboxylation of Epoxides: Catalysed by Ni(II) Complexes</i>	37
1.4.3	<i>Electrocarboxylation of Epoxides: Catalysed by Cu(I) Coordinate Complex</i>	37
1.4.4	<i>Carboxylation of Epoxides Without Electrodes</i>	39
1.4.5	<i>Development of a Non-sacrificial Electrode System</i>	40
1.4.5.1	Photochemical Reduction of CO ₂	41
1.5	Plasma Technology	43
1.5.1	Introduction	43
1.5.2	Gas Breakdown	46
1.5.3	Plasma in and in Contact with Liquids	48
1.5.4	Other Plasma Applications	51
1.5.4.1	Plasma Water Treatment	51
1.5.4.2	Chemical Interaction	54
1.5.4.3	Plasma Medicine	56
1.5.5	Electrical Measurement	57
1.5.5.1	Current, Current Density and Power Dissipation	58
1.6	Summary	59
2.0	EXPERIMENTAL	61
2.1	General Experimental	61
2.1.1	Reagents and Apparatus	61
2.1.2	Determination of % Yield and Calculation of Current Efficiency	62
2.1.2.1	GC/MS Calibration Curves	63
2.1.2.2	Methylation Procedure and Injection Parameter	64
2.1.3	Electrical and Physical Properties	66
2.1.3.1	The Velocity of Gas in a Tube	66
2.1.3.2	Surface Area of Cylindrical Electrode	66
2.1.3.3	Voltage Measurement	67
2.2	Individual Electrochemical Experimental Procedures	67
2.2.1	Electrochemical Setup	67
2.2.2	General Procedure for Carboxylation Using a Sacrificial Electrode	68
2.2.3	General Procedure for Electrocarboxylation Using a Non-Sacrificial electrode	69
2.2.4	Electrode Properties Experiment	69
2.3	Individual Plasma Experimental Procedures and Characterization	71
2.3.1	Plasma Apparatus and Gases	71
2.3.2	Plasma Setup	71

2.3.3	<i>Microplasma Jet Design</i>	72
2.4	Plasma Carboxylation in Wet Solvent	75
2.5	General Plasma Carboxylation in Anhydrous Solvent.....	76
2.6	Plasma Carboxylation Without Reducing Agent.....	76
2.7	Use of Catalyst During Plasma Carboxylation	77
2.8	Formation of 2,3-diphenylpropanoic Acid, Investigation, and Optimization.....	78
2.9	Determination of Reaction Performance by Splitting Plasma Jet.	79
2.10	Screening of Applied Current	80
2.11	Effect of Current Density.....	81
2.12	Plasma Carboxylation of 1-Methoxy-4-(phenylethynyl)benzene.....	82
2.13	Conversion Rate and Current Efficiency Study	83
2.14	Plasma Carboxylation Solvent Optimization.....	84
2.15	Study of Gas Ionization Efficiency.....	85
2.16	Complete Reaction Conversion.....	86
2.16.1	<i>Reaction "A"</i>	86
2.16.2	<i>Reaction "B"</i>	86
2.16.3	<i>Reaction "C"</i>	86
2.16.4	<i>Reaction "D"</i>	87
2.17	Plasma Carboxylation of Alternative Substrate.....	87
3.0	RESULTS AND DISCUSSION	91
3.1	Original Research: Investigation.....	91
3.1.1	<i>Test of Reducing Agent</i>	91
3.1.2	<i>Alternative Substrates</i>	92
3.2	Electrode Properties.....	94
3.3	Application of Cold Atmospheric Plasma in CO ₂ Conversion-Initial Stages.....	95
3.3.1	<i>DC Power Supply Damage</i>	99
3.3.2	<i>Plasma Carboxylation Without the Need for a Reducing Agent</i>	99
3.3.3	<i>Use of Catalyst During Plasma Carboxylation</i>	101
3.3.4	<i>Interesting finding</i>	102
3.3.5	<i>Formation of 2,3-diphenylpropanoic Acid, Investigation, and Optimization</i>	104
3.3.6	<i>Determination of Reaction Performance by Splitting Plasma Jet</i>	106
3.3.7	<i>Carboxylation of 1-Methoxy-4-(phenylethynyl)benzene</i>	110
3.3.8	<i>Screening of Applied Current</i>	111
3.3.9	<i>Effect of Current Density</i>	111

3.3.10	<i>Conversion Rate and Current Efficiency Study</i>	113
3.3.11	<i>Plasma Carboxylation - Solvent Optimization</i>	114
3.3.12	<i>Study of Gas Ionization Efficiency</i>	116
3.3.13	<i>Complete Reaction Conversion</i>	119
3.3.14	<i>Alternative Substrates</i>	125
4.0	CONCLUSIONS AND RECOMMENDATION FOR FUTURE WORKS	128
4.1	Conclusions	128
4.2	Recommendations for Future Work.....	131
5.0	REFERENCES	133

List of abbreviations

BITRE	Bureau of Infrastructure Transport and Regional Economics
Bu ₄ NI	Tetrabutylammonium iodide
CCS	Carbon Capture and Storage
CE	Current Efficiency
CDU	Carbon Dioxide Utilisation
DBD	Dielectric Barrier Discharge
DC	Direct Current
DCM	Dichloromethane
DI	Deionized
DMF	<i>N,N</i> -Dimethylformamide
DMSO	Dimethyl Sulfoxide
E	Electric Field
EIA	Energy Information Administration
EOR	Enhanced Oil Recovery
EGR	Enhanced Gas Recovery
Et	Ethyl
FID	Flame Ionization Detector
GC	Gas Chromatography
GCMS	Gas Chromatography Mass Spectrometry
GHG	Greenhouse Gas
Gt	Gigatone
Hz	Hertz
IARC	International Agency for Research on Cancer
IPA	Isopropyl alcohol

IPCC	Intergovernmental Panel on Climate Change
<i>i</i> -PrOH	Isopropyl Alcohol
IR	Infrared
<i>J</i>	Current Density
LCA	Life Cycle Analysis
mA	Milliampere
Me	Methyl
MW	Molecular Weight
MeCN	Acetonitrile
NASA	National Aeronautics and Space Administration
NMR	Nuclear Magnetic Resonance
PC	Propylene Carbonate
Ph	Phenyl
RF	Radio Frequency
SCCM	Standard Centimetre Cubic per Minute
SLM	Standard Litre per Minute
Te	Temperature of electrons
TEA	Triethylamine
TEOA	Triethanolamine
THF	Tetrahydrofuran
<i>TM</i> SCHN ₂	trimethylsilyldiazomethane
Ti	Temperature of ions
TLC	Thin Layer Chromatography
Torr	~133.3 Pa
UV	Ultraviolet

V	Volt
VOC	Volatile Organic Compound
Ω	Ohm
WMO	World Meteorological Organization

1.0 Introduction

1.1 Aims and Objective

The aim of this research project is to develop a plasma jet enable to harness free electrons formed in the plasma state at atmospheric pressure and room temperature to drive electrosynthesis of organic compounds with carbon dioxide suppressing the need for sacrificial electrode or reducing agent. Up to now, not many chemical interactions have been carried out employing plasma; for instance, the variation of pH measurement was achieved by Go and his team¹ or the reduction of ferricyanide to ferrocyanide was demonstrated by Richmonds.² At the beginning of this work, plasma carboxylation had, to the best of my knowledge not been successfully achieved.

The use of electrons in electrochemistry to incorporate CO₂ into organic compounds has been widely studied.³⁻⁷ The drawback of the majority of electrocarboxylation reactions is the fact that in a redox system the oxidized material (usually a metal) ends up forming toxic compounds⁸. Despite the fact that some improvements have already been made, such as the use of an oxidative agent that discards the need for a sacrificial electrode and the conversion at atmospheric pressure and room temperature achieved by Buckley and coworkers,⁶ there is a need for more improvements.

The application of an atmospheric plasma source at room temperature would overcome the disadvantage of traditional electrochemical processes using a sacrificial electrode or chemical agent since the plasma provides free electrons to the system.

The first step is the replication of electrocarboxylation reaction already carried out successfully and the selection of a suitable substrate. The second step is the design of a plasma jet able to substitute the cathode. After proof of concept, a range of optimization of the process is conducted in order to increase the efficiency of the method and clarify the mechanism of plasma carboxylation. Finally, the identification and characterization of the product formed by NMR and GC-MS.

1.2 Environmental Considerations

The 20th Century was marked by a growing world population resulting in the need for more energy and this resulted in an expansion of the global economy.

Since the beginning of the industrial revolution in the 1760s until nowadays, the need for energy, with a growth rate in the order of 1.9% per year,⁹ along with chemical raw materials has increased exponentially. The main source of energy use is based on the combustion of carbonaceous fuel, which consists mainly of fossil fuels such as coal, natural gas, and petroleum. The combustion of these fossil fuels generates a large amount of carbon dioxide that is released into the atmosphere.¹⁰ Figure 1.1 shows the constantly yearly growth of global emissions of CO₂ from fossil fuel and industry reaching 36.2 Gt CO₂ in 2017, 63% over 1990. Emissions in 2018 are projected to grow at a rate of 2.7% (range: 1.8%–3.7%) reaching 37.1 ± 1.8 Gt CO₂.¹¹

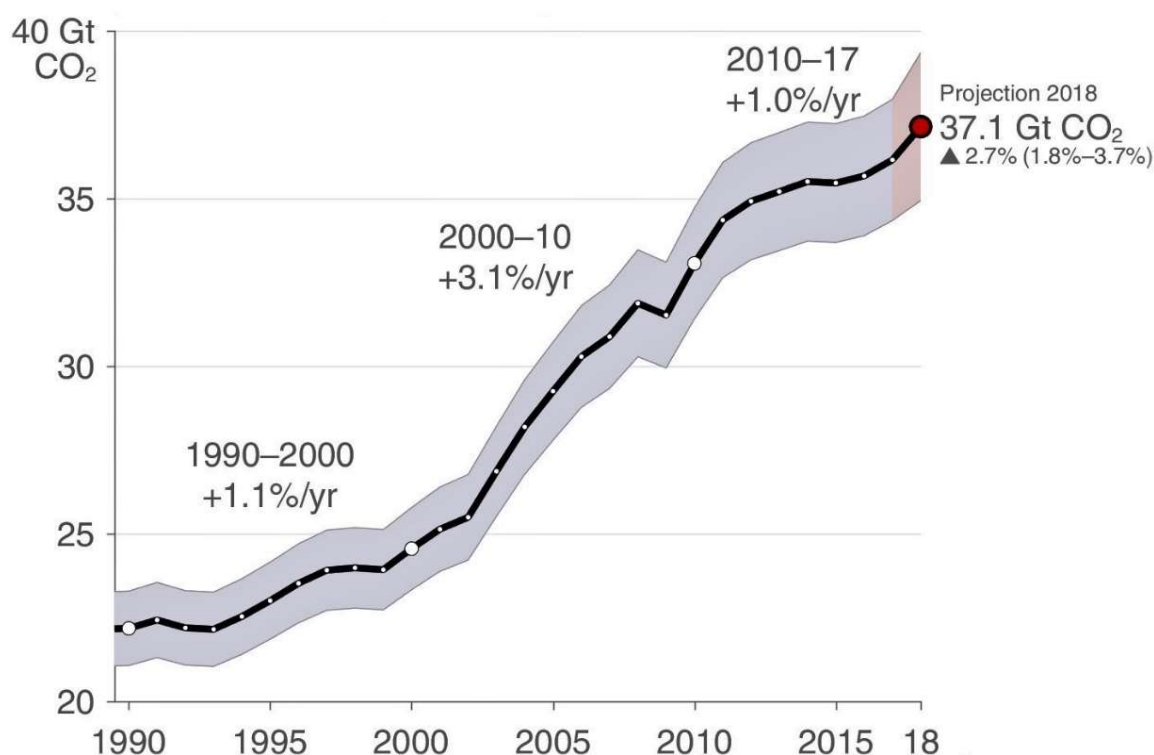


Figure 1.1 Global emissions from fossil fuel and industry from 1990 to 2017 and projection for 2018 .¹¹

Petroleum boosted chemical industry development and due to a lack of knowledge of the effect of carbon dioxide and other greenhouse gases, coupled with a large

amount of cheap fossil fuel available on the market, it was used freely without any thought of the consequences. However, since 1977, Marchetti¹² suggested that rising atmospheric CO₂ levels were a result of the burning of fossil fuel. It is now known that a variety of gases that are released into the atmosphere will cause a negative effect on human health and global warming.¹³

Despite the world's population continues to grow by 1.1% annually,¹⁴ global emissions almost stalled in 2014 with an increase of only 0.5% to 35.7 Gt CO₂ which was the lowest global growth rate since 1998, excluding the recession in 2009. Since the global temperature measurement began in 1880, 2014 was the warmest winter in Europe which helped limit fossil-fuel demand for space heating (Figure 1.2).

China, United States, EU-28 and India account for 61% of all emissions, of which 30% is emitted by China, this large increase in Chinese emissions is mainly due to energy demand after economic reforms since 2000 with growth rates above two digits.¹⁵

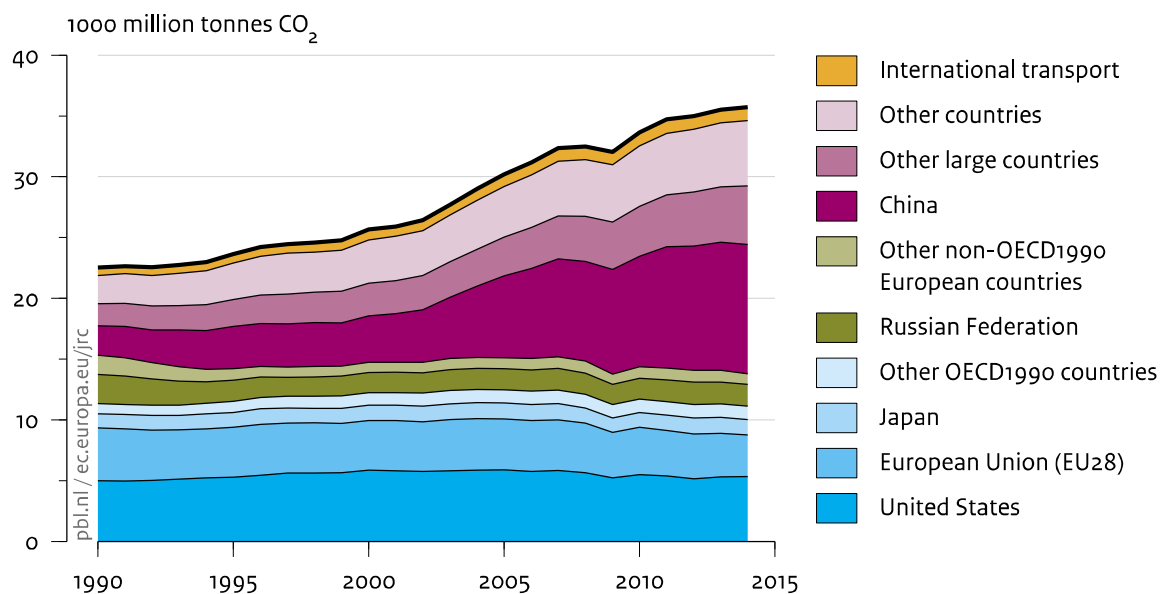


Figure 1.2 Global CO₂ emissions per region from fossil-fuel use and cement production.¹⁵

1.2.1 Greenhouse Gases (GHG)

In the natural greenhouse effect, the greenhouse gases (water vapour, carbon dioxide, methane, NO_x and chlorofluorocarbons) present in the atmosphere, have

the ability to trap some of the heat gained by the sun, keeping the Earth's average surface temperature at around 14°C; without this effect it would be at approximately -19°C. However, the more GHG (greenhouse gases) that are released into the atmosphere the more heat is retained which in turn affect the climate of the planet. These effects are termed anthropogenic (human-caused) climate change.¹³

For hundreds of thousands of years, the snow has been accumulating on the Antarctic and Greenland ice sheet. The pressure of overlying snow has compressed buried layers of snow into ice, trapping pockets of air. Drilling into the ice sheets and extracting the gas from the air pockets, for composition measurement, has proven that the concentration of greenhouse gases has been increasing significantly since the pre-industrial era as displayed in Figure 1.3.¹⁶

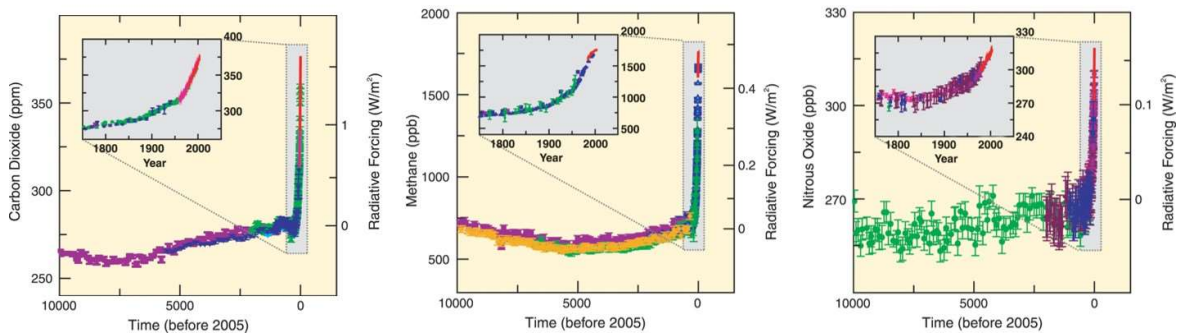


Figure 1.3 Atmospheric concentrations of CO₂, CH₄, and N₂O over the last 10,000 years (large panels) and since 1750 (inset panels). Measurements are shown from ice cores (symbols with different colours for different studies) and atmospheric samples (red lines). The corresponding radiative forcings relative to 1750 are shown on the right-hand axes of the large panels.¹⁶

1.2.2 Global Warming

In addition to the rising of GHG concentration, it has been reported by the IPCC (Intergovernmental Panel on Climate Change) that the Earth's surface has also been warming. Analysis of the temperature data record since 1850 highlights that the last three decades have been successively warmer, providing a correlation between global warming and the concentration of GHG (Figure 1.4).¹⁷

According to the WMO (World Meteorological Organization) report, the hottest years occurred in the 21st century, the global average surface temperature increased by about 0.89 °C (0.69 °C-1.08 °C) in the period 1901-2012.¹⁸

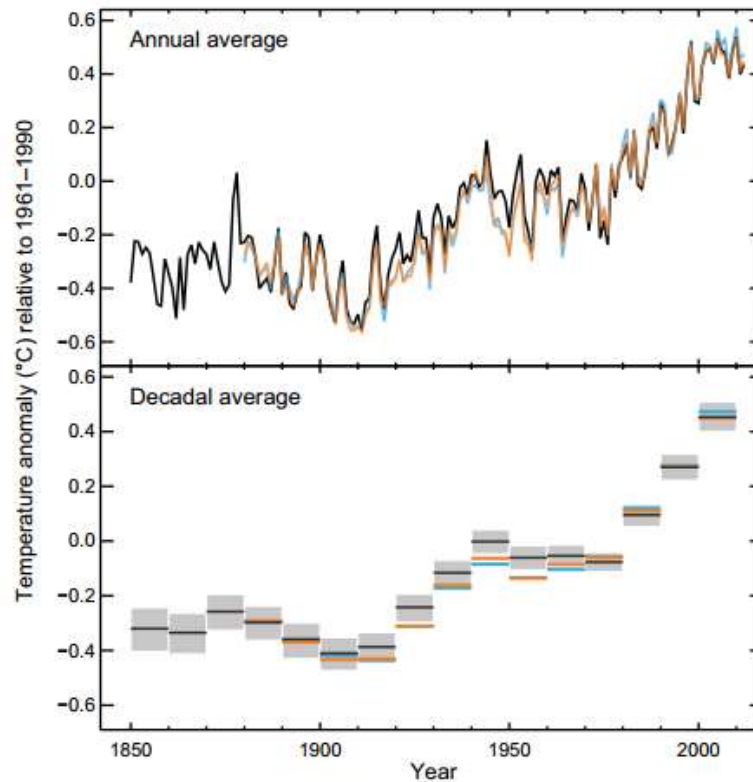


Figure 1.4 Observed globally averaged combined land and ocean surface temperature anomaly 1850-2012 from three data sets.¹⁷

Colours indicate different data sets. Anomalies are relative to the mean of 1961–1990. Observed surface temperature change from 1901 to 2012 derived from temperature trends determined by linear regression from one dataset (orange line). Bottom panel: decadal mean values including the estimate of uncertainty for one dataset (black line).

Global warming will certainly bring some serious consequences for the human population.¹⁹ Research has predicted potential natural disasters due to global warming, for example, increased temperature will cause ice sheets to melt and ocean level to rise. In the period 1901-2010, the average global sea level already increased by 19 cm with an average increase of 1.7 mm per year while only in the past two decades, in the period of 1993-2010, the average global sea level increased by 3.2 mm/year.²⁰ As half of the world population are living in coastal regions, all of them will be affected by the flooding. More frequent and severe weather, dirtier air, higher wildlife extinction rates, more oceans with higher acidity along with other problems are predicted.²¹

There have been some controversial statements saying that the temperature has not been steady over the time.²² Thousand of years ago, the planet was going through an ice age, with glaciers covering much of Europe and North America and

before that, one hundred million years ago, the Earth was very warm which means that climate variations are not unusual.

But first, we already know that CO₂ traps heat and since 1900 after the industrial revolution, CO₂ levels in the atmosphere have been steadily climbing as we burn more, fossil fuel reaching levels that are unprecedented over hundreds of millennia.²² The relationship between global temperature and CO₂ concentration is exemplified in Figure 1.5, for thousands of years the level of carbon dioxide has been fluctuating followed by the changes in temperature, however, for the first time the level of carbon dioxide increased above 280 ppm and continue to rise.²³

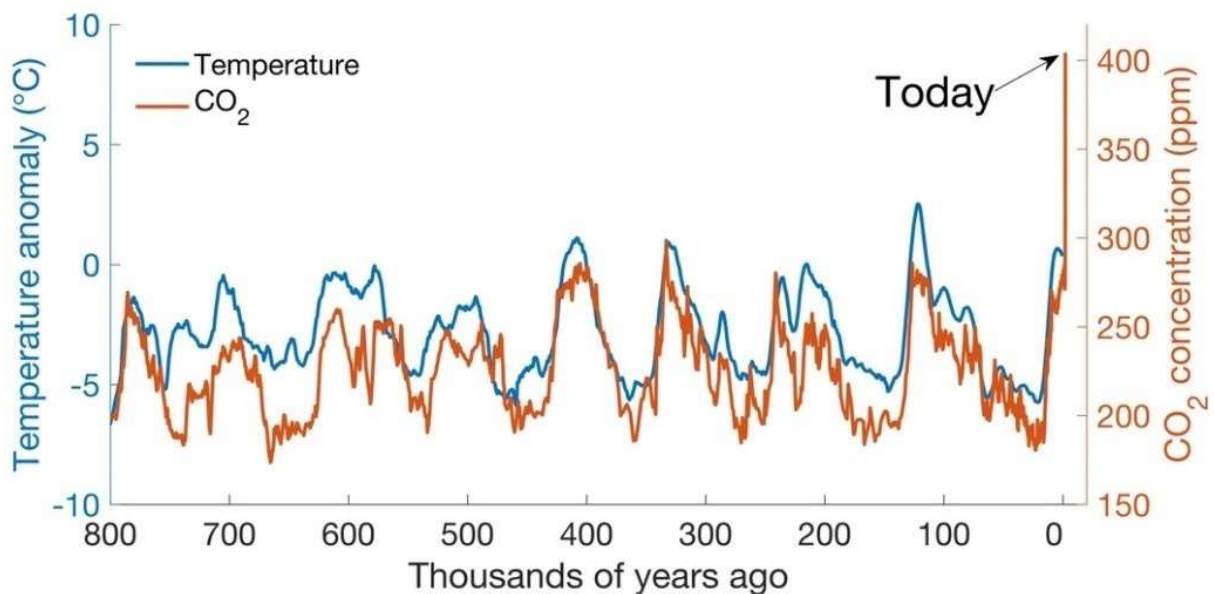


Figure 1.5 Global average temperature and CO₂ concentration changes over 800,000 years.²³

The interesting aspect is that the fastest natural shifts out of ice ages saw CO₂ levels increase by around 35 ppm (parts per million) in 1,000 years, while humans have emitted the equivalent amount in just the last 17 years, so not only our activities are contributing to warming the planet but we are seeing this change occurring very rapidly.

1.2.2.1 Positive Feedback

The amount of warming that occurs because of increased greenhouse gas emissions depends in part on feedback loops. Positive (amplifying) feedback loops

increase the net temperature change from a given forcing (Figure 1.6 Climate Feedback Loops.), while negative (damping) feedbacks offset some of the temperature change associated with a climate forcing. Positive feedback is more problematic as the effect can drastically increase global warming.²⁴ When modeling the carbon cycle, researches have indicated that for every degree Celsius increased of the earth's surface, mechanisms which reflect or reduce heat decrease their effectiveness resulting in increased rate of surface warming. A vicious cycle of decreasing reflection of heat and therefore accelerating global warming occurs. The various different environmental factors which create positive feedback are further described in Figure 1.6 Climate Feedback Loops.²⁵

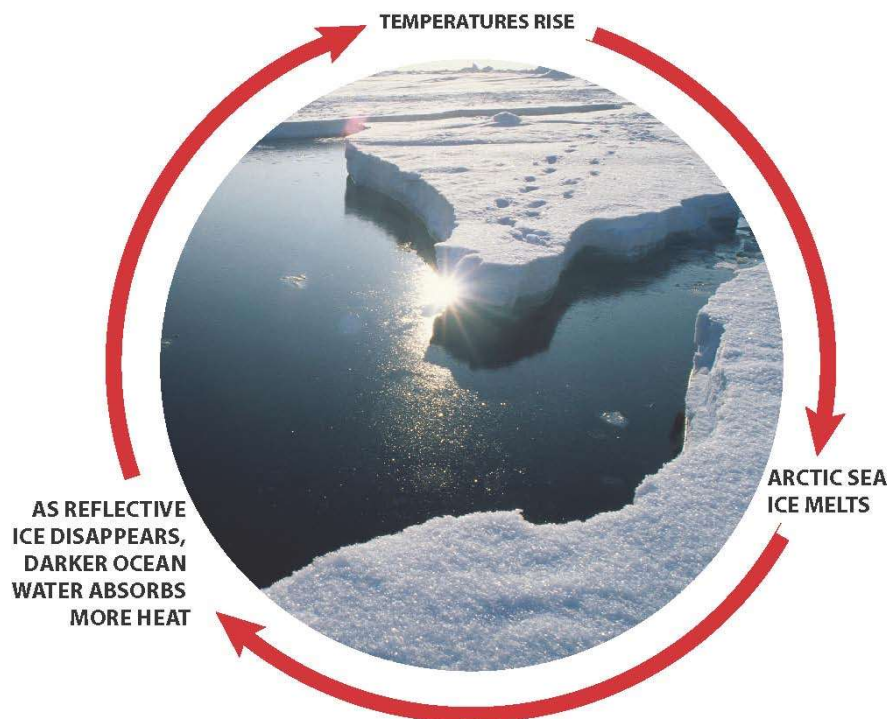


Figure 1.6 Climate Feedback Loops. As the ice melts, less sunlight is reflected back to space and more is absorbed into the dark ocean, causing further warming and further melting of ice.²⁴

1.2.2.2 Arctic Sea

Ice on the Arctic sea reflects sunlight, keeping the polar regions cool and thereby moderating the global climate.²⁶ Figure 1.7 shows that during the last 30 years, the area covered by Arctic sea ice has declined dramatically from 7.0 million km² in 1979 to 4.6 million km² in 2018²⁷ with the most extreme decrease seen in the summer melt season. By exposing the sea to the sun, the fraction of sunlight that

is reflected is significantly reduced, thus more solar energy is absorbed by the sea causing the positive feedback effect, described in the section 1.2.2.1.

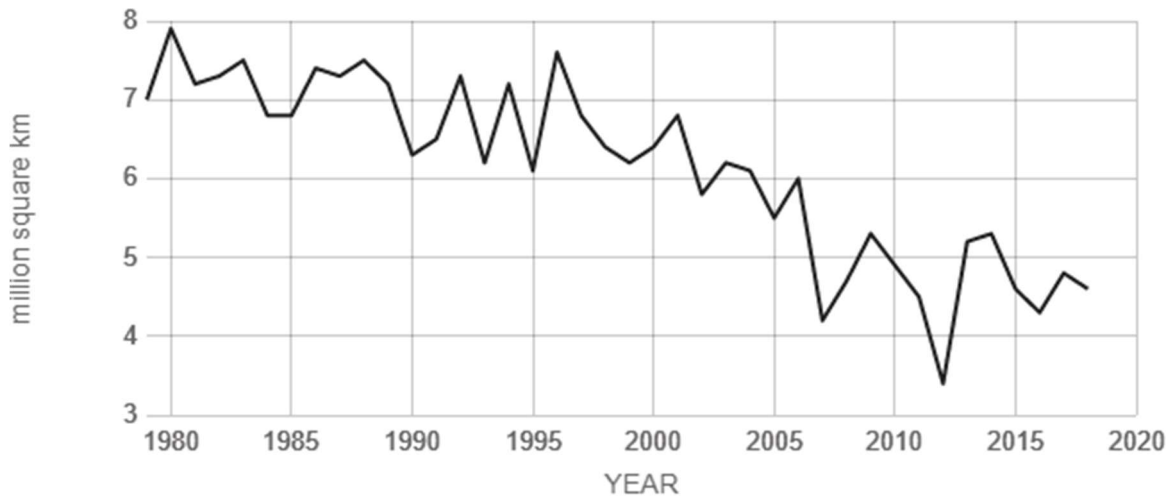


Figure 1.7 NASA satellite observation of average monthly Arctic sea ice extent each September since 1979.²⁷

1.2.2.3 Permafrost

Beneath the frozen depths of the arctic, the icy soil stores an estimated 1.5 trillion tons of carbon, methane and other hydrocarbons.²⁸ These greenhouse gases are locked up in permafrost, frozen ground that covers 24 percent of exposed land in the high latitudes of the Northern Hemisphere, as well as parts of Antarctica and the Patagonian region of Argentina and Chile in the Southern Hemisphere. Such greenhouse gases are escaping the permafrost and entering the atmosphere due to global thawing.²⁷ This thawing process will accelerate the rising of the GHG level in the atmosphere and thus speed up global warming.

1.2.2.4 Sea Temperature

It is known that the ocean absorbs part of the CO₂ from the atmosphere through photosynthesis by plant-like organisms (phytoplankton), as well as by simple chemistry on the formation of bicarbonate. Scientists have discovered that the concentration of carbon dioxide in water depends on the amount of CO₂ in the atmosphere and the temperature of the water.²⁹ Researches indicate that as atmospheric CO₂ increases from pre-industrial levels, the ocean CO₂ concentration also increases. Nevertheless, as water temperature increases, its ability to dissolve CO₂ decreases (Figure 1.8). This means that global warming is expected to reduce

the ocean's ability to absorb CO₂, which in turn will be left in the atmosphere leading to even higher temperatures.³⁰

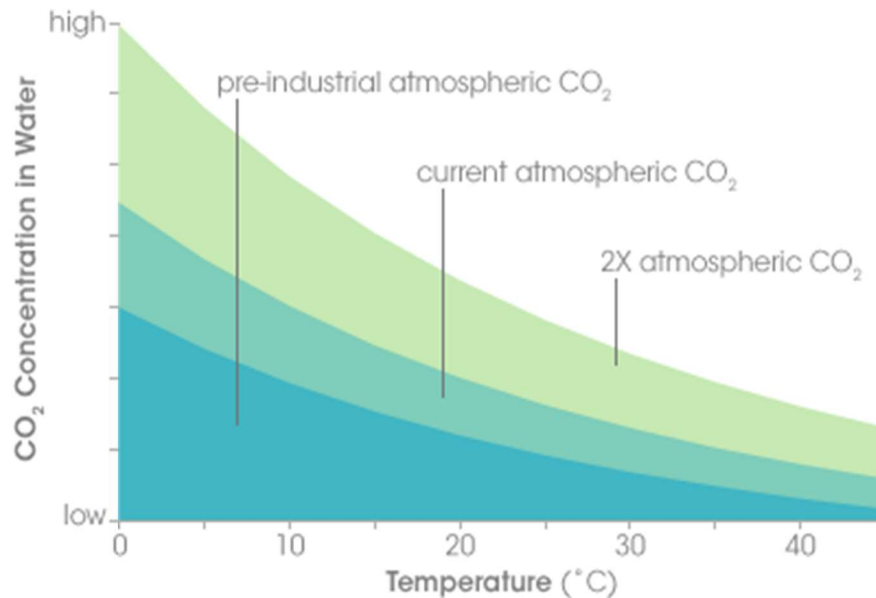


Figure 1.8 Relation of CO₂ available and the ability of water to retain it according to the temperature.²⁹

1.2.3 Petroleum Lifetime

Besides the issues related to GHG emissions, our chemical industry is highly dependent upon oil. Today there are more than 6.000³¹ different products that are made from petroleum, for example, plastics, pesticides, building materials, medical materials, solvents, oil, ink, automotive components, motor gasoline, and distillate fuel besides a wide range of other products.³¹ However, the world's reserves are shrinking, and oil has become harder and harder to find.³²

In 1940, five times as much oil was discovered as consumed. Forty years later, in 1980, the amount of petroleum discovered was just about equaled the amount consumed, as shown in Figure 1.9. By the end of the 21st century, world consumption of petroleum is predicted to be three times the amount that is discovered if current trends continue.³³ It is, therefore, necessary to develop new sustainable raw materials to substitute this fossil fuel.

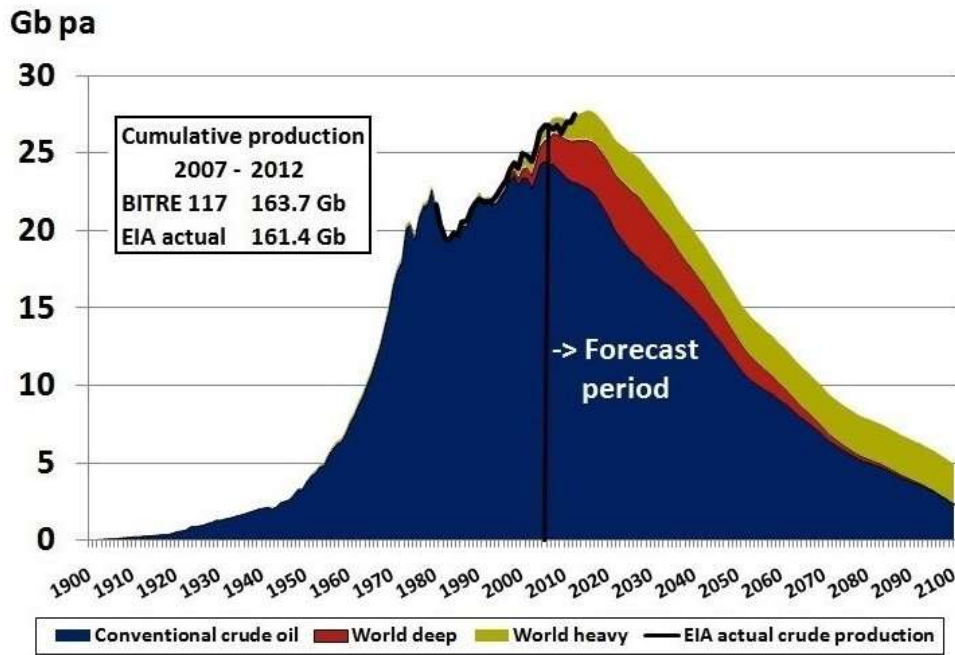


Figure 1.9 World crude oil production and forecast.³²

* Conventional crude oil is oil pumped from wells on land or in water less than 500 metres deep.

* Unit is given in gigabarrel (Gb) of oil.

1.2.4 Proposals to Minimize Climate Change While Reducing the Dependence of Petrochemical Products

There is no one single solution but a combination of techniques, which promise to reduce or stop climate change due to global warming. Some are feasible and depend upon political effort, while others face controversy regarding their efficiency. Some of the techniques illustrated in **Figure 1.10** are briefly explained.

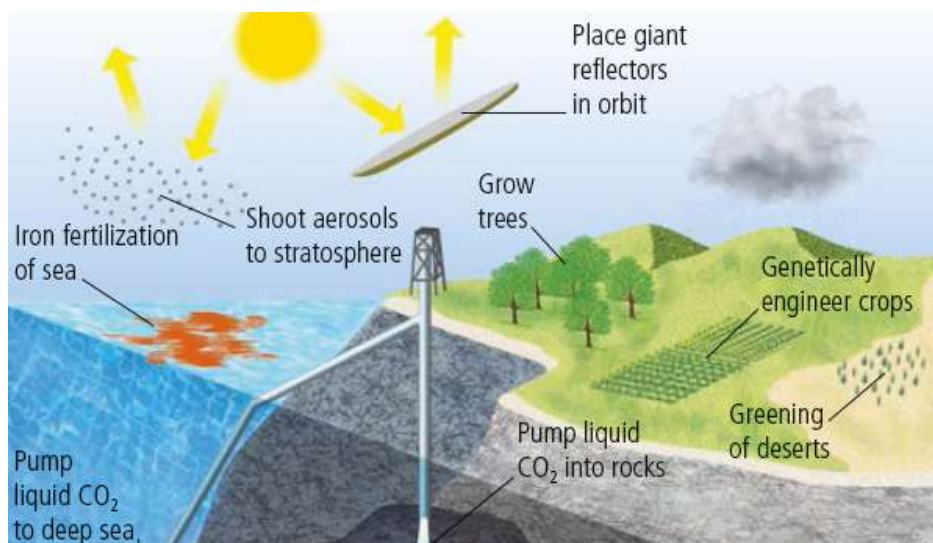


Figure 1.10 Geoengineering solutions to climate change.²¹

1.2.4.1 Solar Shield and Aerosol

This method involves deploying “solar shields” in space that reflect sunlight away from the Earth. Shooting sulfate aerosols into the atmosphere to mimic the cooling impact of volcanic eruptions. It is less costly than other methods that are presented here but could be more dangerous and exacerbate the problem of ozone depletion.³⁴

1.2.4.2 Ocean Iron Fertilization

Ocean iron fertilization is a method in which iron is added to increase and therefore fertilize photosynthetic uptake of CO₂ by phytoplankton, in regions of the ocean where iron is a limiting nutrient. As iron is a trace element necessary for photosynthesis, scientist advocates the idea that by adding iron to the upper ocean would enhance biological productivity, which can benefit the marine food chain, increasing carbon dioxide removal from the atmosphere.³⁵ However, it is uncertain how large an iron addition can be without causing environmental change and also additional effects, such as the resurfacing of nutrient-depleted, low-oxygen waters, which could appear years after an experiment.³⁶

In 1990, Martin suggested that “the phytoplankton growth in major nutrient-rich waters is limited by iron deficiency” and that could offer an approach to mitigating climate change, this theory was supported by the eruption of Mount Pinatubo in 1991 in the Philippines. Watson stated that due to that eruption, approximately 40,000 tons of iron dust was deposited into oceans worldwide. This single fertilization event preceded an easily observed global decline in atmospheric CO₂. A study from 2010 in an oceanic high-nitrate, low-chlorophyll environments (50° N, 145° W) have been highlighted for potential large-scale iron fertilization.³⁷ Iron fertilization stimulated the growth of oceanic *Pseudonitzschia* (nontoxic marine planktonic diatom genus), however, *Pseudonitzschia* produces the neurotoxin domoic acid, causing detrimental marine ecosystem impact.³⁷

1.2.4.3 CCS (Carbon Capture and Storage)

CCS (Carbon Capture and Storage) is a technology in which most of the CO₂ emissions produced from the use of fossil fuels, electricity generation, and

industrial processes are captured, then transported as a liquid through a pipeline or ship into porous geological formations. These formations are typically located several kilometers under the earth's surface, with pressure and temperatures such that carbon dioxide will be in the liquid or 'supercritical' phase.³⁸ The drawback of this method is the fact that it is a palliative solution and may solve the problem for now but in reality, the definitive solution will be left for the future generation to resolve.

Besides just storage carbon dioxide that is captured, CCS can also be used for EHR (Enhanced Hydrocarbon Recovery). This includes EOR (Enhanced Oil Recovery) and EGR (Enhanced Gas Recovery).³⁹ The current process of oil extraction production consists of pumps and in a secondary process injecting water into an oil reservoir to increase the pressure and drive the oil towards the production wells however about 40% of oil is still left behind. EOR is a tertiary method of oil recovery and can enable significant additional quantities of oil to be extracted, in this method only CO₂ or CO₂ mixed with water is injected into the existing oil reservoir pushing the remaining oil towards production wells, this process increases the production while storing carbon dioxide underground.

A similar process can be used to enhance natural gas production, since CO₂ is heavier than natural gas, by injecting it into the base of a depleted gas reservoir causing any remaining natural gas to "float" on top of it driving the natural gas towards the production wells.³⁹

CDU (Carbon Dioxide Utilisation) is also another way which tends to deal with an issue related to CO₂, however, will be thoroughly explained in the next section.

1.3 CDU (Carbon Dioxide Utilisation)

1.3.1 Introduction

Due to the fact that carbon dioxide is a non-polar, thermodynamically and chemically stable molecule under standard conditions, the molecule is difficult to break down and utilize for other uses and is therefore treated as a waste product. Like CCS, CDU also aims to capture CO₂ emissions from point sources such as

power plants and industrial processes, to prevent release into the atmosphere, with the difference in the destination of the captured CO₂.

In this method, carbon dioxide is transformed into different chemicals which contain the carbon of CO₂ or make use of the active 'oxygen atom'. An example would be using CO₂ as a reactant to produce commercially valuable chemical feedstocks. Feedstock production would therefore no longer rely on petrochemical sources, reducing the demand for fossil fuels. Additionally, in order to be even more efficient, the energy used in this process could be derived from a renewable source. Figure 1.11 illustrates the CO₂ utilisation cycle.

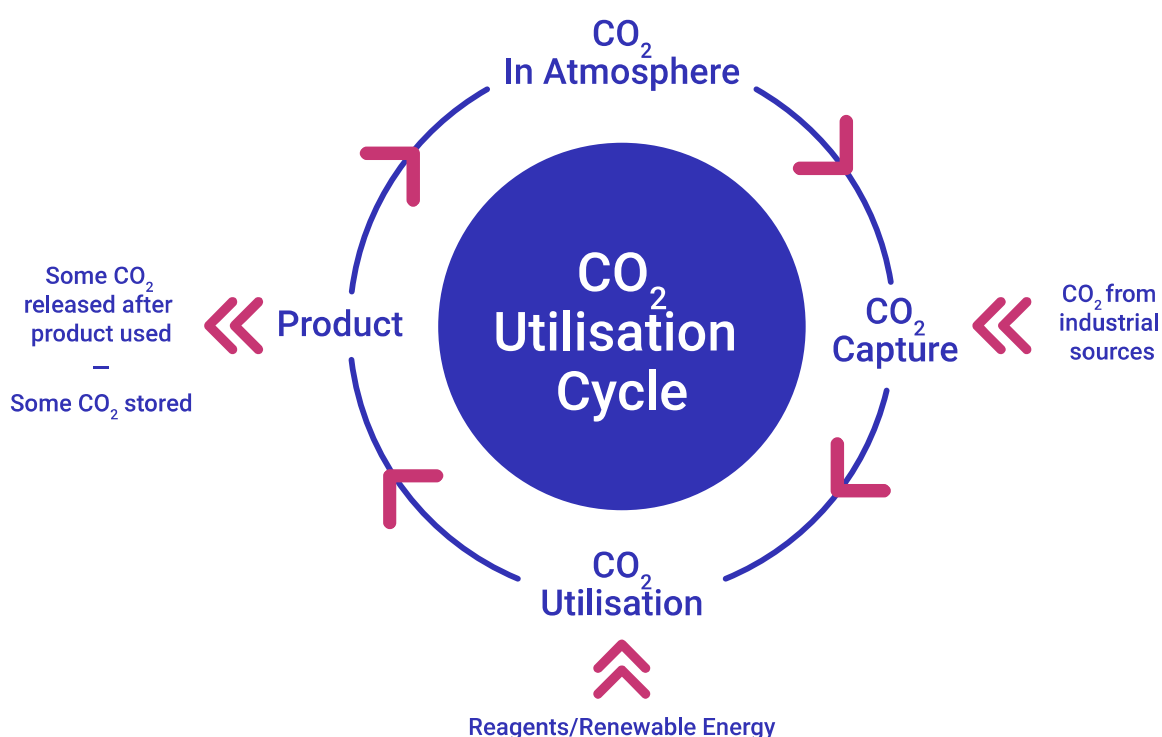


Figure 1.11 The CDU Cycle: Carbon dioxide is captured from the atmosphere or from the industrial exhaust. It is utilized with other materials in manufacture, potentially driven by renewable energy. This delivers valuable products while reducing or avoiding associated emissions to the atmosphere.⁴⁰

Finding a source of CO₂ is easy, only power plants account for roughly 35% of all CO₂ emissions by burning fossil fuel.⁴¹ However, one of the challenges in CDU is the fact that besides the CO₂, flue gas also brings a variety of other gases and impurities (Table 1.1). Dealing with these impurities is somewhat difficult and expensive, the costs are largely influenced by the concentration of CO₂ in the exhaust gas. Table 1.1 summarizes current data on the global largest point of

sources of CO₂ describing emission volumes, concentrations, potential capture volume, and benchmark cost. Common impurities encountered in flue gases may include nitrogen oxides (NO_x), sulfur oxides (SO_x), water vapour (H₂O), and particulate matter (PM), and to address these impurities it is important to know the fundamental mechanisms behind CO₂.⁴²

Table 1.1 Potential sources of waste CO₂ (most recent available estimates).⁴³

CO ₂ emitting source	Global emissions ^a (Mt CO ₂ /year)	CO ₂ content ^a (vol%)	Capturable emissions (Mt CO ₂ /year)	Benchmark capture cost (€ 2014/t CO ₂) [rank]
Coal to power	9031 ^c	12–15	7676	34 [6]
Natural gas to power	2288 ^c	3–10 ^d	1944	63 [9]
Cement production	2000	14–33	1700	68 [10]
Iron and steel production	1000	15	500	40 [7]
Refineries ^e	850	3–13	340	99 [12]
Petroleum to power	765 ^c	3–8	Not available	Not available
Ethylene production	260	12	234	63 [8]
Ammonia production	150	100	128	33 [5]
Bioenergy ^f	73 ^d	3–8 ^d	66	26 [2]
Hydrogen production ^f	54 ^g	70–90 ^h	46	30 [4]
Natural gas production	50	5–70	43	30 [3]
Waste combustion	60 ⁱ	20	Not available	Not available
Fermentation of biomass ^f	18 ^d	100 ^d	18	10 [1]
Aluminium production	8	<1 ^j	7	75 [11]

^aData from Wilcox (2012) if not indicated otherwise.

^cData from IEA (2014) based on the largest point sources suitable for capture and not including the emissions of the large amount of emissions that are caused by small decentral point sources in the mobility and residential sector.

^dData from Metz et al. (2005).

^eRefineries could include ammonia and hydrogen production. A separate listing is nevertheless interesting to differentiate this two high purity from general refinery CO₂ streams. The capturable emission data based on the estimated capture rates should ensure that emissions are not included twice.

^fUndisclosed technological assumptions for emissions volumes and CO₂ content, if not indicated otherwise. For bioenergy and fermentation, emission estimates are only for North America and Brazil.

^gData from Mueller-Langer et al. (2007).

^hData for hydrogen from steam methane reformer from Kurokawa et al. (2011).

ⁱData from Bogner et al. (2007).

^jData from Jilvero et al. (2014), Jordal et al. (2014).

The table above provides general insight into the potential large-scale supply of CO₂ as a commodity. Capture costs are defined as the cost of separation and compression at a single facility disregarding costs of transportation, storage, and

conversion.⁴⁴ It is also recommended that any utilisation technology should follow a study of LCA (Life Cycle Analysis) which evaluates the environmental impacts of all production steps.⁴³

Some industrial process such as ammonia production and fermentation of biomass emits very pure CO₂ requiring only small steps to capture, therefore their emission account for only 2.6% of total 12.7 Gt of capturable emissions (Table 1.1) while coal and natural gas for power generation are responsible for 76% of the 12.7 Gt.⁴³

As shown in Figure 1.12, CO₂ may be used as a gas, liquid, and solid. Today it is used as a refrigerant for food preservation, beverage carbonation, as fire extinguishers, supercritical solvents, and chemical reactant to produce urea, salicylic acid, and dry ice.⁴⁵

For this method to be successful, the whole process needs to have an efficient integration of energy resources, low-cost facility, and high value of chemicals produced as well as the development of new C1 chemicals. Processes that can be used for CO₂ conversion and utilisation include non-catalytic chemical processes,⁴⁶ heterogeneous or homogeneous catalysis,⁴⁷ photochemical and photo-catalytic reduction,⁴⁸ biochemical and enzymatic conversion, electrochemical⁴⁹ and electrocatalytic conversion.¹⁰

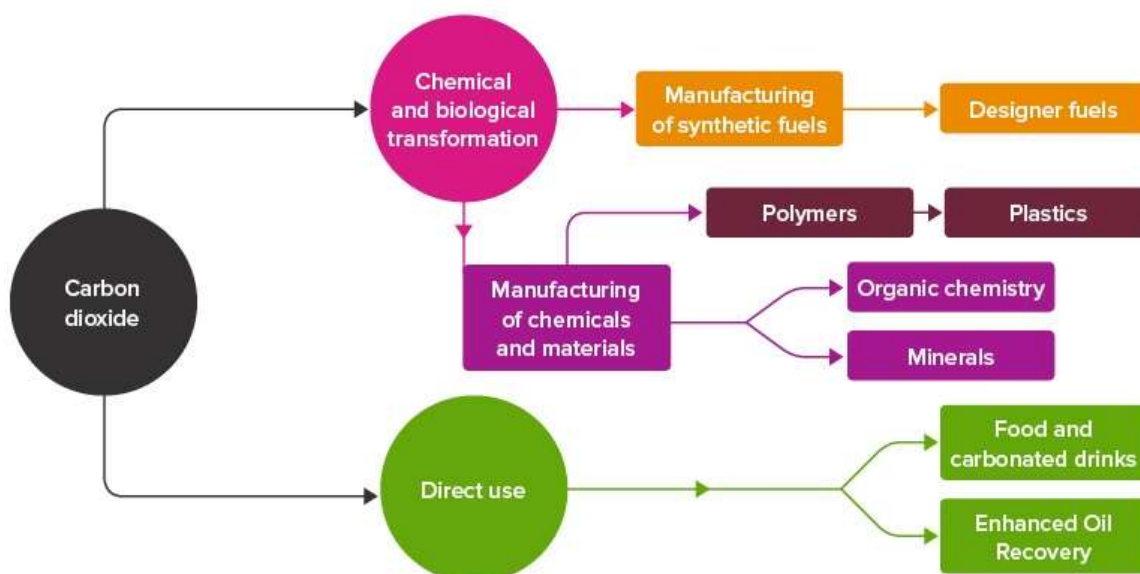


Figure 1.12 - Uses of carbon dioxide.⁴⁵

An overview of possible known conversions is shown in Figure 1.13, where the easier transformations and those most likely to happen are positioned on the left of the figure and as the reactants move to the right of the figure it becomes more stable and difficult to synthesize. The reactant highlighted in red was already successfully being explored by Buckley's group in electrochemical synthesis so it was chosen as substrate in this research due to know reactions and will be thoroughly explained in this report.

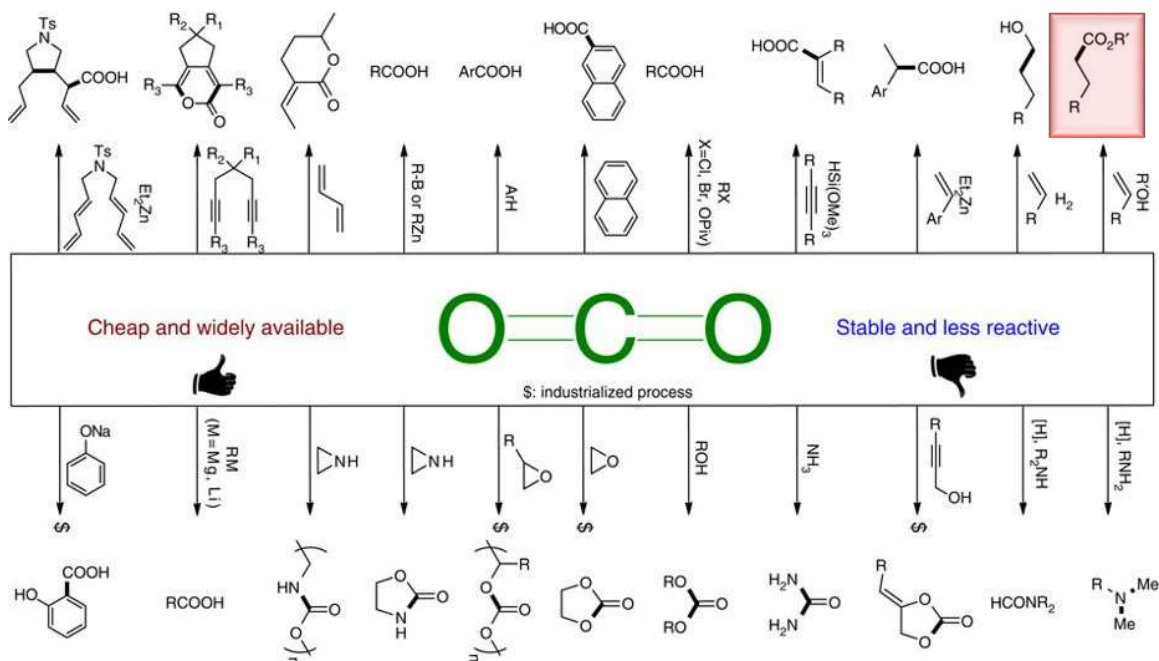


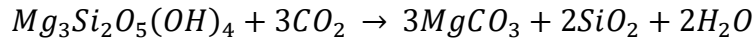
Figure 1.13 - Representative examples using CO₂ as C1 building block in organic synthesis. Along with the rapid development of organometallic chemistry and catalysis, various types of efficient CO₂ transformations have been discovered in the past decades. However, in general, the substrates' scope and efficiency of these reactions are still limited due to the requirement of reactive agents for CO₂ activation. As a result, only a few processes have been industrialized until now (marked by \$).⁵⁰

1.3.2 Applications of CDU

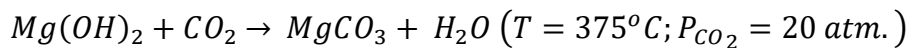
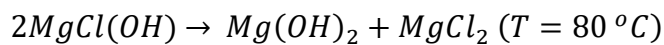
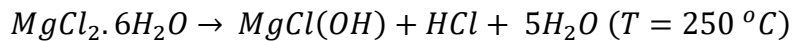
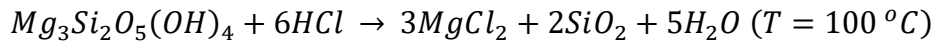
1.3.2.1 Mineral Carbonation

Mineral carbonation is a process where CO₂ is reacted with metal oxides to form carbonates. Calcium and magnesium carbonates are poorly soluble in water and are environmentally harmless minerals that could provide a permanent storage solution for CO₂. Mineral carbonation encompasses a series of reactions that can take place in a single or a multi-step process, in a single-step the extraction of the metal from the mineral matrix and the carbonate precipitation can occur

simultaneously in the same reactor at high pressure. This can take place in a dry or aqueous environment, as follows.⁵¹



In a multi-step process, first, the metal is separated from the mineral matrix, and then the metal in hydroxide form is obtained and reacted with CO₂ to form a carbonate, as shown below.



Some of the advantages of the use of this method include:

- leak-free fixation with no need for long-term monitoring;
- The large potential capacity of CO₂ fixation.⁵¹

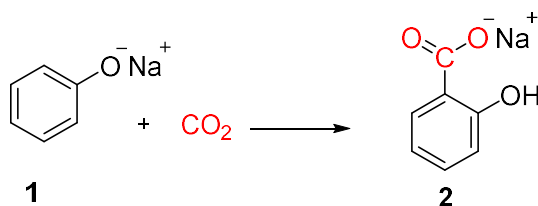
1.3.3 Biofuel from Microalgae

By cultivating microalgae under CO₂, it can be used for biofuel production, since microalgae need CO₂ to complete their photosynthesis. Cultivation of microalgae can be carried out in open raceway ponds and photo-bioreactors, however, a large area is required, and it is still difficult to control the production. The biomass produced needs to be dried and then converted to biofuel through thermochemical or biochemical conversion, including gasification, liquefaction, and pyrolysis.⁵² Microalgae tolerates high CO₂ content in feeding air streams (CO₂ content 5–15%), In comparison to terrestrial plants, which normally absorbs CO₂ in the order of 0,03 to 0,06% which.⁵³

1.3.4 Carboxylation Reactions

A carboxylation reaction is a reaction in which carbon dioxide is fixed to another carbon atom to form a new carbon-carbon bond. There are two purely chemical

carboxylations, which are very common. One is the reaction of an organometallic compound with CO₂ to form a new carbon-carbon bond, in which the carbon-oxygen group of the CO₂ is presumably inserted between the carbon and the metal of the organometallic compound. The other type involves the carboxylation of the metal salt of an enol or phenol. For instance, sodium phenolate **1**, when treated with carbon dioxide at elevated temperatures and pressure will produce the salt, sodium salicylate **2** (Scheme 1) used in the production of aspirin.⁵⁴

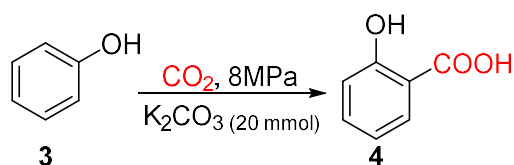


Scheme 1 Carboxylation of a metal salt of phenol.⁵⁴

Research and development of technologies for both sequestration and utilisation of carbon dioxide are urgently necessary. Today there are roughly 750 billion tons of CO₂ in the atmosphere and a net of 13,000 million tons of more carbon dioxide is added annually. The challenge of addressing carbon dioxide is that it is diluted and represents only 0.04% of our atmosphere.⁵⁵ Also CO₂ has high thermodynamic stability ($\Delta G^{\circ} = -396$ kJ/mol) which demands for an energy-intensive activation to drive the desired transformation. Possible energies source that could to be exploited for this purpose includes high temperature, extremely reactive reagents, electricity, pressure or even energy from photons.

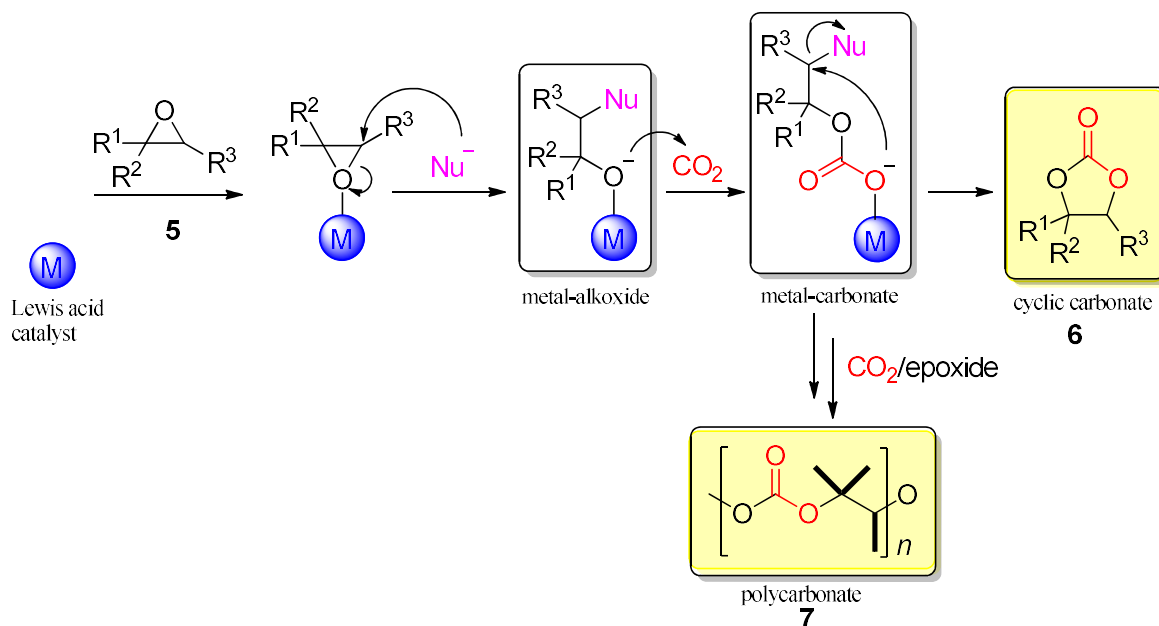
The use of cheap and abundant carbon dioxide as chemical feedstock has been widely investigated as an alternative pathway to close the carbon cycle.^{54,56–58} One of the largest uses of carbon dioxide is for the production of urea, which is one of the most important nitrogen fertilizers in the world.⁵⁹

Salicylic acid **4**, a common medication to help remove the outer layer of the skin was directly synthesized by Takayuri and co-workers from phenol **3** and CO₂ in the presence of potassium carbonate as catalyst.⁶⁰ (Scheme 2)



*Scheme 2 Carboxylation of phenol.*⁶⁰

Formation of cyclic carbonates **6** using carbon dioxide is also another area of research that is growing rapidly^{61–65} due to their applications as polymer precursors, fuel additives or electrolytes in batteries, and their uses as aprotic high-boiling point solvents,⁶⁶ cyclic carbonates can be obtained by direct coupling between CO₂ and oxiranes **5**, also offering a route to produce polycarbonate **7**. Oxiranes are activated by interaction with a Lewis acid (a catalyst which acts as an electron pair acceptor to increase the reactivity of the substrate) through M–O coordination patterns, followed by a nucleophilic attack and subsequent ring-opening, key steps of carboxylation of epoxides are shown in Scheme 3.⁶²



*Scheme 3 Key steps for the coupling of CO₂ and oxiranes to yield cyclic carbonate or polycarbonate.*⁶²
Nu = nucleophile, M = metal complex

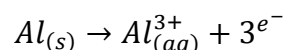
CO₂ can also be converted to fuels, fuels have high energy content, is easy to transport and store, nowadays liquid fuel is majority petroleum-based and contributes with 14% of CO₂ emission if consider only transportation.⁴¹ Direct hydrogenation is a promising alternative, carbon dioxide can be converted into fuels by reduction to methanol⁶⁷ or methane.⁶⁸

1.3.5 Electrochemical Reactions

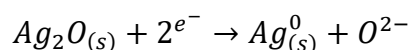
An electrochemical reaction is any process either caused or accompanied by the passage of an electric current and involves in most cases the transfer of electrons between two substances.⁶⁹

Under normal conditions, the chemical reaction is followed by liberation or absorption of heat, however, when allowed to proceed in contact with two electronic conductors and separated by conducting wires, this liberates electrical energy forming an electrical current. Conversely, the energy of an electric current can cause or accelerate any chemical reaction that would not normally occur spontaneously.

The electrochemical cell is defined as two or more half-cells in contact with a common “electrolyte”, it leads to a *redox* reaction which involves a change in oxidation states of the elements. In one of the cells, called the *anode*, oxidation will occur as follows (using aluminium as a representative example).



In the other cell called the *cathode*, the reduction will proceed as follows:



The oxidation and reduction reaction must occur concurrently because the electrons released in the oxidation process will be required in the reduction process. Faraday’s law, states that the rate of electrochemical reaction at an electrode (expressed in terms of gram moles per second per square centimeter of electrode surface) is directly proportional to the current density (expressed in amperes per square centimeter) - i.e. current flowing through the cell divided by the electrode surface area.⁵⁴

Faraday’s first law: The number of moles of a species formed at an electrode during electrolysis is directly proportional to the quantity of electricity transferred at that electrode. Quantity of electricity refers to electrical charge, typically measured in coulombs, which can be defined as:⁷⁰

$$m = (QF) \cdot (Mz) \qquad \text{eq. 1.1}$$

Where m is the mass of the substance altered at an electrode, Q is the total electric charge, $F = 96.485 \text{ C mol}^{-1}$ is the Faraday constant (the amount of charge required to convert 1 mol of substance),⁷¹ M is the molar mass of the substance and z is the valance number of ions of the substance (electrons transferred per ion).⁷⁰ As $Q = I \cdot t$ (I = current and t = time) the *eq 1.1* can be replaced by:

$$m = (I \cdot tF) \cdot (Mz) \quad \text{eq. 1.2}$$

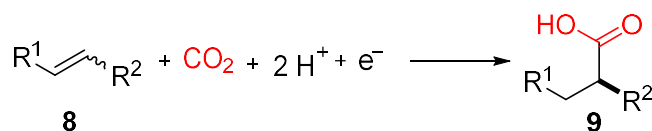
Note that M , F , and z are constants, so that the larger the value of I or t the larger will m be.

1.3.6 Electrocarboxylation

As explained above, carboxylation or carbonation is a chemical reaction that involves the introduction of carbonyl group (C=O) into organic and inorganic compounds to form products such as aldehydes (-CHO), carboxylic acids (R-COOH), esters (RCO₂R), alcohols (-OH) etc...⁷² Electrocarboxylation is the carboxylation reaction where electrons are generated to reduce electrochemically/catalytically carbon dioxide. Solvents with a high solubility for CO₂, such as DMF (*N,N*-Dimethylformamide), are used in the non-aqueous electrochemical reduction of CO₂. The CO₂ concentration in DMF is about 20 times higher than in aqueous solutions, in propylene carbonate and methanol the CO₂ solubility is about eight and five times higher, respectively.⁷³

The number of reports published on the electrocarboxylation of alkenes and alkynes has been increasing substantially.⁷⁴⁻⁷⁷ A carboxylic acid is an organic compound that contains a carboxyl group RC(=O)OH with the general formula of R-COOH, with R referring to the rest of the molecule.⁷⁸ Carboxylic acids are widely used in industry, the global market in 2017 was of 14 billion USD and is forecasted to reach 19 billion USD by 2023. They make up a series of fatty acids which are extremely good for human health such as omega-6 and omega-3. They are also used in the food industry to produce soft drinks, and in the pharmaceutical industry to produce drugs such as aspirin.⁷⁹ The potential of carboxylic acids on the global market and the possibility of synthesizing it using CO₂ at atmospheric pressure and room temperature are one of the reasons of the products produced in this research.

The formation of valuable carboxylic acids by reduction processes of CO₂ and fixation into organic compounds is claimed as means of an energy-efficient method, where only one or two electrons per CO₂ are required as shown in Scheme 4 for olefins **8** where CO₂ is incorporated to form its corresponding carboxylic acid **9**.⁷⁷

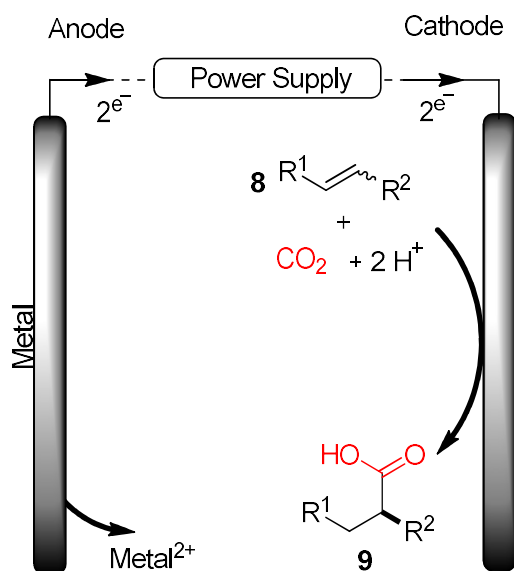


Scheme 4 - General carboxylation of olefins.⁷⁷

1.3.6.1 Use of Sacrificial Electrode in Electrocarboxylation

The majority of researchers have been focused on the fixation of CO₂ in an electrochemical process using sacrificial anodes such as magnesium or aluminium^{80,81} where high efficiency has been demonstrated.

Anodic and cathodic reactions are necessary in all electrocarboxylation process in order to close the electron cycle, an oxidation reaction at the anode is a must to supply electrons to the cathode where the reduction of carbon dioxide will take place, Scheme 5 exemplifies an electrocarboxylation of alkene **8** to form carboxylic acid **9** using a sacrificial anode.



Scheme 5 Overview of electrocarboxylation setup using a sacrificial anode.⁷⁷

Although the use of a sacrificial electrode is widely employed,⁷³ its oxidation leads to the dissolution of the metal as metal ions, and the gradual consumption of the

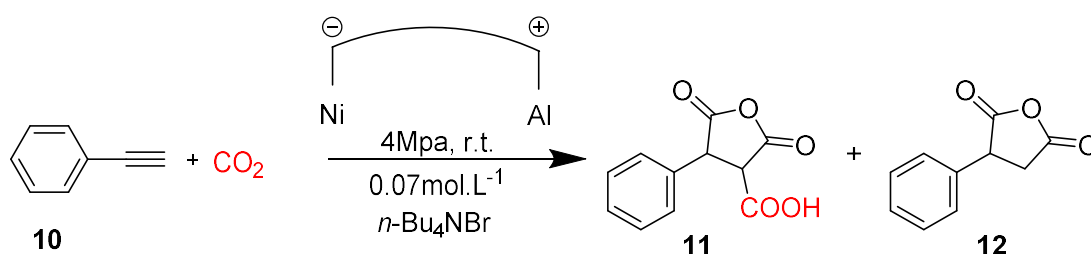
material represents not only an extra cost for industrial application but hinders its use in continuous processes. From the viewpoint of green chemistry, the resulting oxidized metal contaminates the reaction mixture, hence besides the environmental liabilities, an additional purification process is necessary to deal with the waste.^{77,82}

As an alternative to a sacrificial electrode, there have been some researchers who employed what is called sacrificial reagent or reducing agent which donates electron in a redox reaction. The use of tetraalkylammonium salt, for instance, is considered as a sacrificial process since its ions are released into the solution and the salt is consumed during the process.

De Vos and co-workers reported a net incorporation of carbon dioxide in conjugated dienes using tetraethylammonium trifluoroacetate working as either supporting electrolyte and to acetoxyated a conjugated diene, which is also a substrate for cathodic carboxylation.⁸³

1.3.6.2 Electrocarboxylation of Alkynes

The electrochemical fixation of CO₂ into unsaturated hydrocarbons to form new carbon-carbon bonds is an interesting topic because it could afford valuable fine chemicals. Chuanhua and co-workers⁸⁴ have produced saturated carboxylic acid **11** and phenylsuccinic anhydride **12** through electrolysis of phenylacetylene **10** with CO₂ in presence of common metal salts as catalysts (Scheme 6) and Al was used as a sacrificial electrode. This work has shown that the catalyst and electrode play an important role in the conversion achieving up to 70% yield of carboxylic acid **11** on nickel cathode when employing CuI as catalyst.



Scheme 6 Carboxylation of phenylacetylene to form its corresponding carboxylic acid and phenylsuccinic anhydride.⁸⁴

Table 1.2 shows the utilisation of different metal salts and their yield in the experiment described above.⁸⁴

*Table 1.2 Effect of various metal salt catalysts on the electrocarboxylation of phenylacetylene.*⁸⁴

Catalyst ^a	Yield of 11 ^b /%	Yield of 12 ^b /%	η ^c /%
CuI	70	27	73
FeCl ₃	61	30	68
CuCl ₂	52	26	59
FeCl ₂	50	27	58
Pd(OAc) ₂	31	5	27

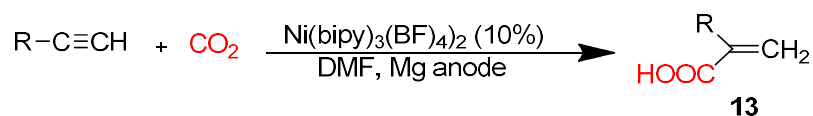
*Experimental conditions: phenylacetylene (2 mmol), DMF (35 mL), CO₂ 4 MPa, room temperature, *n*-Bu₄NBr (2.5 mmol), electricity (4 F•mol⁻¹), current density 10 mA•cm⁻², Ni cathode, and Al anode.*

^a Metal salt catalyst (0.1 equiv.);

^b Total isolated yield based on phenylacetylene and the yield of **11** and **12** were determined by GC/MS;

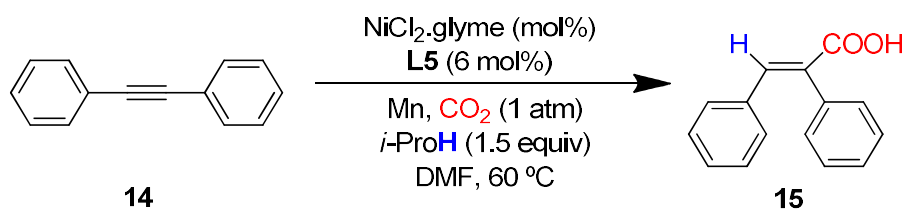
^c $\eta = Q1/Q2$ (η : Current efficiency; Q1: Quantity of electricity consumed in forming product; Q2: Total electricity quantity in the electrolysis).

Nickel complexes have proved in many reports to be an excellent catalyst for carbon dioxide fixation in alkynes but the product formation rely heavily on the nature of the ancillary ligands.^{85–87} In 1989 Duñach and co-workers catalyzed the reaction of carbon dioxide with alkynes to yield selectively α -substituted acrylic acid **13** (Scheme 7) employing Ni(bipy)₃(BF₄)₂.⁸⁶ A magnesium rod was employed in this reaction as a sacrificial anode.



*Scheme 7 Electrocarboxylation of alkyne to form alpha-substituted acrylic acid.*⁸⁶

Later Xueqiang and co-workers found out cocktail consisting of NiCl₂.glyme (5 mol%), neocuproine (**L5**, 6 mol%) and *i*-PrOH (1.5 equiv) in the carboxylation of diphenylacetylene **14** to yield α -phenylcinnamic acid **15** with 94% isolated yield (Scheme 8).⁸⁸ In most of the formation of carboxylic acid through carboxylation process, the source of proton is still not completely clarified, in this study *i*-PrOH was added to guarantee this source.

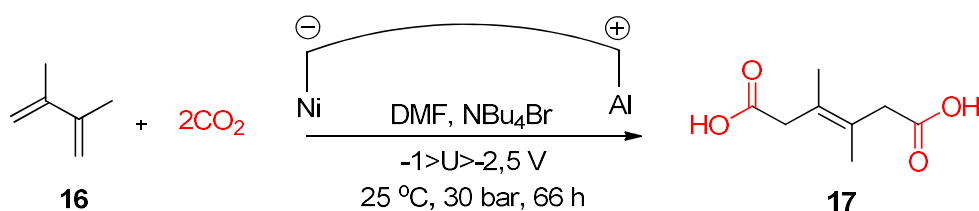


Scheme 8 Carboxylation of diphenylacetylene employing nickel complex.⁸⁸

1.3.6.3 Electrocarboxylation of Unsaturated Hydrocarbons

Nickel was also shown to be effective as a cathode, in the electrocarboxylation of 2,3-dimethyl-butadiene **16** reported by Steinmann and co-workers.⁸⁵ This reaction revealed a highly activated process around the potential of -1.3 V and a change in mechanism around the potential of -2.3 V.

Steinmann explored this reaction using a Ni foam cathode and Al as a sacrificial electrode, although it was necessary to run the experiment under high pressure, hexadienoic acid **17** was obtained (Scheme 9).⁸⁵



Scheme 9 Electrocarboxylation of 2,3-Dimethyl-butadiene.⁸⁵

The various potentials applied in this work provides evidence of selectivity and side product formed, for instance, traces of oxalate were formed at very low potential while carbonate and CO are formed at a high potential as they are basically formed on the metal surface and not through a “free” CO_2 radical.⁸⁵

1.3.6.4 Electroreduction of CO_2 to Form Formic Acid

Formic acid (HCOOH) is the simplest carboxylic acid, it can be formed by the composition of H_2 and CO_2 or decomposed catalytically into hydrogen and carbon dioxide according to the equation as follow:



This reversible process makes formic acid a promising energy storage and as a liquid, could provide a means of H_2 transport and delivery to H_2 refueling stations

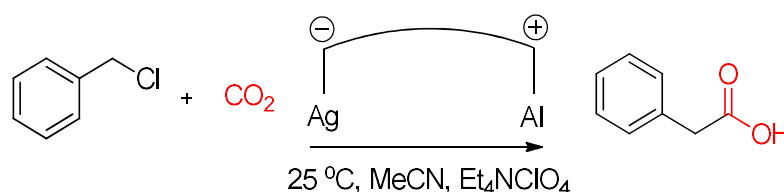
using existing infrastructure, but nowadays, the principal use of formic acid is as a preservative and antibacterial agent in livestock feed.⁸⁹

Xiangjing and co-workers electrochemically reduced carbon dioxide to formic acid in ionic liquid [Emim][N(CN)₂]/water system. The water was introduced to facilitate the high reaction rate by providing protons (H⁺) via water electrolysis at the counter electrode.

In this experiment by employing a [Emim][N(CN)₂] concentration of 0.5 M, the maximum faradaic efficiency of 81.9% was achieved for the production of formic acid from CO₂ electrolysis at a fixed potential of -1.2 V vs RHE (Reversible Hydrogen Electrode).⁹⁰

1.3.6.5 Electrocarboxylation of benzyl chlorides

Carboxylation of benzyl chlorides using silver cathode and aluminium sacrificial anode in CO₂-saturated solvent was reported by Gernarro and coworkers.⁹¹ The reduction potentials of PhCH₂Cl depend on electrode material and it was found that, compared to other cathode materials, the reduction of benzyl chlorides was lowered when silver cathode was used, besides de fact that it occurs at potentials more positive than E_p (peak potential) of CO₂ so the carboxylation of benzyl chlorides takes places with very good yield (94%) without any interference from reduction of CO₂.



Scheme 10 Electrocarboxylation of benzyl chlorides employing silver cathode and aluminium sacrificial anode.⁹¹

1.3.6.6 Electrocarboxylation of Alkenes

Probably one of the first work of electrocarboxylation of alkene was reported by Vasil'ev and coworkers in 1991.⁹² various long and short-chain dicarboxylic acid were obtained by electroreduction of CO₂ in DMF in the presence of acceptors of radical anions. The introduction of ethylene as an acceptor of CO₂ revealed the formation of succinic acid, adipic acid, suberic acid, and oxalic acid. This report

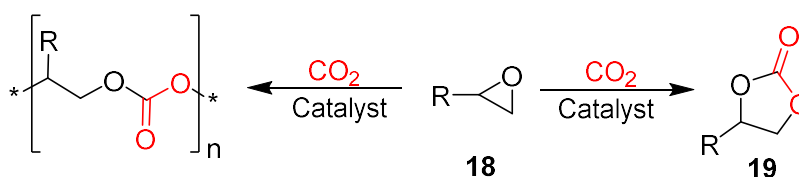
also showed that the selectivity and current efficiency were influenced by experiment parameters, an increase of current density, for instance, lowers the current efficiency with respect of dicarboxylic acids which was increased on the other hand, when the pressure of ethylene is increased.⁹²

1.4 Previous Buckley Group Findings

As mentioned in the introduction, the Buckley group has achieved several improvements in electrochemistry increasing the conversion yield and reducing the environmental impact of the experiment. Overall the electrocarboxylation of organic substrates were followed by the formation of a precipitate at the anode which was overcome by replacing the electrode material by a stable carbon rod and further optimization brought the addition of reducing agent, these achievements will be explained later in this section.

1.4.1 Electrosynthesis of Cyclic Carbonates from Epoxides and Atmospheric Pressure Carbon Dioxide.

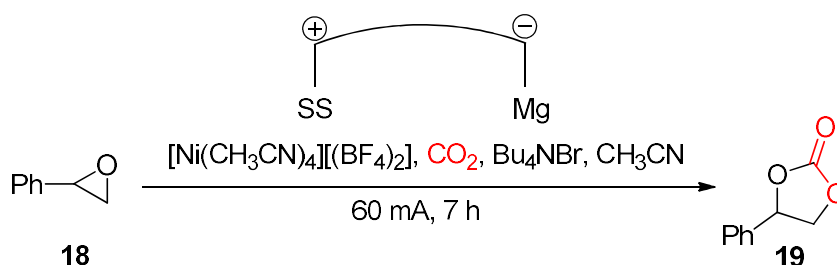
The production of polycarbonates and cyclic carbonates **19** from epoxides **18** and CO₂ is an important approach due to the large range of manufacturing products such as solvents, paint-strippers, biodegradable packaging and other chemical industry including commercial application, however, current methods show some drawbacks such as the use of high-energy input, high pressure and high temperature (Scheme **11**).⁶



Scheme 11 Current processes for CO₂ incorporation into epoxides.

1.4.2 Electrocarboxylation of Epoxides: Catalysed by Ni(II) Complexes

In order to improve the current processes of synthesis of cyclic carbonates **19** by incorporating CO₂ into epoxide, the substrate **18** was catalyzed by [Ni(CH₃CN)₄][(BF₄)₂] in acetonitrile at atmospheric pressure (Scheme 12).

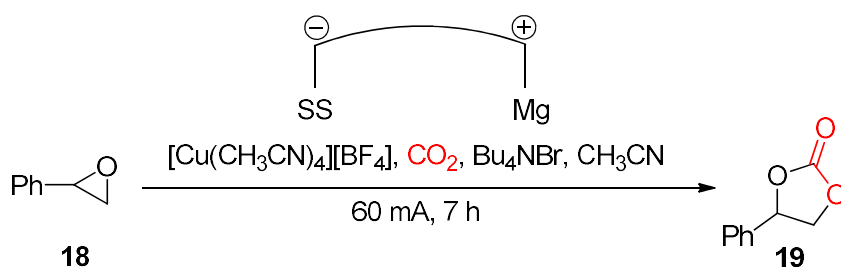


Scheme 12 Electrocarboxylation of styrene oxide employing Ni(II) Complex

The electrochemical setup involved the use of magnesium anode, stainless steel cathode and Bu₄NBr supporting electrolyte (2 eq.), at constant current: 60 mA (7 h), constant CO₂ flow (471 mL·min⁻¹), in the presence of the nickel catalyst (10 mol%) followed by heating at 50 °C (12 h), forming cyclic carbonate **19** in moderate conversion (50%).⁵⁶

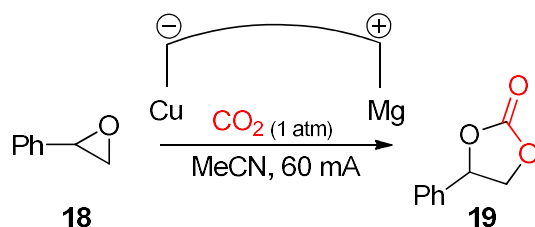
1.4.3 Electrocarboxylation of Epoxides: Catalysed by Cu(I) Coordinate Complex

Due to the poor conversion of cyclic carbonate employing nickel catalyst, In the same research involving the electrocarboxylation of epoxides,⁵⁶ the nickel complex was switched by copper catalyst [Cu(CH₃CN)₄][BF₄], which was cheaper and less toxic when compared to some nickel complexes, it was used in the carboxylation of epoxide **18** yielding cyclic carbonate **19** reaching 75% conversion (Scheme 13). The electrocarboxylation was conducted in acetonitrile employing magnesium anode, stainless steel cathode and Bu₄NBr supporting electrolyte (2.4 eq.), at a constant current of 60 mA (7 h), constant CO₂ flow (471 mL·min⁻¹) in the presence of a copper catalyst (10 mol%).



Scheme 13 Electrocarboxylation of styrene oxide employing Cu(I) complex.

Buckley and co-workers have achieved high conversion of epoxide **18** to cyclic carbonates **19** through electrochemical incorporation using a copper cathode/magnesium anode combination in a single cell under atmospheric pressure applying a current of 60 mA (Scheme 14).



Scheme 14 Use of Copper cathode/magnesium anode in electrochemical reaction to incorporate CO₂ into cyclic carbonate

This work also showed that the type of electrode played an important role when referring to conversion, for instance only 5% was achieved with copper cathode/zinc anode and above 99% using copper cathode/Magnesium anode (Table 1.3).⁶

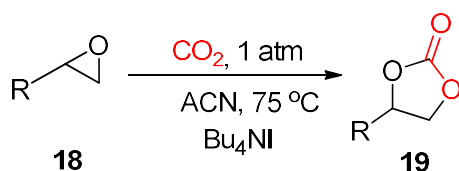
Table 1.3 Electrode screening, conversion of epoxide using different electrodes.

Entry	Cathode	Anode	Conv. (%) ^a
1	Cu	Mg	>99
2	Steel	Mg	75
3	Graphite	Mg	80
4	Cu	Al	75
5	Cu	Sn	10
6	Cu	Zn	5

^a Conversion evaluated from the ¹H NMR spectrum by the integration of epoxide vs. cyclic carbonate peaks.¹²²

1.4.4 Carboxylation of Epoxides Without Electrodes

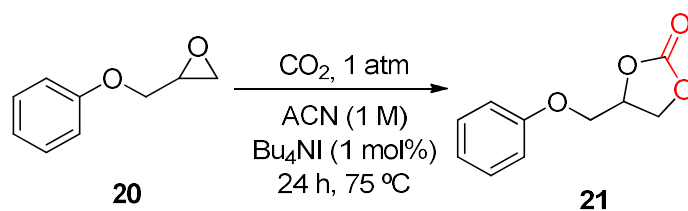
In order to investigate the reaction under control conditions, the carboxylation was also carried without electrodes. At low concentration of epoxide, no conversion was observed in this experiment, therefore, the reaction only takes place at high concentration. The epoxide **18** (1M) was added to a solution of supporting electrolyte (Bu₄NI) in acetonitrile (1:1) and heated to 75 °C under constant CO₂ flow at atmospheric pressure, after 48 h the respective cyclic carbonate **19** was formed (Scheme 15). In the reaction employing the substrate fluorostyrene oxide, for instance, the conversion reached 92%.⁹³ Among the substrates, chlorostyrene oxide, allyl glycidyl ether, and 1,2-epoxyhexane were tested resulting conversions which vary from 42% to 92%.



Scheme 15 Carboxylation of epoxide without electrode.
R=Fluorobenzene, 92.1% conversion
R=Chlorobenzene, 70.4% conversion
R= 3-methoxypropene, 7.4% conversion
R= n-butane, 41.8% conversion

The influence of the molarity of the catalyst (Bu₄NI) on the performance of cyclic carbonate formation was also studied. Phenyl glycidyl ether **20** (1.0 mmol) as starting material was added into a solution of Bu₄NI in MeCN (acetonitrile) to form 4-(Phenoxyethyl)-1,3-dioxolane-2-one **21**. (Scheme 16)

The concentrations studied varied from 0.1 M to 2.0 M of Bu₄NI in MeCN (Table 1.4). The conversion employing 0.1 molar reached only 12.7%, however, when increasing the concentration to 2.0 molar the conversion reached 100%. The experiment concludes that the higher the concentration of the catalyst the higher the conversion to carbonate. However, at a concentration of 2.0 molar, Bu₄NI was not completely soluble in acetonitrile at 75 °C. This process was later developed into a catalytic system employing as little as 1 mol% of Bu₄NI as a catalyst.⁹³



Scheme 16 - Carboxylation of Phenyl glycidyl ether without electrode

Table 1.4 Molarity study of the cyclic carboxylation of Phenyl glycidyl ether reaction.⁹³

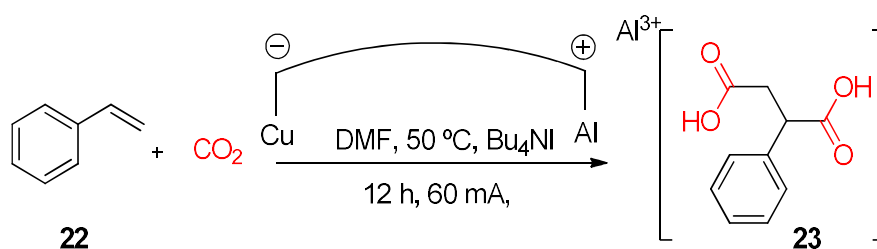
Entry	MeCN:Bu ₄ NI (mol)	Carbonate % (24 h)
1	0.1	12.7
2	0.5	85.0
3	1.0	93.5
4	2.0	100

Although this method overcomes the issue related to the use of the sacrificial electrode, the energy input to keep the reaction at 75 °C during the reaction is relatively high and needs to be taken into consideration.

1.4.5 Development of a Non-sacrificial Electrode System

Volodymyr Tabas previously investigated the flow of electrons and the mechanism of the electrochemical reaction. An initial carboxylation test of styrene **22**, aluminium anode as a sacrificial electrode and copper as a counter electrode at 60 mA for 12 h in MeCN yielded the corresponding dicarboxylic acid **23**. (Scheme 17)

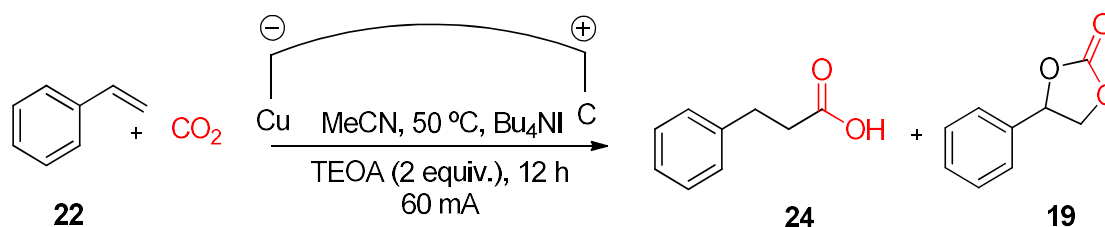
As expected, the target molecule was reduced at the cathode while complimentary oxidation took place at the anode. A corrosion process occurred with the aluminium anode itself to form free metal ions, which provides electrons to the system. The replacement of the aluminium anode by carbon would cease the oxidation of the electrode due to its stability, therefore an electron donor was required to provide an effective substitute.



Scheme 17 - Carboxylation of styrene employing Al as a sacrificial electrode

By consulting the literature, Tabas found out that TEOA (triethanolamine) would be a promising reducing agent and should be able to succeed as an electron donor.

The reaction was then repeated but at this time the aluminium anode was replaced by carbon followed by addition of TEOA (2 equiv.). The experiment worked but not as expected, no dicarboxylic acid was observed but instead, the carboxylation was achieved regioselectively at the terminal β -carbon and as a result monocarboxylic acid 3-phenylpropanoic acid **24** was synthesized followed by formation of cyclic carbonate **19** in a 3:1 ratio, with >99% conversion of the substrate (Scheme 18). Further optimization of this reaction achieved 70% yield of **24** and eliminated the formation of **19**.



Scheme 18 Electrocarboxylation employing TEOA as reducing agent

1.4.5.1 Photochemical Reduction of CO₂

Photochemistry is the branch of chemistry concerned with the chemical effects of light, it naturally occurs through photosynthesis and supplies carbon for all organic compounds on Earth. In chemistry generally, this term is used to describe a chemical reaction caused by absorption of ultraviolet (wavelength from 100 to 400 nm), visible light (400 to 750 nm) or infrared radiation (750 to 2500 nm).⁹⁴ Photocatalytic reduction of CO₂ into CO or formic acid are inefficient or require the use of sacrificial electrode or reducing agent. Solar energy can be used directly as photochemistry or indirect which would require a device to convert solar energy into another mean of energy.

Figure 1.14 represents an experiment conducted by Buckley's group where cyclic carbonate was formed employing Mg sacrificial electrode in a single compartment cell under the CO₂ balloon. In this experiment, a photovoltaic panel was used to convert sunlight into electricity which was then used to drive the reaction.



Figure 1.14 Carboxylation of olefins using solar panel. (Buckley B,R.)

Mul and his coworkers have carefully investigated carbon sources in the photocatalytic CO₂ reduction with copper oxide promoted TiO₂ (Cu(I)/TiO₂),⁹⁵ they reported various metals deposited on TiO₂ accelerating the reduction of CO₂, and that Pd-deposited on TiO₂ (Pd-TiO₂) working as the most efficient photocatalyst for producing CH₄.⁹⁵

Tatsuto and co-workers⁹⁶ reported photocatalyst formation of CH₄ under CO₂ and N₂ showing high formation rate of CH₄ using Pd(2%)-TiO₂, when compared it with nitrogen still showed a little conversion but stopped after 4 h. (Figure 1.15)

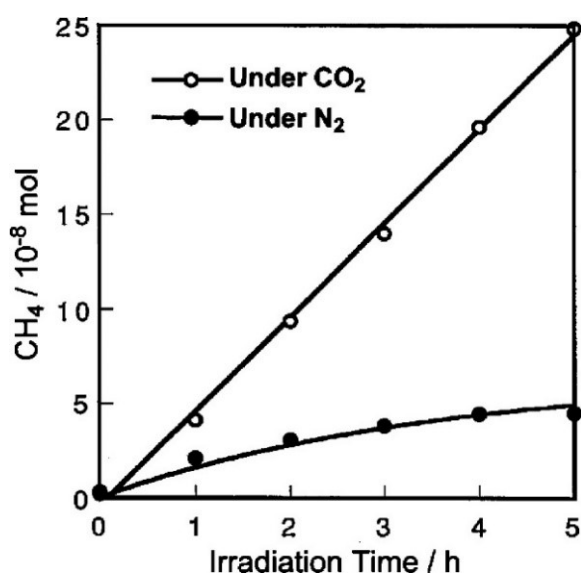


Figure 1.15 Photocatalytic CH₄ formation by Pd(2%)-TiO₂ under CO₂ and N₂ atmospheres.⁹⁶

There has been a significant effort to develop a sustainable way to convert CO₂ into an organic product and mimic nature through artificial photosynthesis, it seems to be the dream for a few scientists. Sodium acrylate is commonly used as a monomer in the production of superabsorber polymers and theoretically could be synthesized from CO₂ and ethylene (Figure 1.16, equation “b”) but yet, represents a very challenging reaction.

The reductive methylation of more widely available arenes to generate toluene and xylenes is also a green alternative and highly interesting (Figure 1.16, equation “d”).⁵⁰ NASA recently launched a big challenge of converting CO₂ into sugar (Figure 1.16, equation “a”) and is offering USD 1 Million for whoever succeeds.⁹⁷ So, photocatalytic or electrocatalytic could be a way to achieve this reaction and make those dreams come true.

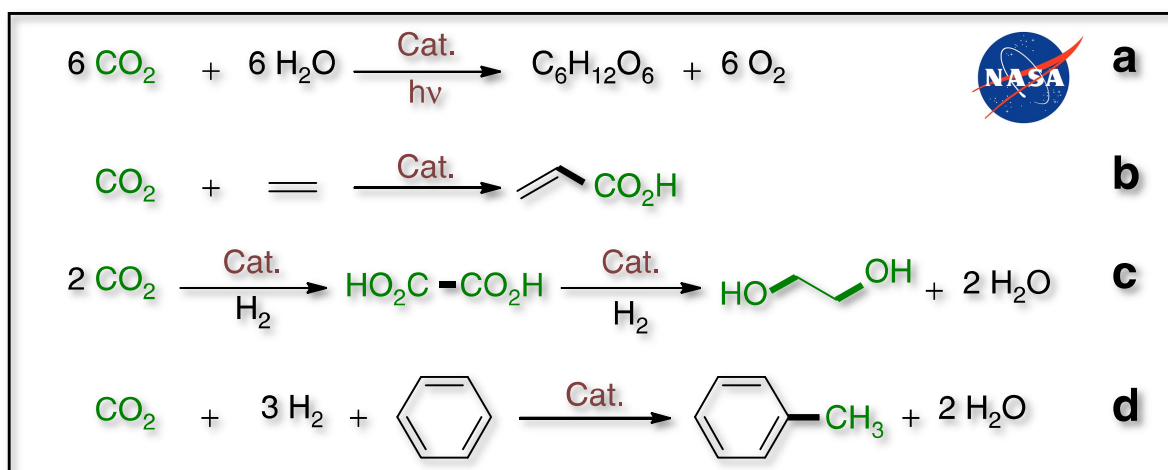


Figure 1.16 (a) Photosynthesis reaction process. (b) Direct synthesis of acrylic acid from ethylene and CO₂. (c) Ethylene glycol synthesis via reductive coupling of CO₂. (d) Reductive methylation of benzene using H₂ and CO₂.⁵⁰

1.5 Plasma Technology

1.5.1 Introduction

Plasma is known as the fourth state of matter where part of the particles in a gas or a liquid are ionized. When the temperature of matter increases at a fixed pressure, its state changes from solid to liquid and from liquid to gas. In the gas state, the atoms of the gas move freely in random directions, but when the temperature further increases the atoms decompose into freely moving charged

particles. This occurs in equilibrium with the temperature of the ions or the bulk gas and is called the plasma state, where the main feature is the commonly charged particle density.

Furthermore, when a gas flow is exposed to an electric field, the free electrons are accelerated acquiring Kinetic energy. If the gas has either low pressure or if the electric field is high enough then a dissociation upon collision of the electrons to a certain point occurs, where the gas becomes electrically conductive. At this point, the non-equilibrium plasma and discharge phenomena are seen in the form of spark or lightning.⁹⁸ Following dissociation of the gas molecule, there is also radical dissociation which is produced as a by-product. The type of radical produced will rely on the gas phase present, for example in the presence of hydrogen, the radicals are atomic hydrogen (H^+).⁹⁸

Plasma encompasses the majority of matter in the universe; for instance, the sun is made of plasma, the majority of stars are made of plasma, lightning is also a form of plasma occurring in nature as well as the Aurora Borealis. The Aurora Borealis is formed at near-space altitude, the Earth's magnetic field interacts with the charged particles from the Sun. The particles which are denser in the pole region, are trapped by the magnetic field causing ionization of neutral particles in the atmosphere emitting light of the aurora (Figure 1.17).⁹⁹



Figure 1.17 Northern lights in Iceland. (Picture taken by A.Randi at Aurora Reykjavik Exhibition Center – Iceland, 2018)

Although plasma occurs naturally it can also be effectively made-man and is already employed in industry as light source, in material processing, nuclear fusion, propulsion of spacecraft and much more. These forms of equilibrium plasma are very hot in the order of 10.000 K but can reach up to 20.000 K. In the coatings industry, for instance, powder material is introduced into a plasma jet where is melted and accelerated towards a surface to be coated, the droplets rapidly solidify and form a deposition layer. On the contrary, non-equilibrium plasma can be as cold as room temperature.¹⁰⁰ Non-equilibrium atmospheric pressure plasmas are non-thermal meaning that the temperature of the electrons is not in equilibrium with the temperature of the ions or bulk. In the laboratory, discharges are electrically driven heating the mobile electrons and the ions efficiently exchange energy with the background gas. Hence $T_e > T_i$ where T_e is the temperature of electrons and T_i is the temperature of ions.⁹⁸

One of the main features that make plasma a very interesting technique for applications in chemistry is the ability to generates active species such as, free radicals and metastable species allowing reactions to occur at a much lower temperature than in conventional methods.¹⁰¹ The radicals formed dissolve in the media altering its composition, molecules have electrons removed or added in presence of plasma making them positively or negatively charged, for instance in the presence of air, the plasma formed can produce NO, HNO₂, HNO₃, H₂O₂, etc. In solution, Nitric Oxide reacts with other species to form nitrogen dioxide (NO₂) which in the presence of aqueous solution dissolves to form nitrous and nitric acid.¹⁰²

Another big advantage of plasma is the fact that the discharge can operate at atmospheric pressure, which discards the necessity of expensive and complex vacuum system. This results in a reactor or plasma jet that is easy and simple to design. Although this field is still in its infancy, there are several different types of plasmas and applications. Varying gas composition, electrode, wall configuration, and electric characteristic, including DC (Direct Current) or AC (Alternating Current) and high-frequency power supply, more energy can be channeled into specific excitation and reactions. Table 1.5 illustrates some but not all-important non-thermal plasmas along with their energization and typical application.¹⁰³

Table 1.5 Overview of non-thermal discharge types and their most common applications.¹⁰³

Type of plasma	Gap (mm)	Plasma	Energization	Typical Application
Corona	10 - 300	Filaments	Pulsed/DC	Gas cleaning/Dust precipitation
Corona with barrier	10 - 30	Filaments	Pulsed	Gas and water cleaning
Barrier with packed bed	3 - 10	Filaments	AC	Chemical conversion
Plates with barrier	1 – 5	Difuse	AC	Surface treatment
Surface discharge	1 – 5	Filaments	AC	Surface treatment
Plasma jet	0.5 - 10	Diffuse	AC/RF	Local surface
Microdischarge	0.1 - 1	Diffuse	AC/RF	Chemical conversion

1.5.2 Gas Breakdown

In 1889 Frederich Paschen published what is today known as Paschen's law where the breakdown voltage (the voltage necessary to start a discharge or electric arc) between two electrodes is a function of gap distance in metres d and pressure in Pascals p of the medium gas, A is the saturation ionization in the gas at a particular E/p (Electric field/pressure) B is related to the excitation and ionization energies. The constants A and B were found to be constant for any given gas where $A = 112.50 \text{ (kPa}\cdot\text{cm}^{-1})$ and $B = 2737.50 \text{ V/(kPa}\cdot\text{cm}^{-1})$ which can be described as follows:¹⁰⁴

$$V = \frac{Bpd}{\ln(Apd) - \ln\left[\ln\left(1 + \left(1 + \frac{1}{\gamma_{SE}}\right)\right)\right]} \quad \text{eq. 1.3}$$

To fully understand this mechanism imagine a vacuum chamber without any plasma, when the voltage is applied across this tube free electrons will be released

which will be moving towards the anode, according to the density of the inner gas the electrons may collide with neutral atom, this is when the ionization begins creating positive ions which are accelerated towards a cathode, when the ions collide with the electrode, there is a finite probability γ that a secondary electron will be emitted which in turn, will ionize more neutral atoms, this process is called “secondary electron emission”. This secondary electron emission will depend on the cathode material, the state of the surface, the type of gas and electric field. Typically values of γ in discharge range from 0.001 to 0.1.¹⁰⁵ The positive ions will appear in a form or a stream or spark towards the cathode. When each electron creates enough ions to release a secondary electron from the cathode, the mechanism becomes self-sustaining and the breakdown occurs.

Paschen found that each type of gas responded at a different breakdown voltage due to its metastable state, also at normal pressure, the voltage needed to cause an arc reduced as the gap size was reduced but only to a certain point. As the gap was reduced further, the voltage required to cause an arc began to rise and again exceeded its original value. This lead to Paschen’s curve showed in Figure 1.18.¹⁰⁰

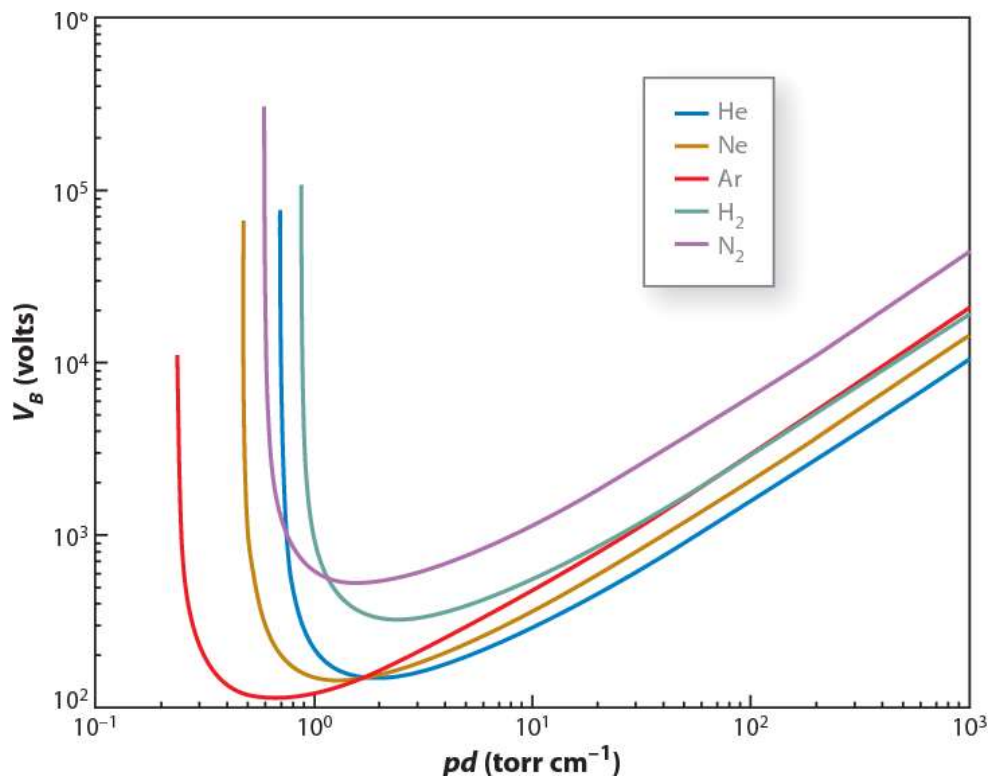


Figure 1.18 Paschen ionization curves obtained for helium (He), neon (Ne), argon (Ar), hydrogen (H₂), and nitrogen (N₂). V_B (breakdown voltage, in volts) as a function of pd (pressure·distance, in torr·cm⁻¹). Assumes parallel plate electrodes.¹⁰⁶

The Paschen's curve was developed studying the breakdown voltage of various gases between parallel metal plates varying the gas pressure and gap distance. The breakdown voltage is a minimum V_{\min} at some intermediate value $pd = (pd)_{\min}$.

At higher pressures (above a 760 torr) the breakdown characteristics of a gap are a function (generally not linear) of the product of the gas pressure and the gap length, usually written as $V = f(pd)$, where p is the pressure and d is the gap distance.

1.5.3 Plasma in and in Contact with Liquids

Probably the first work involving plasma-liquid interaction was published by Henry Cavendish in 1785, in his experiment, he reported the production of nitric acid by an electric spark in the air.¹⁰⁷ The interaction of plasma with liquids is an increasingly important topic in the field of plasma science and technology. The complex physical and chemical processes that occur when plasma contacts liquids offer a rich source of many short-lived chemical species that are critical for many applications. Biomedical, water treatment, chemical conversion, material science, and environmental remediation are all areas where non-thermal plasma in and in contact with liquid is bringing more attention each year. However, as discussed above, different design, electrical characteristic, and carrier gases are employed for each specific application. Essentially, non-thermal plasma in and in contact with liquids takes place in the gas phase, even when referring to plasma formation in liquid, it needs to be formed in bubbles. Initially, the high energy delivered by the power supply is first used to evaporate the liquid surrounding the high voltage electrode, generating gas bubbles, which in turn are ionized by the electric field. One of the possible mechanisms for the production of bubbles at the initial stage of electrical breakdown is through *Joule heating* by ionic conduction inside the liquid, the power of one joule heating can be calculated as $P = \sigma E^2$ where σ is the electrical conductivity of the liquid and E is the electrical field.¹⁰⁰ The temperature near the electrode is usually high due to energy dissipated in the liquid. Freedman and his colleagues are conducting some research on the formation of plasma in liquids without bubbles as it is promising to be more energy-efficient besides the

fact that the production of *in situ* active species reduces the transportation losses and eliminates storage and residual remediation of external chemical sources.¹⁰⁸

Discharge in and in contact with liquids can be subdivided into three different groups:

- a) Direct liquid phase discharge
- b) Discharge in the gas phase with a liquid electrode.
- c) Discharge in bubbles in liquids.

Non-thermal discharge direct in the liquid is known as a “direct liquid streamer” or “corona discharge”, generally, the pin-to-plate or plate-to-plate configuration is the most common. Discharge in the gas phase with liquid electrode typically consists of a metal pin suspended over a water electrode and can be excited by DC, arc or pulsed excitation, in this case, a current is transported through the water electrode by ions. For the bubble discharge in liquids, a pulsed excitation must be used as the displacement current and should be larger than the conduction current. If this is not the case, the liquid in the reactor will act as a pure resistor.¹⁰⁹

Figure 1.19 illustrates the reactor commonly designed for these three types of plasma generator.

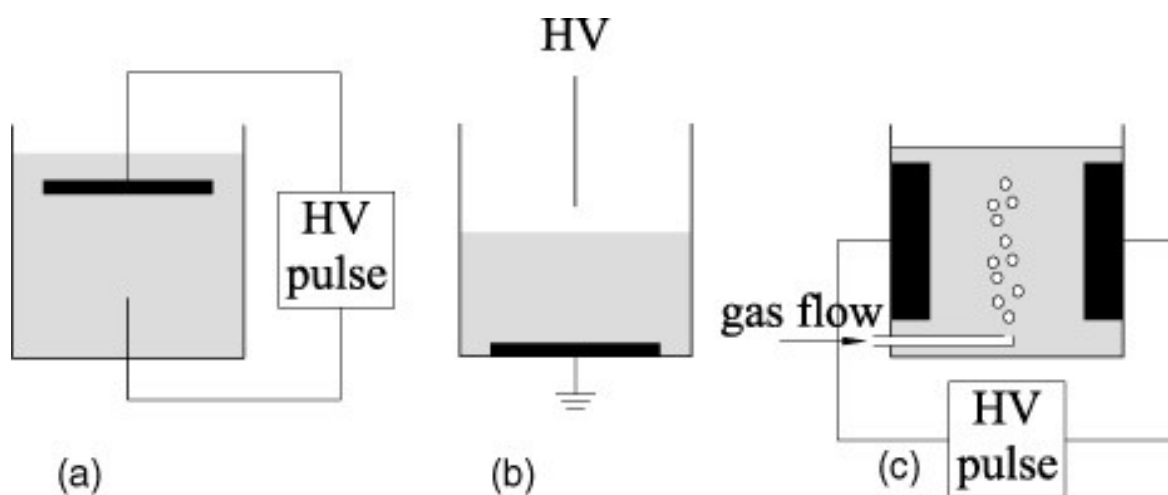


Figure 1.19 Typical configurations for the discharges in and in contact with liquids. (a) Direct liquid phase discharge (b) gas phase discharge with liquid (c) bubble discharge reactor.¹¹⁰

Electrical discharge in liquids is also divided into partial discharge (or pulsed corona discharge) this type of discharge does not reach the second electrode and its branches are called streamers, and full discharge (Arc or pulsed spark discharge)

is when the discharge reaches the second electrode, Figure 1.20 shows the full discharge in water.¹⁰⁰

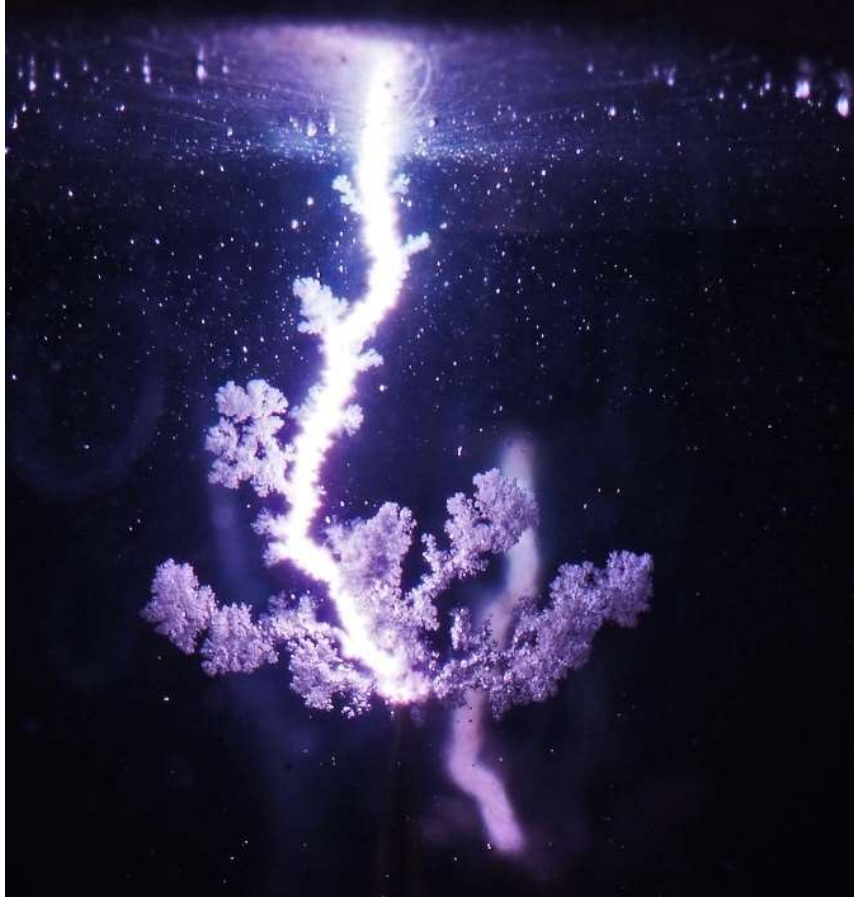


Figure 1.20 Pulsed arc plasma discharge in water (IOP Science).¹¹¹

For a liquid with high electrical conductivity more current will freely move through it resulting in higher power density in the channel, higher plasma temperature and higher ultraviolet (UV) generating more acoustic waves so just by changing the conductivity all these parameters mentioned are changed, nevertheless, the electric field (current density) tends to be the same, one technique to increase the electric field is simply by changing the thickness of the tips of the needle electrode, as the electric field is inversely proportional to the radius of the needle tip.¹⁰⁰ The electric field at the tip of the needle can be calculated as:

$$E \sim \frac{V}{r} \quad \text{eq. 1.4}$$

Where r is the curvature of the needle tip and V is the voltage. However, as demonstrated by Sunka and his team,¹¹² a sharper needle tends to erode quicker

due to the high temperature.¹¹² The erosion of an electrode with pulse electric discharge in water results in particles of metal and metal oxide being formed in the liquid.¹¹³

1.5.4 Other Plasma Applications

1.5.4.1 Plasma Water Treatment

Today the population growth, economic development of developing countries and the continual increase of safe clean water consumption is a concern, mainly due to poor water treatment and distribution. According to the WHO (World Health Organization), diarrhoeal disease is responsible for the death of 1.5 million people per year of which 58% could be averted through safe drinking water, sanitation and hygiene.¹¹⁴

Water contamination can be attributed to several factors such as chemical fouling, lack of wastewater treatment and deficient clean water treatment and distribution. In 2010, more than 500 million eggs were recalled after dangerous levels of Salmonella were detected, it is believed that were caused by groundwater contaminated by animal feces.¹¹⁵

Traditional chemical treatment, UV (ultraviolet) radiation and ozone have been implemented to inactivate these bacteria, however, these approaches have some drawbacks; chlorination can render some toxic species in potable water, UV and ozone application although proved to be practical in inactivating bacteria in water, the effectiveness depends on the adherence to a regimented maintenance schedule. Plasma methods combined with UV radiation, chemicals, and a high electric field have been shown to be an effective alternative to conventional methods. Sunka and co-workers have shown that for low concentrations of organic contaminants dissolved in water, lower-energy corona and glow discharge processes are useful, and for high concentrations of organic compounds in the liquid phase, larger energy-arc and pulsed-arc type processes may be more effective.¹¹⁶

Due to the discharge of industrial process among other activities, phenol and its derivatives are widely distributed contaminants in groundwater and surface water.

Phenols are harmful contaminants at very low concentration.¹¹⁷ Chlorine is normally used as a disinfectant in water treatment plants, and undesirable chlorophenols will consequently form when phenols are present. Other methods such as activated carbon extraction and chemical oxidation suffer from low efficiency, high cost, and formation of by-products. Low-temperature plasma generates active species such as OH, H, O, H₂O₂, O₃, etc.¹¹⁸ With its strong oxidation ability, it can effectively remove the organic pollutants from water.¹¹⁹ Sato and his colleagues have successfully removed phenol from contaminated water employing gliding arc discharge above a water solution, the decomposition is shown in Figure 1.21. Figure “A” illustrates the removal of phenol as a function of treatment time where after 12,7 min 100 % of phenol was removed, also in the figure “B” the removal of phenol is faster when bubbling oxygen due to the radicals formed.¹²⁰

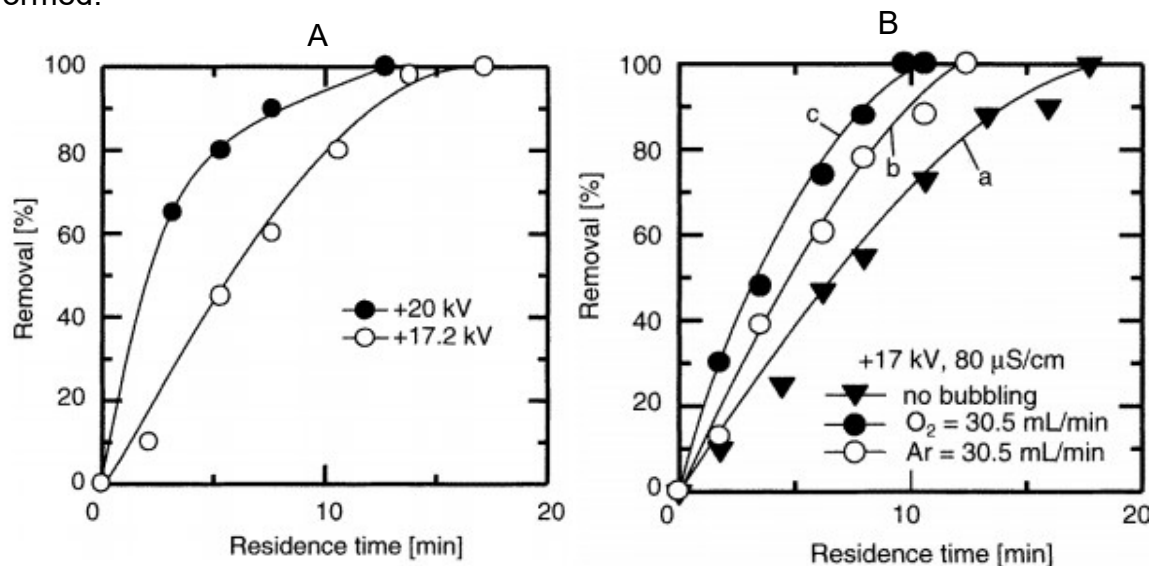
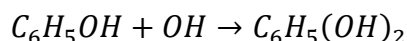
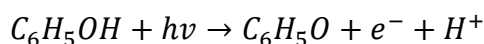


Figure 1.21 experiment results for the removal of phenol by a streamer corona discharge in the solution (A) Dependence of phenol removal on residence time for peak-pulse voltages of +17.2 and +20 kV (B) Effect of gas bubbling on the phenol removal efficiency at a +17 kV peak-pulse voltage.¹²⁰

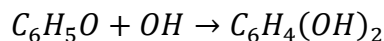
The mechanism proposed for phenol removal from water solution starting with oxidation provided by OH radicals is as follows:¹²⁰



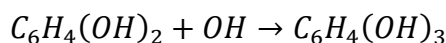
The dihydroxy cyclohexadienyl radical decays to form phenoxy radical C₆H₅O. Phenoxy radical can also be directly formed under the activation of ultraviolet light produced by the discharge.



C_6H_5O will further react with OH forming hydroquinone and pyrocatechol (dihydroxybenzenes).



Dihydroxybenzenes are also attacked by OH radicals to form $C_6H_4(OH)_3$.



$C_6H_4(OH)_3$ further reacts with oxygen to form 1,2,4-trihydroxybenzenes. According to Sun and co-workers, the opening of the aromatic rings leads to the formation of low molecular weight compounds which are also oxidized through hydroxylation and hydration which will form carbon dioxide.¹²⁰

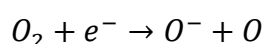
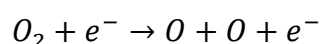
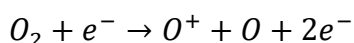
VOC Removal

VOCs (Volatile Organic Compounds) are carbon-containing organic chemicals that have low water solubility and high vapour pressure. The most common VOCs found in drinking water are chlorinated solvents (carbon tetrachloride, 1,2-dichloroethane, methylene chloride, etc.) and fuel components (benzene, toluene, xylenes, etc.). These pollutants contaminate the water through gasoline or oil spills, as well as underground tank and pipe leakage. In addition, there are many chlorinated solvents present in household products as well as adhesive and cleaning products have find their way into the water supply.¹⁰⁰

As mentioned before, chlorination is the most widespread technique used as an oxidative agent, nevertheless, chlorine is likely to produce chlorinated organic compounds such as dioxins and dioxin-like compounds, which are toxic to humans, and plants. RO (Reverse Osmosis) and active carbon are frequently used approaches to purify water, but these are high-cost technologies and are not as efficient for low concentrations. The application of non-thermal plasma directly into aqueous solution generates reactive chemical radicals and molecular species, together with shock waves and UV radiation. This process is effective even for large volumes at low concentrations. Pulsed corona and DBD (Dielectric Barrier Discharge) have been successfully applied for removal of volatile hydrocarbons, aromatic compounds and chlorine-containing compounds.¹²¹

1.5.4.2 Chemical Interaction

With the continuous development of plasma medicine¹²² and materials synthesis, the interaction of reactive species generated at the surface of liquids in contact with non-thermal plasma and the liquid has become an important research topic.¹²³ The wide variety of active species formed at plasma state can be dissolved and react at the interface or bulk of the liquid. The main advantage of non-thermal plasma related to chemical interactions is the high chemical efficiency, as there is only a little or no thermal loss, most of the input energy is harnessed into chemical conversion. The fast electrons and the energetic photons can, therefore, trigger many different chemical processes.¹⁰³ Two classes of reactions can be observed when plasma is formed at the surface of a liquid. Reaction initiated by electrons which are short-lived species and those reactions initiated by gaseous neutral species. In the end, the species formed will be a combined reaction with electrons and the stable species present. A good example of a combined reaction is the production of ozone by non-thermal plasma generated in air; as illustrated below when at an initial stage free oxygen is produced by electron impact, then ozone is created by reaction with the free radicals.



Indeed, ozone has been produced by DBD's since 1857 by Siemens¹²⁴ and many other types of DBD ozone generators have been developed and investigated.¹²⁵ The reactive species formed will rely mostly on the background gas and can be tracked by measuring the pH. With oxygen or argon as the background gas, the electrolytic reaction between plasma electrons and the gas will yield ions of hydroxide (OH⁻) in excess making the solution more basic. While the reaction under nitrogen and oxygen gas will form NO by the Zeldovich Mechanism (production of active nitrogen from molecular nitrogen in the gas phase).¹²⁶ Which will react with oxygen to form NO₂ (nitrogen dioxide) and by dissolving in aqueous solution will form HNO₂ (nitrous acid) and HNO₃ (nitric acid) making the solution more acidic.¹⁰⁷

Variation of pH measurement was carried out by Go and his team, where plasma formation under different gases was conducted in a 0.34 M of NaCl solution using Pt (platinum) foil as counter electrode, in the experiment the same voltage and current was applied so that the net number of electrons transferred was the same, the measurement was taken as a function of plasma exposure time as can be seen in Figure 1.22.¹

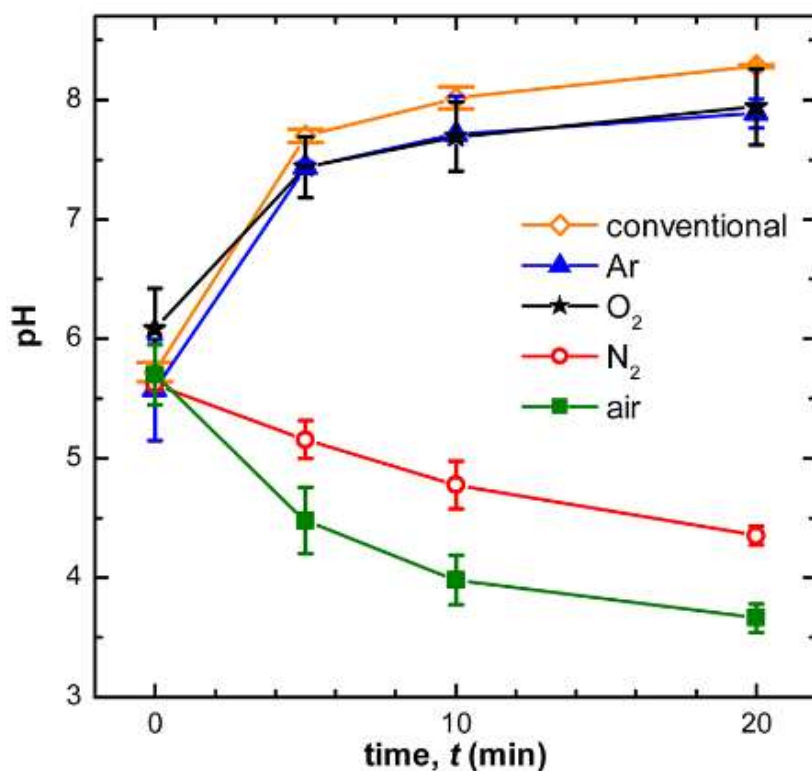


Figure 1.22 pH of the NaCl solution in direct contact with the microplasma jet measured as a function of time for various ambient gases.¹

Under Ar and O₂ gas, the pH increased, as you would expect, a conventional cell with Pt cathode would also do. This suggests that the plasma electrode causes the dissociation of Cl₂ and generation of OH⁻, but when operating in air or N₂ the solution became acidic which could explain the production of HNO₂ and HNO₃ as mentioned above.

Traditionally in an electrochemical system, charge-transfer reactions take place between solid-liquid interfaces¹²⁷ where two electrodes are immersed in an electrolytic solution, the electric potential differences lead to a charge-transfer reaction, nevertheless, the electrochemical reaction is not limited by solid-liquid interfaces, insulators have been charged and introduced to a range of charge-

transfer reactions.¹²⁸ Also, previous studies demonstrate charge transfer reaction through glow discharge electrolysis.¹²⁹ Richmonds and co-workers reported a reduction of $[\text{Fe}(\text{CN})_6^{3-}]$ (ferricyanide) to $[\text{Fe}(\text{CN})_6^{4-}]$ (ferrocyanide) using DC non-thermal atmospheric plasma discharge. In addition, the group were able to demonstrate the relationship between the current employed and the conversion rate, as demonstrated in Figure 1.23.²

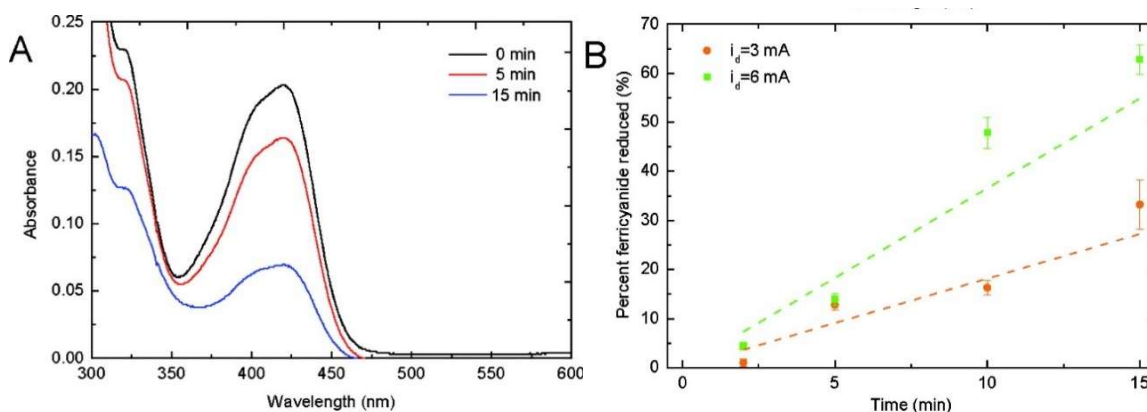


Figure 1.23 (A) UV-vis absorbance spectra of solutions of ferricyanide after exposure to the plasma for 0 min, 5 min, and 15 min (discharge current, $i_d = 6$ mA), (B) percent of ferricyanide reduced in solution as a function of time at discharge currents (i_d) of 3 and 6 mA.²

1.5.4.3 Plasma Medicine

Low-temperature atmospheric dielectric-barrier discharge jets have been shown to be effective on the sterilization of surgical instruments that are often contaminated by both bacteria and proteinaceous matters.¹³⁰ Quasi-thermal plasmas (thermal plasma) have been used in medical practice for blood coagulation in wound treatment and surgery in the form of cauterization devices (argon plasma coagulators, argon beam coagulators and so forth).¹³¹ However, studies conducted by Fridman and co-workers¹³² and undependably by Kalghatgi¹³³ indicate that high temperature is not a prerequisite for plasma-induced blood coagulation. Plasma stimulation of *in vivo* blood coagulation was conducted with live hairless SKH1 mice (the hairless type of mice used to conduct skin research). Applying DBD plasma treatment for 15 s could coagulate the blood at the surface of a cut saphenous vein and a vein of a mouse as shown in Figure 1.24.

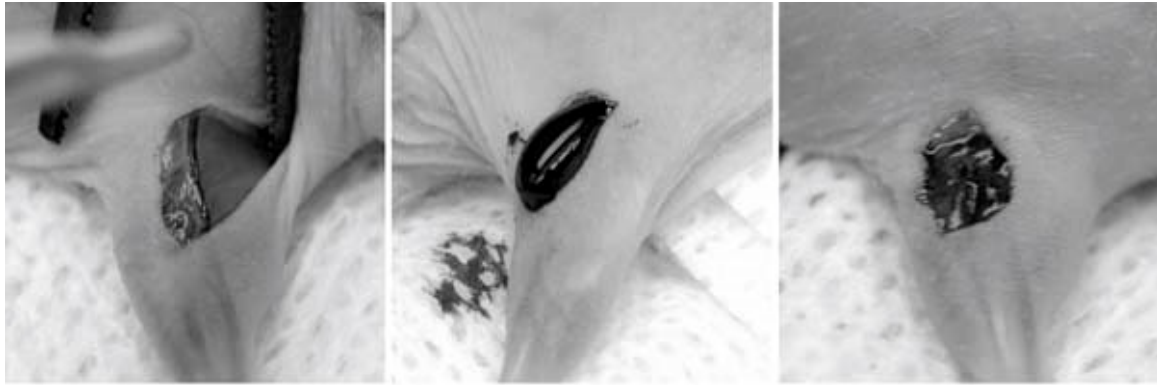


Figure 1.24 Blood coagulation of a live animal, (left) Saphenous vein, (middle) if left untreated following a cut the animal will bleed out, (right) cut treated with DBD plasma. Plasma processes and polymers (2008).¹²²

The picture on the left shows the saphenous vein, which is the major vein vessel for a mouse, when leaving the cut untreated (middle) the animal will continue bleeding out but after 15 s of treatment using $0.8 \text{ W}\cdot\text{cm}^{-2}$ of DBD plasma (right) the animal stopped bleeding completely.¹²²

It has also been shown that plasma can be employed efficiently to combat fungal diseases, experiments with *Candida albicans* (common fungi present in a hospital as well as public places) were carried out and after 5 s of plasma treatment, the fungi were reduced to about 10^{-4} of the original level.¹³⁴ Even for cancer therapy, CAP (Cold Atmospheric Plasma) interaction with tissue allows targeted cell removal without necrosis such as cell disruption, CAP affects cells via a programmable process called apoptosis which is a multi-step process leading to cell death and this process is the one inherent to cells in the human body.¹³⁵

1.5.5 Electrical Measurement

Although considerable effort has been devoted to the investigation of atmospheric pressure discharge, the physics of this discharge is still not completely understood. Especially in the case of plasma in contact with liquid where the discharge occurs between a metal pin and a liquid anode, only some phenomenological properties have been reported.¹³⁶ When the high voltage anode is in contact with liquid, the anode becomes the whole liquid and not the electrode alone so any calculation should consider this theory. An important observation is that the interaction of plasma with liquid does not change significantly the pH of the electrolyte, for instance in a solution of sodium hydroxide with pH 11.6, the drop in pH is only 0.6

with plasma discharge at 50 mA for 2.5 h.¹³⁷ However, in the case of distilled water the change in pH is noticeably more evident and will heavily depend on the gas nature. A recent investigation showed that the lower the pH the conductivity is higher.¹³⁸

When generating any type of plasma, it is important to record various electrical features of the system. In some cases, the information is simply collected through specific equipment while others can be calculated.

1.5.5.1 Current, Current Density and Power Dissipation

Electric current is a flow of electric charge. In electric circuits, this charge is often carried by moving electrons in a wire. It can also be carried by ions in an electrolyte, or by both ions and electrons such as in ionized gas (plasma).¹³⁹ It can be simply calculated using Ohm's law, Ohm's law states that $I = \frac{V}{R}$ where I =current in units of Amperes, V is the potential difference in units of Volts and R is the resistance in units of Ohms.

Current density is a measure of the density of an electric current. It is defined as a vector whose magnitude is the electric current per cross-sectional area. In SI units, the current density is measured in amperes per square meter, as considering that all reaction takes places at the electrode surface, we can calculate the current density as follows:

$$I = \int J \cdot dA \quad \text{eq. 1.5}$$

Where I is the current in amperes, J is the current density per unit area in a material with finite resistance and A is the area in meter, from this equation we can rewrite as:

$$J = \frac{I}{A} \quad \text{eq. 1.6}$$

Any resistor in a circuit that has a voltage drop across it dissipates electrical power. The cathode/anode voltage drop is measured by extrapolating the linear curve of the burning voltage as a function of the inter-electrode distance to zero. The voltage drop in the liquid can be calculated by calculating the resistance of the water

electrode between the cathode spot and the metal electrode at the bottom of the liquid cathode.¹⁴⁰ Where

$$(p = i^2 \times R) \quad \text{or} \quad \left(p = \frac{V^2}{R}\right) \quad \text{eq. 1.7}$$

1.6 Summary

In conclusion, we can see that greenhouse gases present in our atmosphere, mainly carbon dioxide, trap some of the heat gained by the sun, and, since the industrial revolution, anthropogenic activities are in fact increasing significantly the concentration of these gases, resulting in what is known as global warming. In addition, the industry is heavily dependent on limited source of petrochemical resources. All these data are attracting the attention of scientists around the world to find solutions to shift our industry to non-petroleum-based products and also to reduce the concentration of carbon dioxide in the atmosphere. Global warming and climate change are a long process and with the amount of CO₂ that has already been released into the atmosphere there is nothing we could do to avoid its effects; however, it is still possible to mitigate the effect and actions are urgent. If is not to be concerned with the effects which we are already witnessing, with the positive feedback, the global warming process will accelerate to a point where it will be out of control and the future will be unprecedented.

In face of this issue, researchers around the world are working on the development of ways to stop carbon emission or to reduce the concentration of those gases in our atmosphere, such as solar shield, iron fertilization, carbon capture and storage, and carbon dioxide utilisation.

Carbon dioxide utilisation has been widely approached and in the electrosynthesis field, excellent results have been achieved. For instance, the carboxylation of phenol to make salicylic acid was reported by Takayuri.⁶⁰ The incorporation of carbon dioxide in conjugated dienes reported by Vos and co-workers or the electrocarboxylation of phenylacetylene presented by Chuanhua are also other examples. All of these reports were presented with a good conversion and energy efficiency and was claimed to be a good alternative to address the issue related to

carbon dioxide, but what all of them have in common, is the use of a sacrificial electrode to generate free electrons which is vital in an electrochemical reaction. The drawback of the use of sacrificial electrodes is the resulting oxidized metal requiring its collection and disposal or recycling if possible. As an alternative, an inert electrode along with a reducing organic agent can sometimes be employed which again requires a further process to be separated from the products and disposed of.

Plasma technology has been known since 1785 but its industrial use has brought more attention in the last 20 years. For example: Application in medicine, automotive industry, surface material modification, water treatment and chemical interaction of the active species formed at plasma state.

Nevertheless, the possibility of using a plasma jet in contact with liquid, harnessing the free electrons to interact with other substrates, like the reduction of $[\text{Fe}(\text{CN})_6^{3-}]$ to $[\text{Fe}(\text{CN})_6^{4-}]$ reported by Richmonds and co-workers, aroused interest of Buckley's group and opens a new research area employing it in the traditional electrochemical process as alternative of sacrificial electrode or reducing agent in the carboxylation process.

2.0 Experimental

2.1 General Experimental

2.1.1 Reagents and Apparatus

All ^1H and ^{13}C NMR spectra were measured at 400 and 100 MHz respectively using a Jeol ECZ spectrometer and analyzed with Delta software. The solvent used for ^1H and ^{13}C NMR spectroscopy was CDCl_3 using TMS (tetramethylsilane) as the internal reference. For polar compounds, deuterated dimethyl sulfoxide was used. Chemical shifts are given in ppm (parts per million) and J values are given in Hz (Hertz).

All chromatographic manipulations used silica gel as the adsorbent. Reactions were monitored using TLC (Thin Layer Chromatography) on aluminium-backed plates. TLC was visualized by UV radiation at a wavelength of 254 nm.

DMF (*N,N*-dimethylformamide) was obtained from Sigma Aldrich at $\geq 99\%$ although some experiments were conducted under dried DMF from the same supplier and were used without further purification. To obtain dry DMF, the solvent was stored over activated molecular sieves 3\AA for at least 24h before use. In order to activate the molecular sieves, they were taken into the microwave and exposed to $600\text{ }^\circ\text{C}$ for 20 min, then stored under nitrogen.

Gas Chromatography was employed to monitor the experiments. An Agilent HP GC system 6890 series fitted with an SPB $^{\text{®}}$ -5 Capillary GC Column $30\text{ m} \times 0.25\text{ mm}$ ($L \times \text{I.D.}$), $df\ 0.25\ \mu\text{m}$ or a GC/MS (Gas Chromatograph Mass Spectrometry) from Shimadzu GC-2010 Plus with Restek Rtx $^{\text{®}}$ -5Sil MS Column $30\text{ m} \times 0.25\text{ mm}$ ($L \times \text{I.D.}$) was used. Programmed was developed during this research with an initial oven temperature of $60\text{ }^\circ\text{C}$ for 1 min, oven program rate of $10\text{ }^\circ\text{C}\cdot\text{min}^{-1}$ up to $260\text{ }^\circ\text{C}$ for 1 min and injection temperature of $220\text{ }^\circ\text{C}$. The shift is given by retention time (min) and Voltage (V).

2.1.2 Determination of % Yield and Calculation of Current Efficiency

GC/MS is somewhat rapid and reliable analysis and was used to determine the percentage of conversion and to calculate the current efficiency of carboxylation experiments not only in electrochemistry but also in plasma experiments. Once the parameters were set, it was found to be an easy way to evaluate the conversion rate and work out the optimization of the experiment.

The percent yield is equal to the actual yield divided by the theoretical yield of the product multiplied by 100:

$$GC\ Yield_{(\%)} = \left(\frac{Actual\ Yield_{(g)}}{Theoretical\ Yield_{(g)}} \right) 100 \quad eq. 2.1$$

Where the theoretical yield is the maximum amount of product that can be produced in a reaction which can be calculated as follow:

$$Theoretical\ Yield_{(g)} = \left(\frac{mass\ of\ substrate_{(g)}}{Mw\ substrate_{(g/mol)}} \right) Mw\ Product_{(g/mol)} \quad eq. 2.2$$

The actual yield is the concentration of the product in mol/L obtained by the GC calibration curve and calculated as follow:

$$Actual\ Yield_{(g)} = Conc.\ Product_{(mol/L)} \cdot Vol_{(L)} \cdot Mw\ Product_{(g/mol)} \quad eq. 2.3$$

CE (Current efficiency) describes the efficiency with which charge (electrons) is transferred in a system and can be calculated as the formula below.

$$CE_{(\%)} = \left(\frac{grams_{(product)}}{Theoretical\ g_{(product)}} \right) 100 \quad eq. 2.4$$

Where:

$$Theoretical\ g_{(product)} = Moles_{(product)} \cdot Mw_{(product)} \quad eq. 2.5$$

$$Moles_{(product)} = \left(\frac{Moles_{(electrons)}}{n} \right) \quad eq. 2.6$$

$$Moles_{(electrons)} = \left(\frac{Amperes \cdot t_{(s)}}{Faraday\ Constant} \right) \quad eq. 2.7$$

$$Faraday\ Constant = 96,485\ and$$

$$n = n^{\circ}\ of\ electrons$$

2.1.2.1 GC/MS Calibration Curves

Both the Agilent HP GC or the Shimadzu GC/MS used to identify and quantify the concentration of chemicals present in the experiments, has a FID (Flame Ionization Detector). As any normal flame, the flicker is not constant and so the ionization might produce some variation in the integrated area of the spectra. To overcome these variations and generate more accurate quantitative analysis, an IS (Internal Standard) is required. An IS is a known concentration of a known substance which is added in every sample and its purpose is to behave like the analyte.

As the spectra will only provide the integrated area of the injected compound, a calibration curve of each known substance is necessary, so any specific area is related to a specific concentration. The calibration curve utilized was prepared as follows: For each substrate or product, 0.2 mol/L of stock solution was prepared, from the stock solution, 5.0 mL of solutions (0.01, 0.02, 0.04, 0.06, 0.08 and 0.1) mol/L were prepared, the preparation of different concentrations of solutions are arbitrary and the more data collected, more accurate will be the calibration curve. Subsequently, 500 μ L of each one of the prepared solutions was added into a 2.0 mL GC vial along with 50 μ L of I.S. naphthalene 0.05 mol/L in methanol.

All these samples were injected in the GC under the same conditions. To produce the calibration curve, the integrated area of the substrate was divided by the integrated area of the IS, and, for each of these ratios a corresponded concentration was plotted in excel forming a curve which gives a formula, the formula is then used to calculate the concentration of each product. The R^2 generated along with the formula is the "proportion of variance in y attributable to the variance in x" so the closest R^2 to 1.0 means that the GC is more accurate.

It is extremely important that the analyte is injected following the same conditions stated in the calibration curve procedure such as the volume of the sample, volume, and concentration of the IS and the calculus of the ratio.

Figure 2.1 below shows the calibration curve of the *trans*-Stilbene **28** followed by the calibration curve of methyl-2,3-diphenylpropanoate (Figure 2.2) which is the corresponding product of carboxylation and methylation of *trans*-Stilbene.

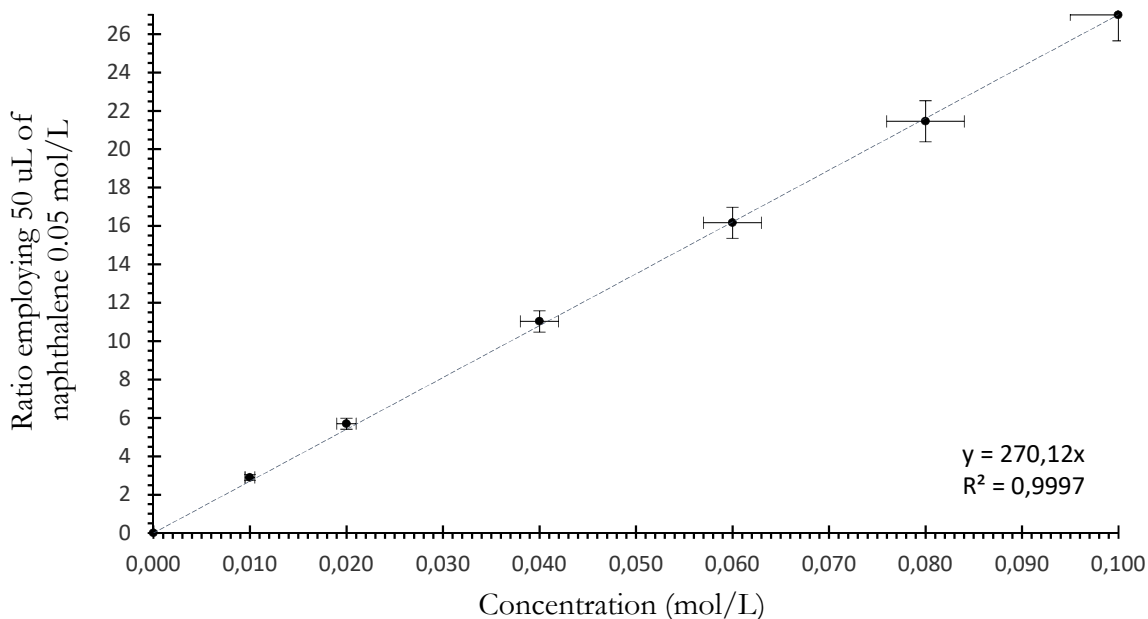


Figure 2.1 Calibration Curve of *trans*-Stilbene

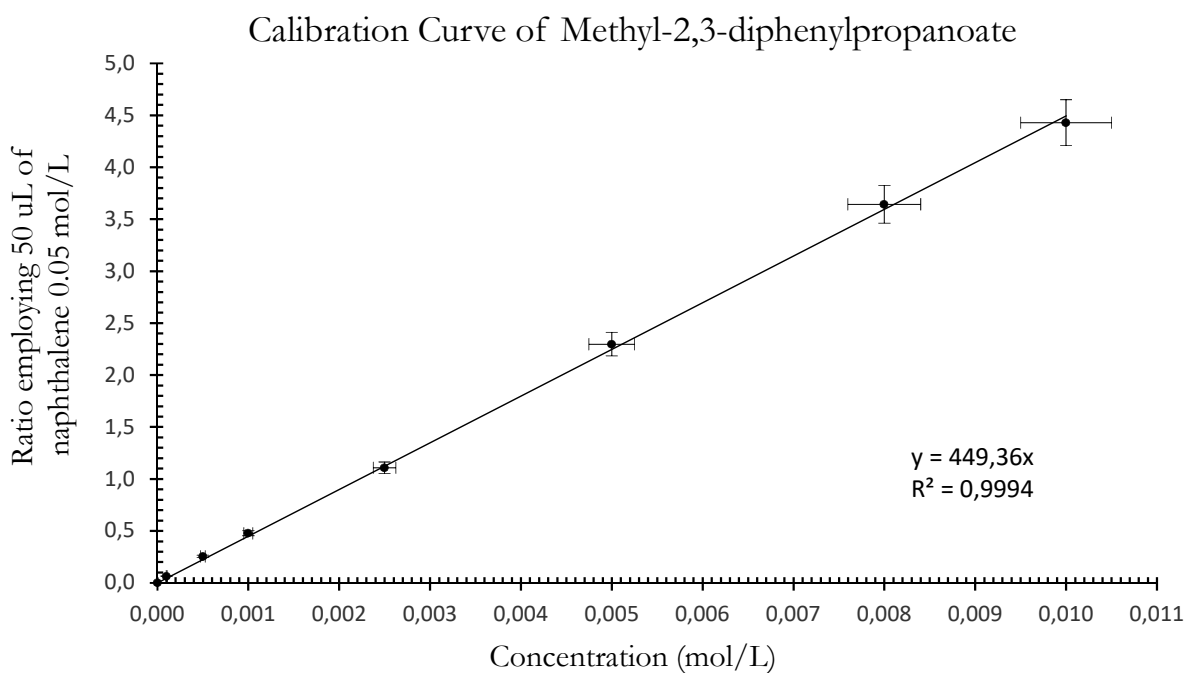


Figure 2.2 Calibration Curve of Methyl-2,3-diphenylpropanoate

2.1.2.2 Methylation Procedure and Injection Parameter.

When the reaction was being monitored by GC/MS, the SPB®-5 Capillary GC Column was used, as this column is mainly made of dimethyl siloxane (95%) by injecting polar compounds as the carboxylic acid, it will likely be adhered on the wall of the column and not produce reliable results. To overcome this scenario,

$TMSCHN_2$ (trimethylsilyldiazomethane) was employed as an efficient reagent for methylation of carboxylic acids.¹⁴¹ Although there are other methods of methylation available, $TMSCHN_2$ is easier, efficient and quick to use. The carboxylic acid with a methyl group attached is easier to quantify and fully integrate. In face of this, the product identified by GC/MS spectra and reported here is the methyl ester of the specific acid. The same methylation technique was used when the product was purified through the column chromatography using silica gel and then characterized by 1H NMR spectroscopy.

As standard method for sampling and analysis using GC/MS, 500 μ L of the reaction mixture is injected in a 2.0 mL GC/MS vial along with 50 μ L of internal standard naphthalene 0.05 mol/L in methanol and the addition of $TMSCHN_2$ dropwise (roughly 3 drops). This methylation is followed by every experiment in this research. Preparation of methyl ester was achieved by the addition of $TMSCHN_2$ dropwise until a yellow colour persisted. This method was tested and showed that to get complete methyl-2,3-diphenylpropanoate, the reaction needs to be stirred for at least 30 min, the methylation was completed as shown in Table 2.1.

Table 2.1 - Time of reaction to complete the methylation of carboxylic acid

Product	Time of stirring (min)	Formation of methyl ester (mmol)
Methyl-2,3-diphenylpropanoate	10	0.92
	30	2.06
	45	2.07

Before the injection, the GC/MS was conditioned as follows:

Table 2.2 - GC/MS injection parameters

Oven Temp. Program Rate ($^{\circ}C$ /min)	Temperature($^{\circ}C$)	Hold Time(min)
-	60	1.00
20	140	0.75
8.0	200	1.00
25	260	1.35

Injection temperature: 220 °C

Injection mode: Split

Total Flow: 64.3 mL/min

Column Flow :1.20 mL/min

Column oven initial temperature of 60 °C for 1 min

2.1.3 Electrical and Physical Properties

Some important calculations considered in this research are explained in this section as follows:

2.1.3.1 The Velocity of Gas in a Tube

In this calculation, I neglected the internal rugosity of the tube and the density of the air and simply used as a reference for future comparison, for the pressure I considered 1 atm, so the velocity of a gas in a tube when the plasma strikes is calculated as follows:

$$v = \frac{Qa}{60\pi \left(\frac{d}{2}\right)^2} \quad eq.2.8$$

Where v is the velocity of the gas in the unit of $m \cdot s^{-1}$; Qa is the flow of the gas in the unit of $m^3 \cdot min^{-1}$ and d is the diameter of the tube in m .

2.1.3.2 Surface Area of Cylindrical Electrode

The majority of the electrodes used in this research are cylindrical so to calculate the area in contact with the liquid I considered one base circle πr^2 plus the side area of the cylinder which is a parallelogram of height h :

$$A = \pi r^2 + 2\pi r \cdot h \quad eq.2.9$$

Where the area A is given in m^2 , r is the radius of the cylinder in the unit of m and h is the height of the cylinder in the unit of m .

2.1.3.3 Voltage Measurement

The high voltage applied in the system was measured using Brandenburg 507R DC power supply connected to an electrode. The low voltage was measured using an oscilloscope Tektronix 1012 connected across a 2.166 K Ω resistor, this technique allows the calculation of the current through the system, current density, and power dissipation using ohms law.

2.2 Individual Electrochemical Experimental Procedures

2.2.1 Electrochemical Setup

In order to conduct the electrochemical reaction, the equipment should be set up according to Figure 2.3

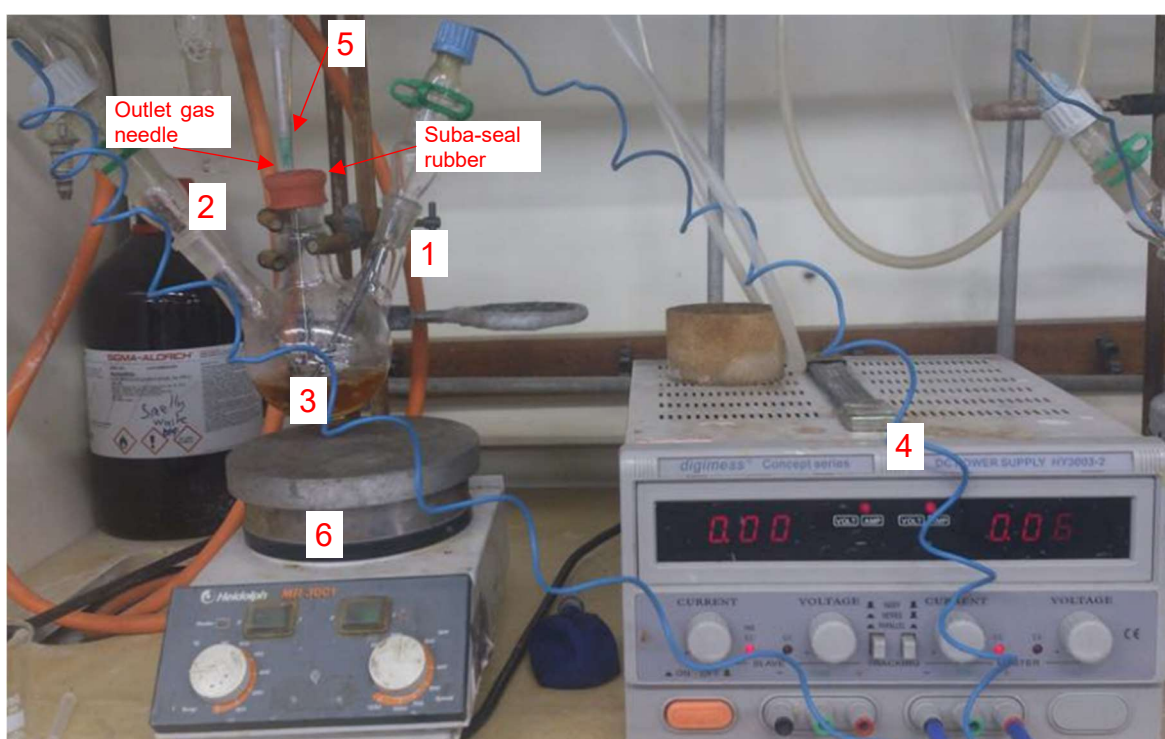
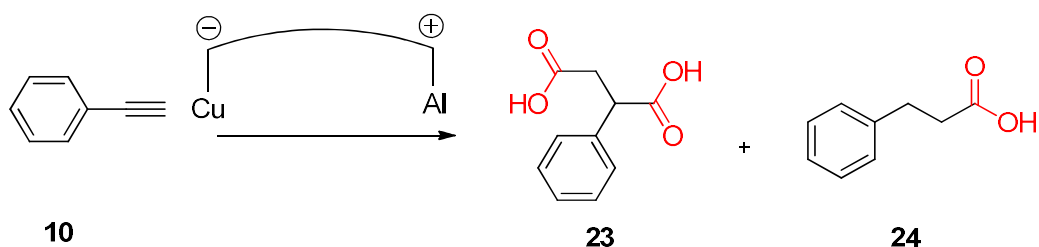


Figure 2.3 - Electrochemical setup equipment

It consists of an anode (1) where the oxidation takes place; Cathode (2) where the reduction takes place, the electrodes are immersed in the liquid at 1.0 cm with a distance of 3 cm of each other; 100 mL single compartment cell with three-neck (3); DC The power supply (4); Inlet CO₂ needle (5) and the magnetic stirrer (6). The compartment is sealed with suba-seal rubber septa with an outlet gas needle to

keep the positive pressure. The connectors of the electrodes were properly sealed. Some of the characteristics of this setup are variable and were changed during the optimization of the experiment, for instance, the size of three-neck compartment cell was adjusted according to volume of solvent employed and the size and material of anode and cathode were also changed.

2.2.2 General Procedure for Carboxylation Using a Sacrificial Electrode



In a single compartment cell of 100 mL with three-neck a solution containing phenylacetylene **10** (0.10 g, 1.0 mmol), Bu₄NI (Tetrabutylammonium iodide) (0.18g, 0.5 mmol), and DMF (*N,N*-dimethylformamide) (50 mL) was prepared. A stream of CO₂ (10 SCCM) was continuously introduced into the mechanical stirred homogeneous solution. Copper cathode and aluminium anode were placed into the three-neck flask and a constant current of 60 mA was maintained during the reaction. After 2 h of reaction, the power supply was turned off and 500 μ L of sample was injected in a 2.0 mL GC vial along with internal standard in methanol (50 μ L), this solution was methylated according to injection parameters 2.1.2.2. Identification and quantification of the products were done by GC/MS. The resulted mixture of the experiment was acidified by addition of HCl (37%)/H₂O (1:1, 10 mL), extracted with diethyl ether (3 x 20 mL) and washed with brine (5 x 20 mL) until DMF is completely removed. Traces of water from combined organic layer were removed with MgSO₄ and the solvent was evaporated to dryness to afford an amber oil. (99% of conversion with a ratio of dicarboxylic acid: monocarboxylic acid of 3:1).

These experimental conditions were used to extract carboxylic acid throughout the electrochemical experiments carried out by Buckley group and as the group achieved great extraction results I decided to keep the methodology.

2.2.3 General Procedure for Electrocarboxylation Using a Non-Sacrificial electrode

In a single compartment cell of 100 mL with three-neck, a solution containing phenylacetylene **10** (0.10 g, 1.0 mmol), TEOA (Triethanolamine) (0.30 g, 2.0 mmol), Bu₄NI (0.18 g, 0.5 mmol) and DMF (50 mL) was prepared. A stream of CO₂ (10 SCCM) was continuously introduced into the mechanical stirred homogeneous solution. Carbon fiber cathode and carbon fiber anode were placed into the three-neck flask and a constant current of 60 mA was maintained during the reaction. After 2 h of reaction, the power supply was turned off and 500 µL of sample was injected in a 2.0 mL GC vial along with internal standard in methanol (50 µL), this solution was methylated according to injection parameters 2.1.2.2. Identification and quantification of the products were done by GC-MS. The resulted mixture of the experiment was acidified by addition of HCl (37%)/H₂O (1:1, 10 mL), extracted with diethyl ether (3 x 20 mL) and washed with brine (5 x 20 mL) until DMF is completely removed. Traces of water from combined organic layer were removed with MgSO₄ and the solvent was evaporated to dryness to afford an amber oil. (99% of conversion with a ratio of dicarboxylic acid: monocarboxylic acid of 3:1).

2.2.4 Electrode Properties Experiment

The purpose of this experiment is to understand the variations of current for a specific potential applied employing electrode of different materials, and the effect of electrolytic salt, this result is essential for the optimization process. In a single compartment cell of 100 mL with three-neck flask, Bu₄NI (0.18 g, 0.5 mmol) was dissolved in DMF (50 mL). Under constant stirring, carbon fiber anode and carbon fiber cathode were placed into the tree-neck flask and the solution was electrolysed at a constant current of 50 mA and the potential (V) was recorded. Different types of anode and cathode along with the concentration of solute were tested and for each of those tests, the potential measurement was recorded. (Table **2.3**)

Table 2.3 – Electrical properties of electrodes vs electrolyte concentration

Cathode	Anode	Bu₄NI concentration (mmol)	Current (mA)	Voltage (V)
C	C	0.0	1	60
Ni	Ni	0.0	1	60
Cu	Cu	0.0	1	60
C	C	0.5	50	22.3
Ni	Ni	0.5	50	29.8
Cu	Cu	0.5	50	24.2
C	C	1.0	50	13.8
Ni	Ni	1.0	50	15.9
Cu	Cu	1.0	50	16.3
C	C	1.5	50	10.9
Ni	Ni	1.5	50	12.6
Cu	Cu	1.5	50	16.8
C	C	2.0	50	9.3
Ni	Ni	2.0	50	11.4
Cu	Cu	2.0	50	10.7
C	C	2.5	50	7.8
Ni	Ni	2.5	50	10.3
Cu	Cu	2.5	50	12.3
C	C	3.0	50	7.6
Ni	Ni	3.0	50	8.6
Cu	Cu	3.0	50	12.3

The outcome of this experiment can be seen in section 3.2

2.3 Individual Plasma Experimental Procedures and Characterization

2.3.1 Plasma Apparatus and Gases

The apparatus of plasma experiment will be detailed in section 2.3.2. Gases were obtained from BOC Group Limited as listed in Table 2.4.

Table 2.4 - List of gases used in plasma experiment

Product	CAS n°	Purity %
Argon	7440-37-1	99.999
Helium	7440-59-7	99.996
Carbon Dioxide	124-38-9	99.8

2.3.2 Plasma Setup

The initial system was designed according to Figure 2.4, it consists of a carbon dioxide cylinder (11) connected into 3 necks round bottom flask of 100 mL (8). Argon (1) is connected into the grounded (6) microplasma jet (7) which operate as the cathode. The microplasma jet was manufactured with a 3D printer at Wolfson School of Mechanical/Loughborough University it works at direct current (D.C.) under atmospheric-pressure and has 4 channels to allow up to 4 simultaneous jets (the channels are necessary to investigate the optimal numbers of channels striking during the reaction aiming the best conversion efficiency) and a 0,8 mm stainless-steel grounded needle which features as cross-field plasma jet, this type of plasma generation was chosen because allows the electrons to be driven towards the liquid more efficiently than linear field.¹⁴² MKS PR4000B gas flow controller (2) is connected at both cylinders, background gas (1) and, CO₂ (11) in order to control gas flow. Brandenburg DC power supply model 507 R (500 V to 5 kV, 5 mA) (10) is connected to the carbon fiber anode (9) through high voltage wire. Surface mount resistor 4 x 470 kΩ ±5% 3W (3) is connected in parallel with each of the plasma channels to limit the current and a 2.166 kΩ ±5% 0.25W (4) current measuring resistor placed along the ground wire. An oscilloscope Tektronix model TSD1012

(5) is connected at both output side of the current measuring resistor (4) which measure the voltage drop upon it, the information provided by oscilloscope is further used to calculate the current (mA). Stirring plate (12) was placed underneath the flask to keep the solution constantly homogeneous.

During the research, this design has slightly changed allowing the optimization of the experiment, for instance, argon cylinder was temporarily exchanged by helium, and the design of the microplasma jet also changed which will be detailed in the session 0.

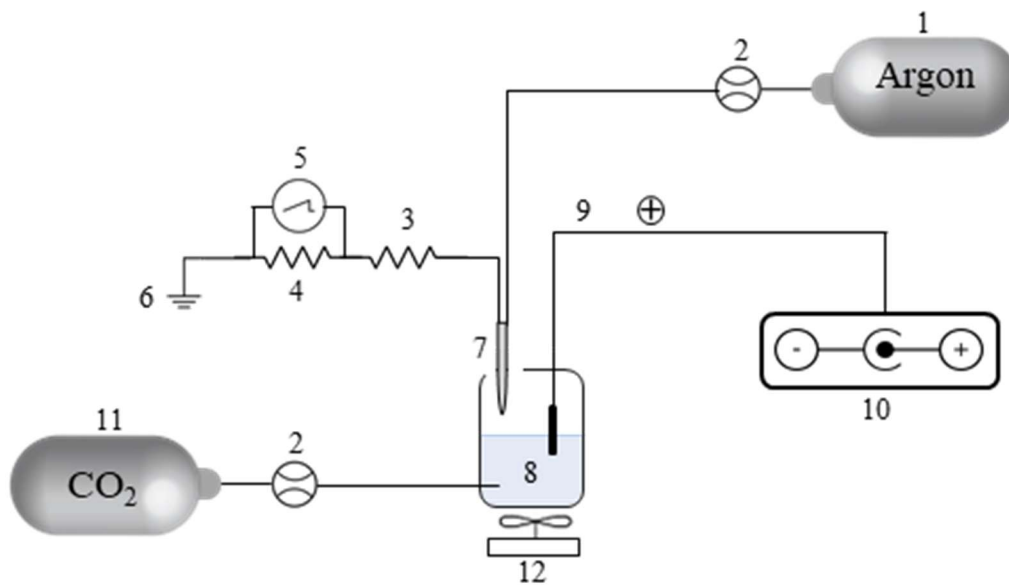


Figure 2.4 - Plasma System Setup

1-Argon cylinder, 2-gas flow controller, 3-surface mount resistor, 4-current measuring resistor, 5-oscilloscope, 6-grounding, 7-microplasma jet, 8- three-neck flask, 9-anode, 10- DC power supply, 11-CO₂ cylinder, 12-stirring plate.

2.3.3 Microplasma Jet Design

The plasma device consists of a DC atmospheric pressure microplasma jet manufactured at Wolfson School of Mechanical/Loughborough University. It is cross-field plasma jet type (where the electric field is perpendicular to the flow of gas) designed in a such way where the height of the 0.8 mm needle and the height of the body the of the jet could be adjusted by twisting the screw on the top of the jet body, by changing the position of the needle in relation to the dielectric tube and the gap between the tip of the needle and the surface of the liquid, result in a variation of the resistance of the system and by doing so change the characteristic

of the plasma, as seen in the section 1.5.3 There are two different options of gas flow which is through the center of the needle and around the outside of the needle through the tube. The plasma jet works as cathode and the electrode connected to the high voltage is the anode, although the whole liquid will be potentialized with high voltage, this configuration would allow the current to flow from anode towards the cathode and as the electrons flow in the opposite direction of the current, it will bombard the solution with electrons, which will be needed for the reaction to occur. The design of the jet is shown in Figure 2.5.

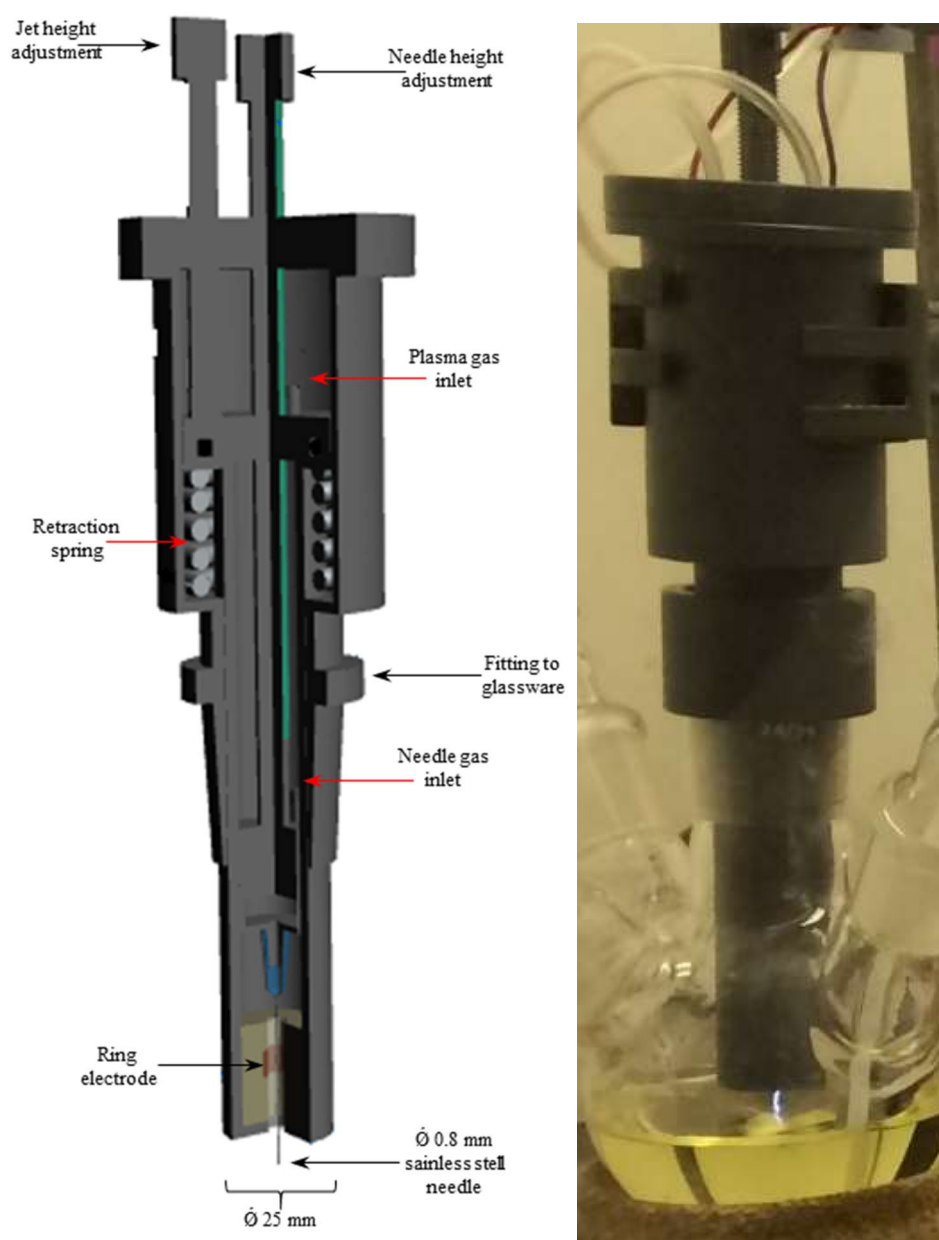


Figure 2.5 - First DC plasma jet used in this research, the computational design on the left and the picture on the right.

As mentioned in the previous section, the design of the plasma jet changed significantly (Figure 2.6). We tried to make something which could be simple to the point of being 3D printed, with a connection in the body making it easy to switch.

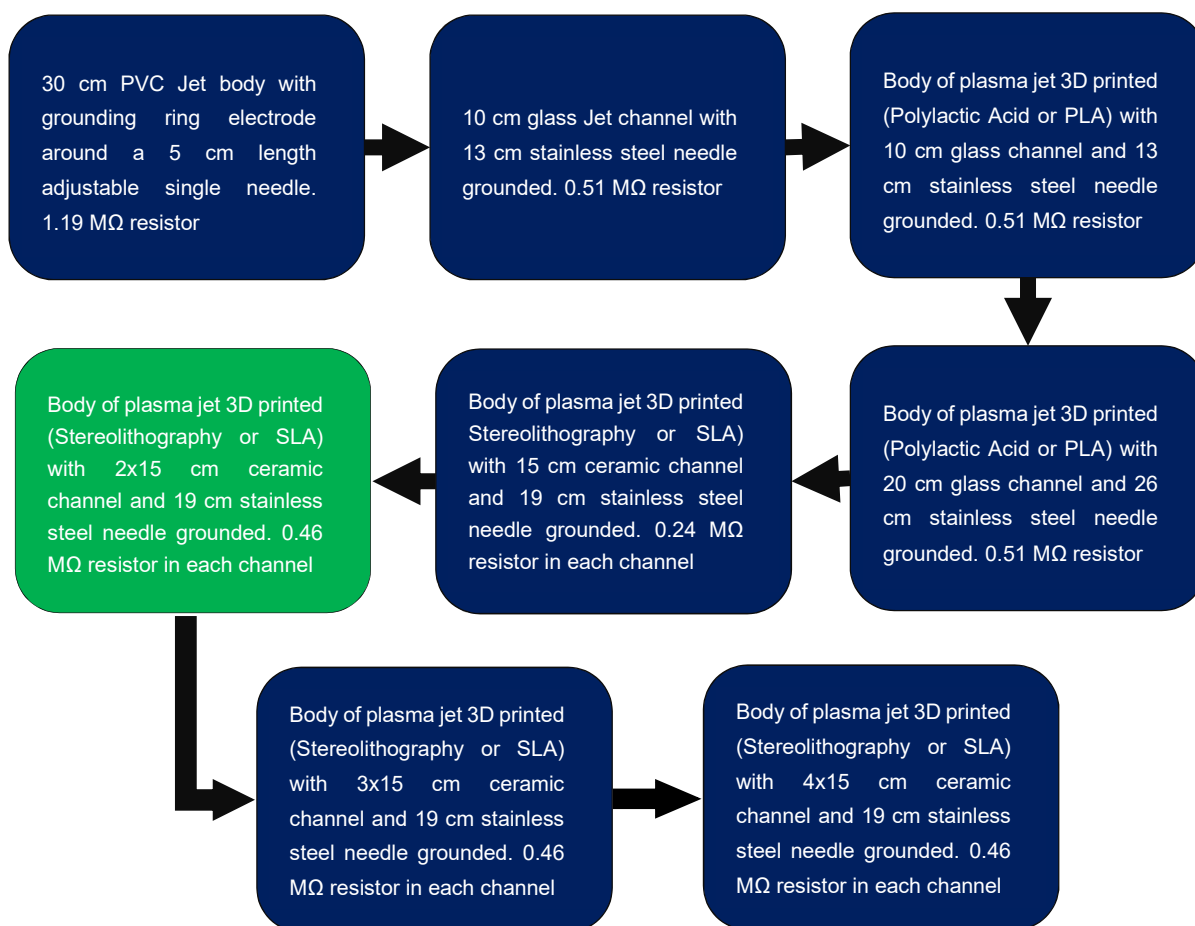


Figure 2.6 Variety of designs of plasma jet. The green box is the plasma jet used in the optimized experiment.

With a collaboration of my co-workers from electrical engineering, Alexander Wright and Alexander Shaw, the plasma jet used in the optimized experiments was designed and one of the new features was the possibility of connecting up to 4 jets simultaneously (Diagram 1, green box). In the design of the first jet, there was accumulation of the evaporated solvent during an experiment, the condensation of solvent at the tip of the plasma body was due to the large flat surface at the tip, which ended up damaging the plastic body. The diameter of the new body was reduced from 25 mm to 7 mm with 150 mm length and the material selected was ceramic (Figure 2.7).

With this plasma jet, we could explore some different experiments such as needle materials and dimensions, and, split the current into multiple jets. Moreover, the design along with material made it more resistant.

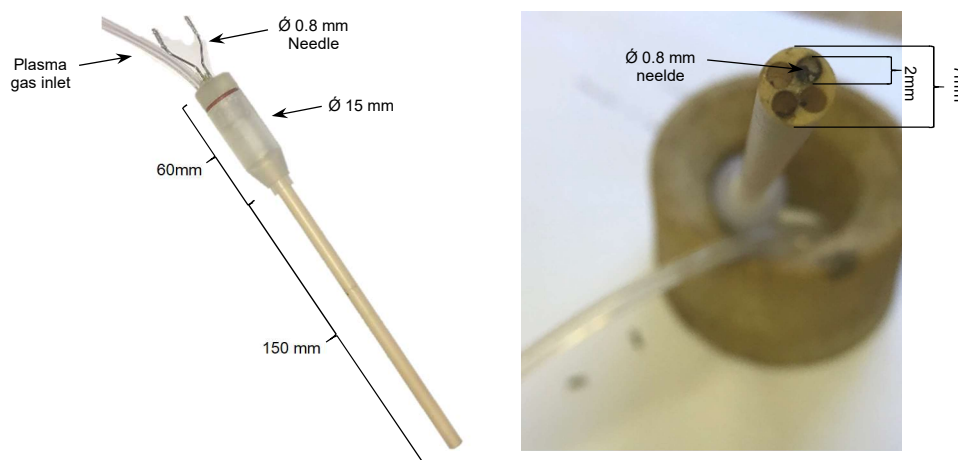
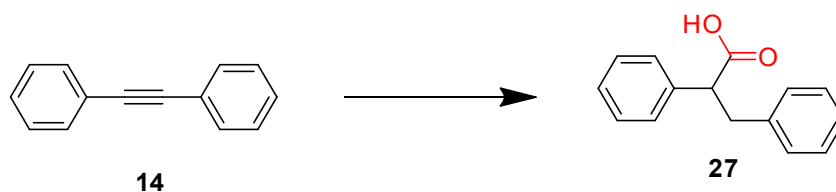


Figure 2.7 - DC plasma jet 3D printed

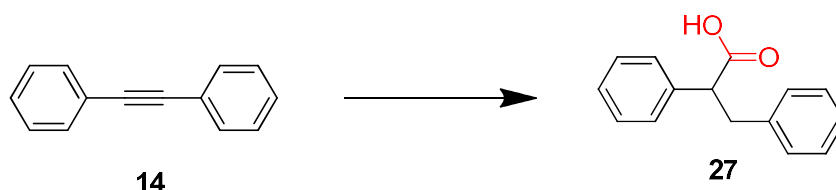
2.4 Plasma Carboxylation in Wet Solvent



In a single compartment cell of 100 mL with three-neck, a solution containing diphenylacetylene **14** (0.18 g, 1.0 mmol), TEOA (0.30 g, 2.0 mmol), Bu₄NI (0.55 g, 1.5 mmol) and DMF:H₂O (5:1, 50 mL) was prepared. A stream of CO₂ (10 SCCM) was continuously introduced into the mechanical stirred homogeneous solution. Carbon fiber anode (0.09 cm d. x 0.50 cm length) was placed in the three-neck flask and argon cathode single streamer microplasma jet (1.0 SLM) connected to a 1.19 MΩ resistor was positioned 5 mm above the surface of the liquid and ignited in the exit flow. DC power supply was adjusted to 1.6 kV giving 1.74 V across measuring resistor (2.17 kΩ) to get a constant current of 0.8 mA. After 3 h of reaction, the power supply was turned off and 500 μL of the sample was injected in a 2.0 mL GC vial along with internal standard in methanol (50 μL), this solution was methylated according to injection parameters 2.1.2.2. Identification and quantification of the product was done by GC/MS. For ¹H NMR analysis, the

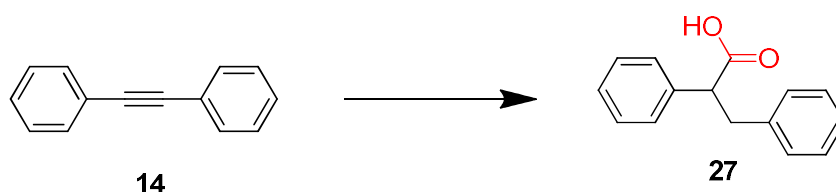
resulted mixture of the experiment was acidified by addition of HCl (37%)/H₂O (1:1, 10 mL), extracted with diethyl ether (3 x 20 mL) and washed with brine (5 x 20 mL) until DMF is completely removed. Traces of water from combined organic layer were removed with MgSO₄ and the solvent was evaporated to dryness to afford an amber oil. No carboxylation reaction was observed.

2.5 General Plasma Carboxylation in Anhydrous Solvent



According to the plasma carboxylation in wet solvent procedure (section 2.4) I modified the following parameter as: Anhydrous DMF (50 mL); Argon cathode with single streamer microplasma jet (1.0 SLM) connected to a 239.9 K Ω resistor; DC power supply was adjusted to 1.0 kV giving 4.0 V across measuring resistor (2.17 k Ω) to get a constant current of 1.85 mA. ¹H NMR spectra showed 0.66% of conversion of the starting material diphenylacetylene into 2,3-diphenylpropanoic acid **27**.

2.6 Plasma Carboxylation Without Reducing Agent

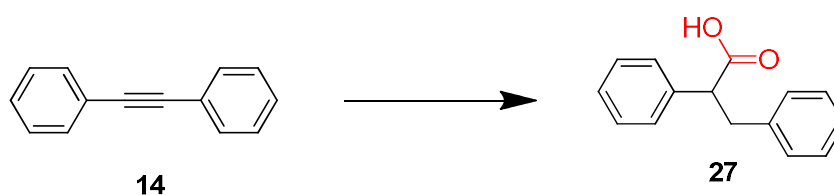


Following the general plasma carboxylation in anhydrous solvent (chapter 2.5), two experiments were carried out (employing TEOA and without TEOA) the following parameters were modified as: Bu₄NI (0.37g, 1.0 mmol); Argon cathode with single streamer microplasma jet (0.5 SLM); DC power supply was adjusted to 1.15 kV giving 8.0 V across measuring resistor (2.17 k Ω) to get a constant current of 3.7 mA. The reactions were monitored by GC/MS and the results are shown in Table **2.5**

Table 2.5 - test of plasma carboxylation with and without reducing agent

Experiment	Product (% yield) 90 min reaction	Product (% yield) 180 min reaction	Product (% yield) 270 min reaction	Product (% yield) 360 min reaction
Without TEOA	0.06	1.2	2.2	4.3
Employing TEOA	0.17	1.8	3.1	3.8

2.7 Use of Catalyst During Plasma Carboxylation



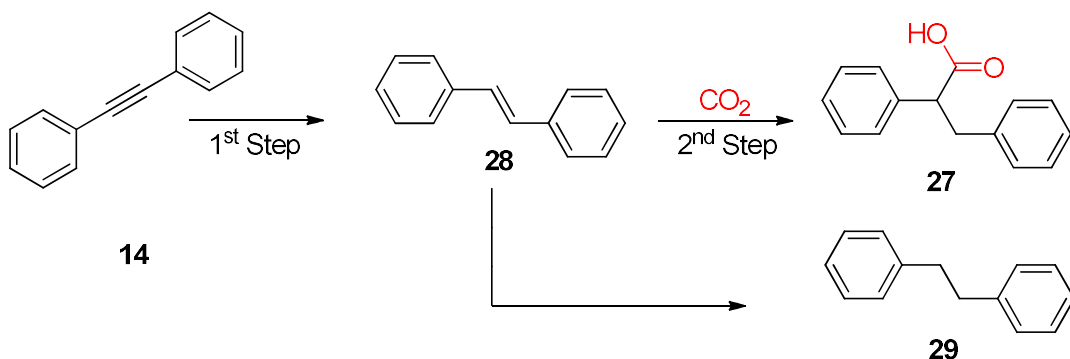
According to the plasma carboxylation in wet solvent procedure (section 2.4) I modified the following parameter as: Single compartment cell of 25 mL with three-neck; Diphenylacetylene **14** (0.09 g, 0.5 mmol); Removed TEOA; Et₄NI (Tetraethylammonium iodide) (0.13 g, 0.5 mmol); Catalyst (5% mmol); Anhydrous DMF (10 mL); Argon cathode with single streamer microplasma jet (0.5 SLM) connected to a 0.24 MΩ resistor; DC power supply was adjusted to 1.35 kV giving 10 V across measuring resistor (2.17 kΩ) to get a constant current of 4.6 mA; 2 h of reaction. The reaction was monitored by GC/MS and the results of the variety of catalysts tested in this experiment are shown in **Table 2.6**.

Table 2.6 - Screening of catalyst employed in the plasma carboxylation of diphenylacetylene

Catalyst	GC/MS Yield (%)
No Catalyst	3.2
RuCl ₃ · 3H ₂ O	2.2
MgBr ₂	1.4
CuBr ₂	1.4
NiCl ₂ glyme	0.6
NiCl ₂ -6H ₂ O	1.9

% yield of carboxylic acid was monitored by GC/MS and calculated according to section 2.1.2

2.8 Formation of 2,3-diphenylpropanoic Acid, Investigation, and Optimization.



According to the plasma carboxylation in wet solvent procedure (section 2.4) I modified the following parameter as: Single compartment cell of 50 mL with three-neck; Substrate (0.5 mmol); Removed TEOA, Et₄NI (0.13 g, 0.5 mmol); Anhydrous DMF (25mL); Argon cathode with single streamer microplasma jet (0.5 SLM) connected to a 0.24 MΩ resistor; DC power supply was adjusted to 1.35 kV giving 10 V across measuring resistor (2.17 kΩ) to get a constant current of 4.6 mA; 2 h of reaction. The reaction was monitored by GC/MS and the results of the variety of catalysts tested in this experiment are shown in Table 2.7. After extraction of the product, the combined organic extracts were purified by column chromatography on silica affording 2,3-diphenylpropanoic acid **27**¹⁴³.

¹H-NMR (400 MHz, CDCl₃) δ 7.33-7.04 (m, 10H, 10 × H_{Ar}), 3.81 (dd, *J* = 9.1, 6.6 Hz, 1H, H5), 3.59 (s, 3H, H12), 3.38 (dd, *J* = 13.8, 9.1 Hz, 1H, H6), 2.98 (dd, *J* = 13.8, 6.6 Hz, 1H, H6') ppm

¹³C-NMR (101 MHz, CDCl₃) δ 174.0 (C11), 139.2 (C4 or C7), 138.8 (C4 or C7), 129.1 (2 × CH_{Ar}), 128.8 (2 × CH_{Ar}), 128.5 (2 × CH_{Ar}), 128.1 (2 × CH_{Ar}), 127.5 (C1 or C10), 126.5 (C1 or C10), 53.7(C5), 52.1 (C12), 39.9 (C6) ppm

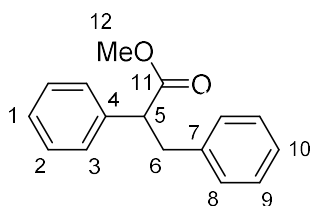
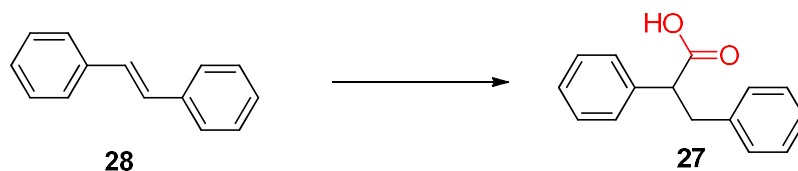


Table 2.7 Comparison of plasma carboxylation of alkene and alkyne with and without CO₂

Substrate	Gas dissolved in the solvent	<i>trans</i> -Stilbene formation (mmol/L)	Bibenzyl formation (mmol/L)	GC Yield (% product)
Diphenylacetylene	CO ₂	0.58	0.01	1.7
Diphenylacetylene	He	1.78	0.81	0.0
<i>trans</i> -Stilbene	CO ₂	-	0.78	4.0

Experiment conditions: Single plasma jet, 4.6 mA, 2 h reaction, 0.5 mmol of solute, 25 mL of DMF
% yield of carboxylic acid was monitored by GC/MS and calculated according to section 2.1.2
When He was employed in the carboxylation of the alkyne, no carboxylic acid formation was observed.

2.9 Determination of Reaction Performance by Splitting Plasma Jet.



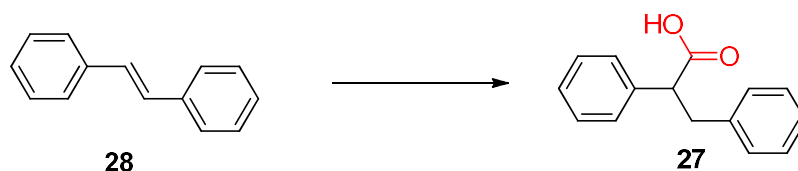
According to the plasma carboxylation in wet solvent procedure (section 2.4) I modified the following parameter as: Single compartment cell of 25 mL with three-neck; *trans*-Stilbene **28** (0.04 g, 0.2 mmol); Removed TEOA, Et₄NI (0.03 g, 0.1 mmol); Anhydrous DMF (10 mL); Argon cathode microplasma jet (0.35 SLM, 1.9 m/s) with 1, 2, 3, and 4 streamers, connected to a 0.47 MΩ resistor; DC power supply was adjusted according to the number of plasma streamer discharge giving 18.0 V across measuring resistor (4.99 kΩ) to get a total constant current of 3.6 mA; 1 h of reaction. The reaction was monitored by GC/MS (Retention time of product **27**: 16.5 min, MW = 240) and the results are shown in Table 2.8.

Table 2.8 Reaction of trans-Stilbene employing different jet configurations.

Number of microplasma channels	DC power input (KV)	Voltage across 4.99 k Ω resistor	Current (mA)	GC Yield (%)
1	1.65	18	3.6	7.3
2	1.10	18	3.6	8.3
3	0.75	18	3.6	7.0
4	0.65	18	3.6	5.6

Experiment conditions: Argon single plasma jet, 3.6 mA, 1h, 0.1 mmol solute, 10 mL % yield of carboxylic acid was monitored by GC/MS and calculated according to section 2.1.2

2.10 Screening of Applied Current



According to the plasma carboxylation in wet solvent procedure (section 2.4) I modified the following parameter as: Single compartment cell of 50 mL with three-neck; *trans*-Stilbene **28** (0.18 g, 1.0 mmol); Removed TEOA, Et₄NI (0.13 g, 0.5 mmol); Anhydrous DMF (25.0 mL); Argon cathode with double streamer microplasma jet (0.35 SLM, 1.9 m/s) connected to a 0.47 M Ω resistor; DC power supply was adjusted to (0.60, 0.80, and 0.9) kV to give currents of (2.50, 3.50, and 4.57) mA respectively; Measuring resistor of 5.03 k Ω ; 2 h of reaction. The reaction was monitored by GC/MS (Retention time of product **27**: 16.5 min, MW = 240) and the results are shown in Table 2.9.

Table 2.9 Screening of applied current in plasma carboxylation of *trans*-Stilbene.

DC power input (KV)	Voltage across 5.03 k Ω resistor	Current (mA)	GC Yield (% product)
0.90	23.0	4.57	2.97
0.80	17.6	3.50	2.13
0.60	12.6	2.50	1.24

Experiment conditions: Argon double plasma jet, 2 h, 1.0 mmol solute, 25 mL

% yield of carboxylic acid was monitored by GC/MS and calculated according to section 2.1.2

2.11 Effect of Current Density

According to the plasma carboxylation in wet solvent procedure (section 2.4) I modified the following parameter as: Single compartment cell of 25 mL with three-neck; *trans*-Stilbene **28** (0.04 g, 0.2 mmol); Removed TEOA, Et₄NI (0.03 g, 0.1 mmol); Anhydrous DMF (10 mL); Argon cathode double streamer microplasma jet (0.35 SLM, 1.9 m/s) connected to a 0.47 M Ω resistor; DC power supply was adjusted to 1.10 kV giving 18 V across measuring resistor (4.99 k Ω) to get a constant current of 3.6 mA; 1 h of reaction.

The size of carbon fiber anode varied, where the larger the area of the electrode in contact with liquid, the lower the current density. The reaction was monitored by GC/MS, (Retention time of product **27**: 16.5 min, MW = 240) and the results are shown in Table 2.10.

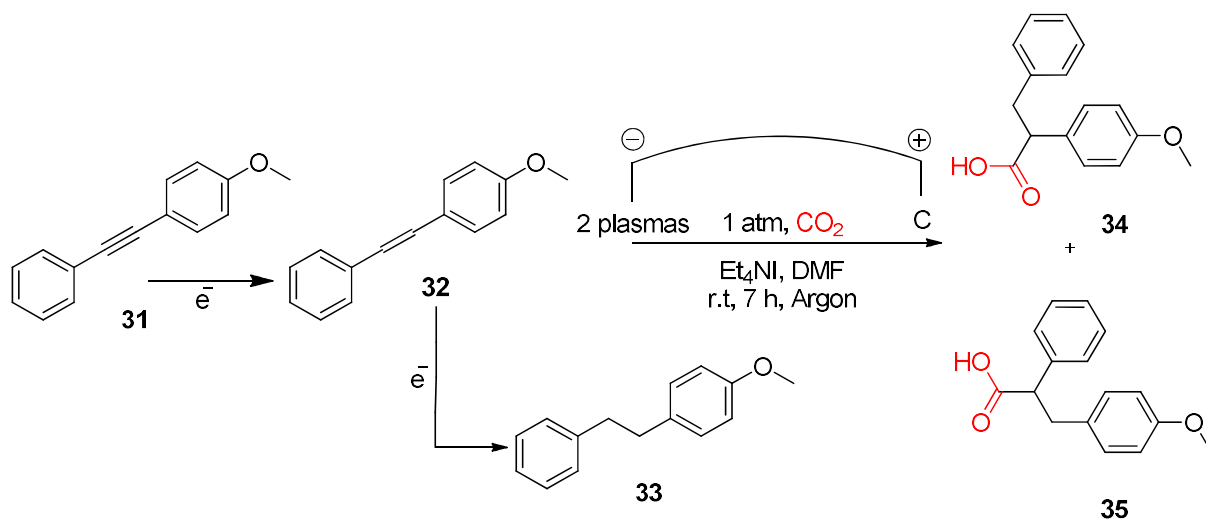
Table 2.10 Interference of current density in the % of yield in plasma carboxylation of *trans*-Stilbene

Surface area of electrode cm ²	Current density (mA/cm ²)	GC Yield (% product)
0.97	3.70	9.03
0.50	7.17	9.17
0.19	19.13	9.39

Experiment conditions: Argon double plasma jet, 3.6 mA, 1 h, 0.2 mmol solute, 10 mL

% yield of carboxylic acid was monitored by GC/MS and calculated according to section 2.1.2

2.12 Plasma Carboxylation of 1-Methoxy-4-(phenylethynyl)benzene (phenylethynyl)benzene



According to the plasma carboxylation in wet solvent procedure (section 2.4) I modified the following parameter as: Single compartment cell of 25 mL with three-neck; 1-methoxy-4-(phenylethynyl)benzene **31** (0.21, 1.0 mmol); Removed TEOA; Et_4NI (0.03 g, 0.1 mmol); Anhydrous DMF (10 mL); Carbon fiber anode (0.19 cm^2); Argon cathode double streamer microplasma jet (0.35 SLM, 1.9 m/s) connected to 0.47 M Ω resistor; DC power supply was adjusted to 1.10 kV giving 18 V across measuring resistor (4.99 k Ω) to get a constant current of 3.6 mA; 7 h of reaction. The reaction was monitored by GC/MS, (Retention time of product **27**: 15.6 min, MW = 270) and the results are shown in Figure 2.8.

After extraction of the product, the combined organic extracts were purified by column chromatography on silica affording a mix of 2-(4-methoxyphenyl)-3-phenylpropanoic acid **34** and 3-(4-Methoxyphenyl)-2-phenylpropionic acid **35** (0.037g, 17.8% isolated yield). 1H -NMR (500 MHz, $CDCl_3$) δ 7.33-6.74 (m, 20H, 20 \times H_{Ar}), 3.84-3.80 (1H), 3.79-3.77 (2H), 3.76-3.74 (1H), 3.40-3.31 (1H), 3.03-2.94 (1H). ^{13}C -NMR (125 MHz, $CDCl_3$) 207.2, 130.0, 129.2, 129.0, 128.8, 128.4, 128.2, 127.6, 126.5, 114.1, 113.8, 77.6, 77.4, 77.1, 76.8, 55.3, 55.3, 53.5, 52.3, 39.5, 38.6, 31.1, 1.1

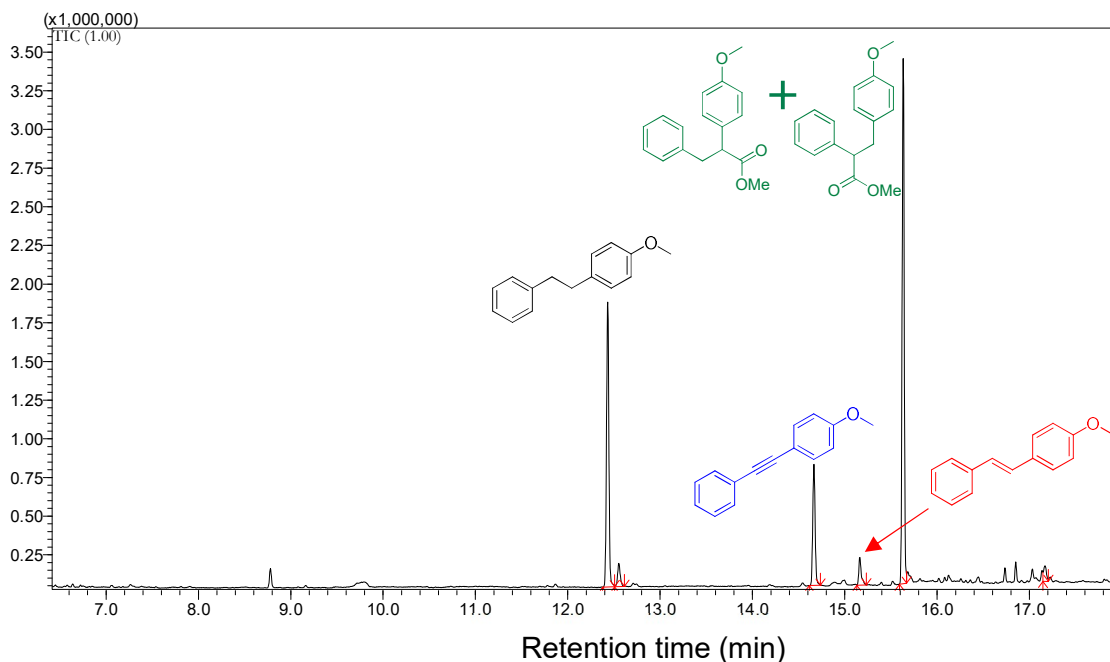
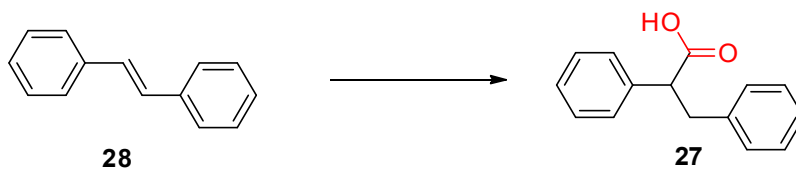


Figure 2.8 - GC-MS spectra of plasma carboxylation of 1-methoxy-4-(phenylethynyl)benzene before purification
 Experiment conditions: Argon double plasma jet (0.35 SLM), constant CO₂ (10 SCCM), 3.6 mA, 7 h, 1.0 mmol solute, 0.1 mmol of Et₄Nl, 10 mL of DMF

2.13 Conversion Rate and Current Efficiency Study



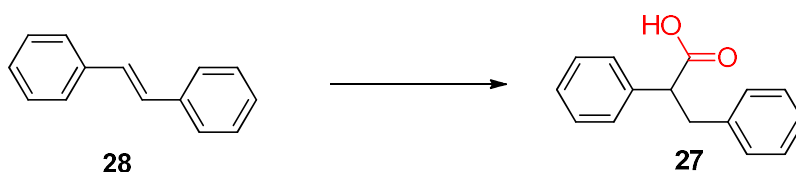
According to the plasma carboxylation in wet solvent procedure (section 2.4) I modified the following parameter as: Single compartment cell of 25 mL with three-neck; *trans*-Stilbene **28** (0.04 g, 0.2 mmol); Removed TEOA, Et₄Nl (0.03 g, 0.1 mmol); Anhydrous DMF (10 mL); Carbon fiber anode (0.19 cm²) ; Argon cathode double streamer microplasma jet (0.35 SLM, 1.9 m/s) connected to a 0.47 MΩ resistor; DC power input was adjusted to (1.0, 1.1, 1.2, and 1.25) KV to give currents of (2.8, 3.4, 4.0, and 4.6) mA respectively; 2 h of reaction. The reaction was monitored by GC/MS, (Retention time of product **27**: 16.5 min, MW = 240) and the results are shown in **Table 2.11**.

Table 2.11 - Interference of current density in the percentage of yield in plasma carboxylation of *trans*-Stilbene

DC power input (KV)	Voltage across 4.99 k Ω resistor	Current (mA)	GC Yield (% product)	Current Efficiency (%)
1.0	14.0	2.8	15.0	28.6
1.1	17.0	3.4	18.5	29.1
1.2	20.0	4.0	21.6	28.8
1.25	23.0	4.6	23.1	26.8

Experiment conditions: Argon double plasma jet (0.35 SLM), constant CO₂ (10 SCCM), 2.8 mA, 2 h, 0.2 mmol solute, 0.1 mmol of Et₄NI, 10 mL of DMF.

2.14 Plasma Carboxylation Solvent Optimization



According to the plasma carboxylation in wet solvent procedure (section 2.4) I modified the following parameter as: Single compartment cell of 25 mL with three-neck; *trans*-Stilbene **28** (0.04 g, 0.2 mmol); Removed TEOA, Et₄NI (0.03 g, 0.1 mmol); Solvent (10 mL); Carbon fiber anode (0.19 cm²) ; Argon cathode double streamer microplasma jet (0.35 SLM, 1.9 m/s) connected to a 0.47 M Ω resistor; DC power input was adjusted to 1.15 KV giving 18 V across measuring resistor (4.99 k Ω) to get a constant current of 3.6 mA; 1 h of reaction. The reaction was monitored by GC/MS, (Retention time of product **27**: 16.5 min, MW = 240). Over 9 different solvents were tested in this experiment, the solvents were chosen because they are claimed to be less harmful to the environment than DMF. The results are shown in Table 2.12.

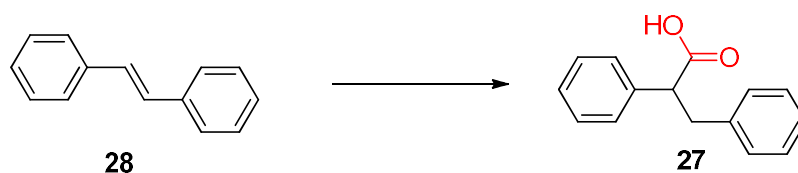
Table 2.12 Alternative solvent study on plasma carboxylation of *trans*-Stilbene

Entry	Solvent	GC Yield (% product)
1	DMF	10.4
2	DCM ^b	≤ 0.1
3	THF ^{a, b}	≤ 0.1
4	Cyrene	≤ 0.1
5	Methanol ^{a, b}	≤ 0.1
6	Acetonitrile ^b	≤ 0.1
7	DMSO	≤ 0.1
8	Propylene Carbonate	0.2
9	D-Limonene	≤ 0.1

^a The substrate was dissolved in DMF (1.0 mL) before dissolution with solvent

^b Condenser Graham connected to the three-neck flask

2.15 Study of Gas Ionization Efficiency



According to the plasma carboxylation in wet solvent procedure (section 2.4) I modified the following parameter as: Single compartment cell of 50 mL with three-neck; *trans*-Stilbene **28** (0.18 g, 1.0 mmol); Removed TEOA, Et₄Ni (0.13 g, 0.5 mmol); Anhydrous DMF (25 mL); Carbon fiber anode (0.19 cm²); Argon cathode double streamer microplasma jet (0.35 SLM, 1.9 m/s) connected to a 0.15 MΩ resistor; DC power input was adjusted to 0.65 KV giving 23 V across measuring resistor (5.03 kΩ) to get a constant current of 4.6 mA; 2 h of reaction. The reaction was monitored by GC/MS, (Retention time of product **27**: 16.5 min, MW = 240). The results are shown in Table 2.13.

Table 2.13 Carboxylation of *trans*-Stilbene under helium and argon background plasma gas

Entry	Background plasma gas	GC Yield (% product)	Current Efficiency (%)
1	Helium	2.4	14
2	Helium	1.7	10
3	Argon	5.3	31
4	Argon	5.8	34

Experiment conditions: Double plasma jet (0.35 SLM), constant CO₂ (10 SCCM), 4.6 mA, 2 h, 1.0 mmol solute, 0.5 mmol of Et₄NI, 25 mL of DMF, carbon anode.

2.16 Complete Reaction Conversion

2.16.1 Reaction “A”

According to the plasma carboxylation in wet solvent procedure (section 2.4), the reaction was repeated with the modification of the following parameter: Single compartment cell of 25 mL with three-neck; *trans*-Stilbene **28** (0.04 g, 0.2 mmol); Removed TEOA, Et₄NI (0.03 g, 0.1 mmol); Anhydrous DMF (10 mL); Carbon fiber anode (0.19 cm²); Argon cathode double streamer microplasma jet (0.35 SLM, 1.9 m/s) connected to a 0.46 MΩ resistor; DC power input was adjusted to 1.05 kV giving 18 V across measuring resistor (4.99 kΩ) to get a constant current of 3.6 mA; 21 h of reaction; The reaction was monitored by GC/MS, (Retention time of product **27**: 16.5 min, MW = 240). (GC Yield: 43.4%, C.E: 6.1%).

2.16.2 Reaction “B”

The experiment described in section 2.16.1 was repeated, therefore, with substitution of electrolytic salt Et₄NI by LiBF₄ (Lithium Tetrafluoroborate) (0.009 g, 0.1 mmol) at a constant current of 3.6 mA for 13 h and the result obtained was: (Yield: 35.3%, C.E: 8.0%).

2.16.3 Reaction “C”

The experiment described in section 2.16.1 was repeated for the third time with the modification of the following parameters: Employed the electrolytic salt LiBF₄

(0.009 g, 0.1 mmol) in substitution of Et₄Nl, DMF was prepared with 2-propanol (IPA) making a solution of DMF:IPA (10 mL) (95:5), at a constant current of 3.6 mA for 14 h (Yield: 57.2%, C.E: 14.0%).

2.16.4 Reaction “D”

The experiment described in section 2.16.1 was repeated for the fourth time with the modification of the following parameters: All glassware dried in the oven at 125°C for 24 h, solvents were dried with activated molecular sieves 3A for 24 h. Argon was connected into drying column filled with silica gel previously dried in the oven at 125 °C for 24 h and CO₂ was connected into drying column filled with molecular sieves 3A previously activated in microwave at 600 °C for 20 min. The substrate was carboxylated for 5 h (Yield: 49.3%, C.E: 29.1%) (0.037 g, 17.8% isolated yield).

2.17 Plasma Carboxylation of Alternative Substrate

According to the Reaction “B” procedure (section 2.16.4), the reaction was repeated employing a variety of substrate listed in Table 2.14, the carboxylation was carried for 1 h and monitored by GC/MS. The reaction time of 1 h conducted in this experiment is intended only to observe the possibility of carboxylation of different substrates.

Table 2.14 List of more substrates exposed to plasma carboxylation

Entry	Substrate		GC Yield (% product)	^a Mass-spectrum
1	Styrene	22	3.1	<i>Figure 2.9</i>
2	Phenylacetylene	10	3.9	<i>Figure 2.10</i>
3	4-tert-Butylstyrene	38	6.4	<i>Figure 2.11</i>
4	1,1-Diphenylethylene	36	6.4	<i>Figure 2.12</i>
5	4-Methoxystyrene	40	6.6	<i>Figure 2.13</i>
6	cis-Stilbene	30	6.4	<i>Figure 2.14</i>

Experiment conditions: Double plasma jet (0.35 SLM), constant CO₂ (10 SCCM), 3.6 mA, 1 h, 0.1 mmol solute, 0.1 mmol of LiBF₄, DMF:IPA (10 mL) (95:5), carbon anode.

^a is the GC spectra of GC/MS analysis and mass-spectrum of corresponding methyl ester of carboxylic acid.

Substrate Styrene **22** and the retention time of its corresponding carboxylic acid methyl 3-phenylpropanoate (6.2 min, MW = 164) (Figure 2.9).

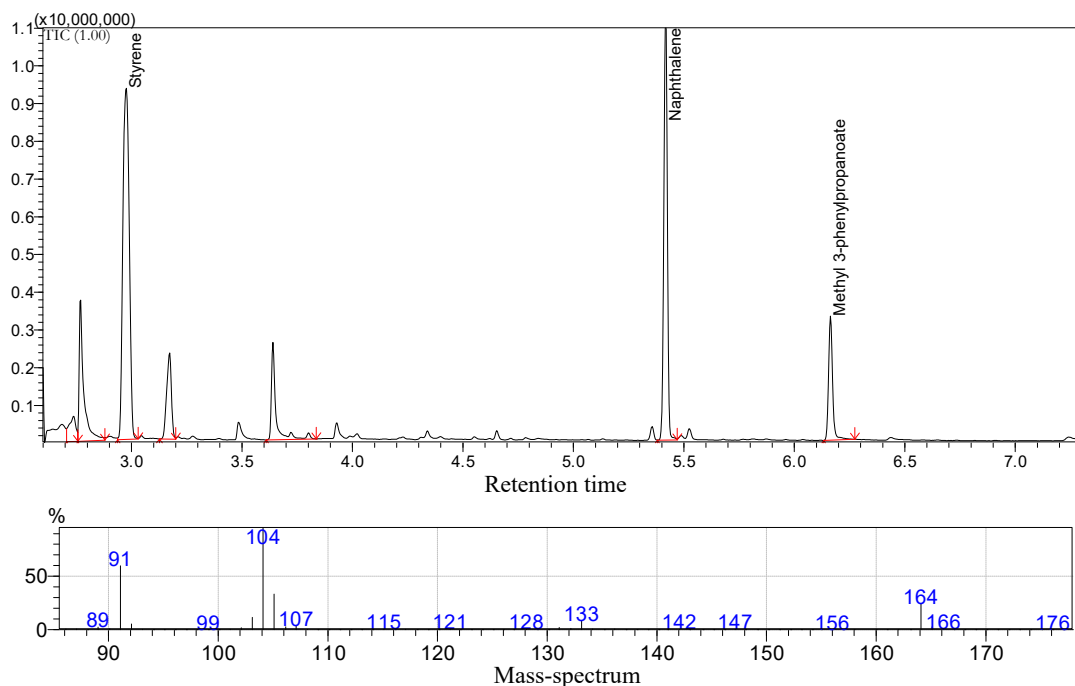


Figure 2.9 - GC-MS spectra of plasma carboxylation of Styrene and the mass-spectrum methyl 3-phenylpropanoate.

Substrate Phenylacetylene **10** and the retention time of its corresponding carboxylic acid methyl 3-phenylpropanoate (6.2 min, MW = 164) (Figure 2.10).

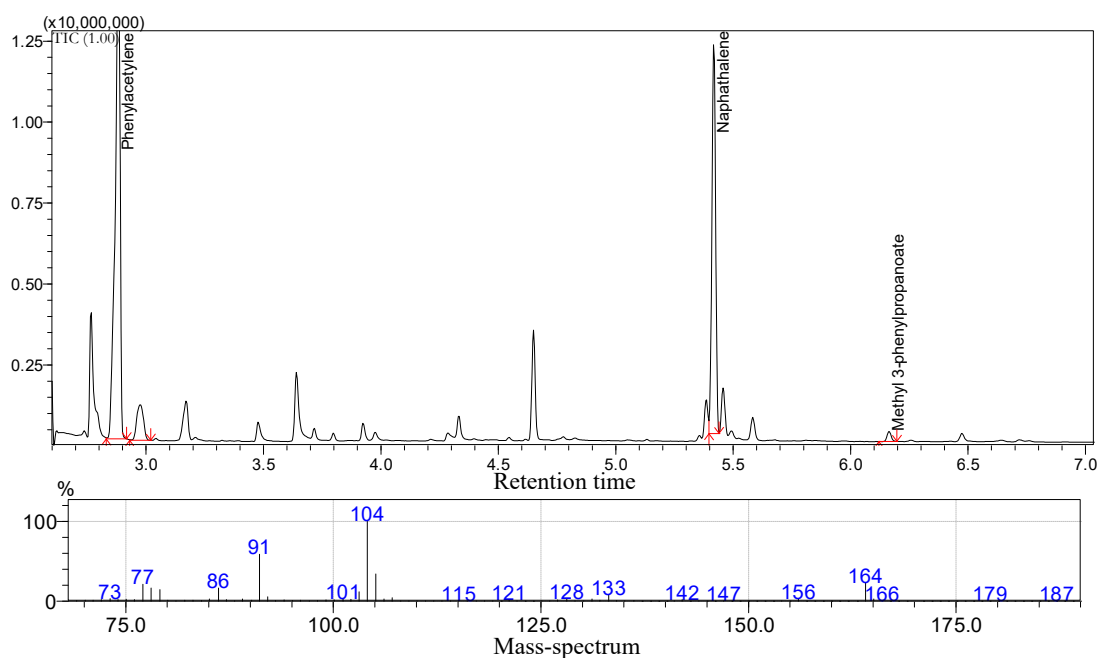


Figure 2.10 - GC-MS spectra of plasma carboxylation of Phenylacetylene and the mass-spectrum of methyl 3-phenylpropanoate.

Substrate 4-tert-Butylstyrene **38** and the retention time of its corresponding carboxylic acid methyl 3-(4-tert-butylphenyl)propanoate (9.9 min, MW = 220) (Figure 2.11).

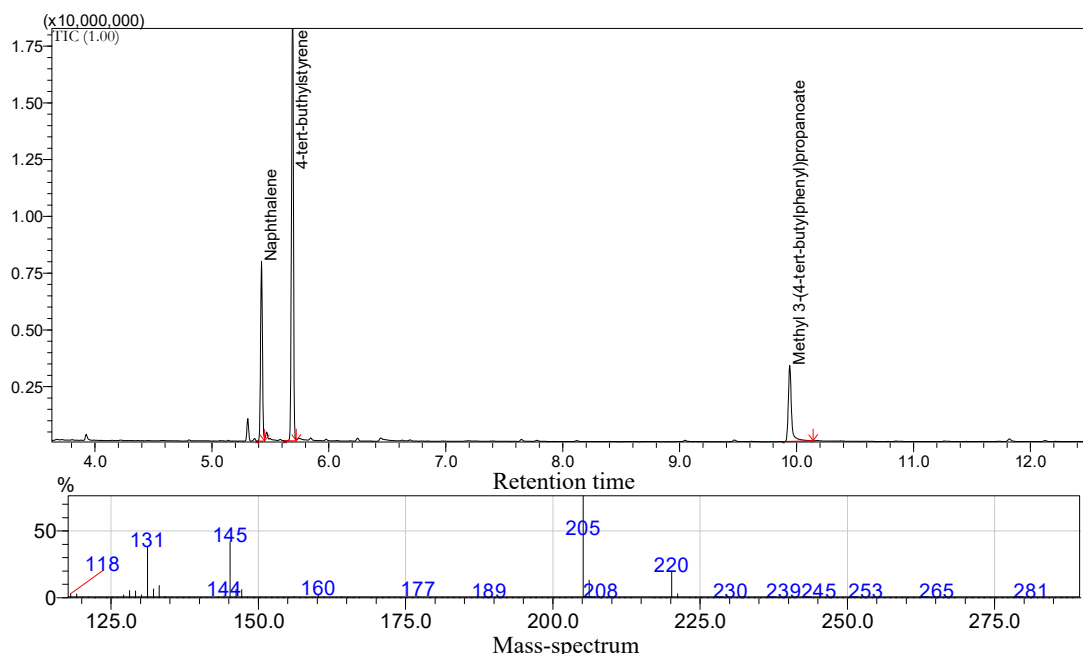


Figure 2.11 - GC-MS spectra of plasma carboxylation of 4-tert-butylstyrene and the mass-spectrum of 3-(4-tert-butylphenyl)propanoate.

Substrate 1,1-Diphenylethylene **36** and the retention time of its corresponding carboxylic acid Me 3,3-Diphenylpropanoic acid (15.7 min, MW = 240) (Figure 2.12).

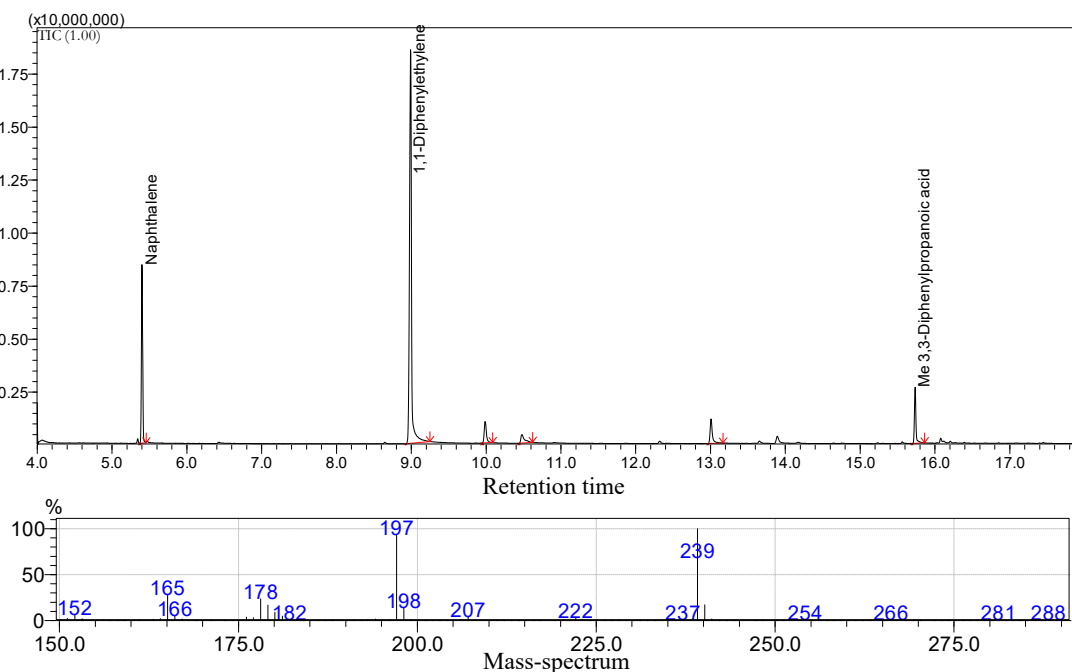


Figure 2.12 - GC-MS spectra of plasma carboxylation of 1,1-Diphenylethylene and the mass-spectrum of Me 3,3-Diphenylpropanoic acid.

Substrate 4-Methoxystyrene **40** and the retention time of its corresponding carboxylic acid Methyl 3-(methoxyphenyl)propanoate (9.1 min, MW = 194) (Figure 2.13).

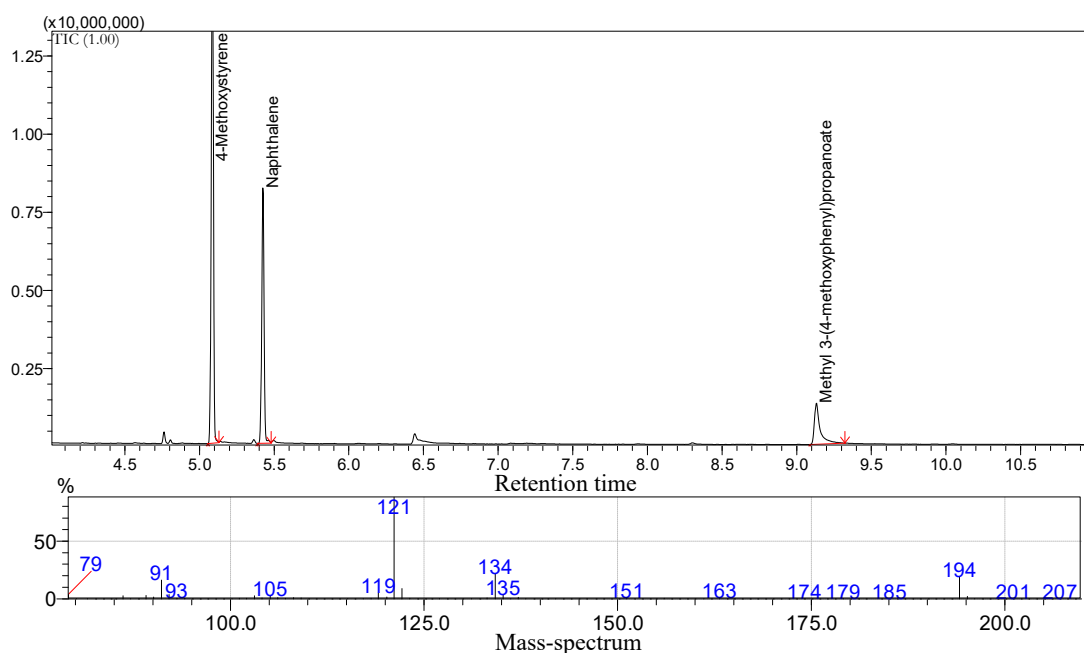


Figure 2.13 - GC-MS spectra of plasma carboxylation of 4-Methoxystyrene and the mass-spectrum of Methyl 3-(methoxyphenyl)propanoate.

Substrate *cis*-Stilbene **30** and the retention time of its corresponding carboxylic acid Methyl 3-phenylpropanoate (12.6 min, MW = 240) (Figure 2.14).

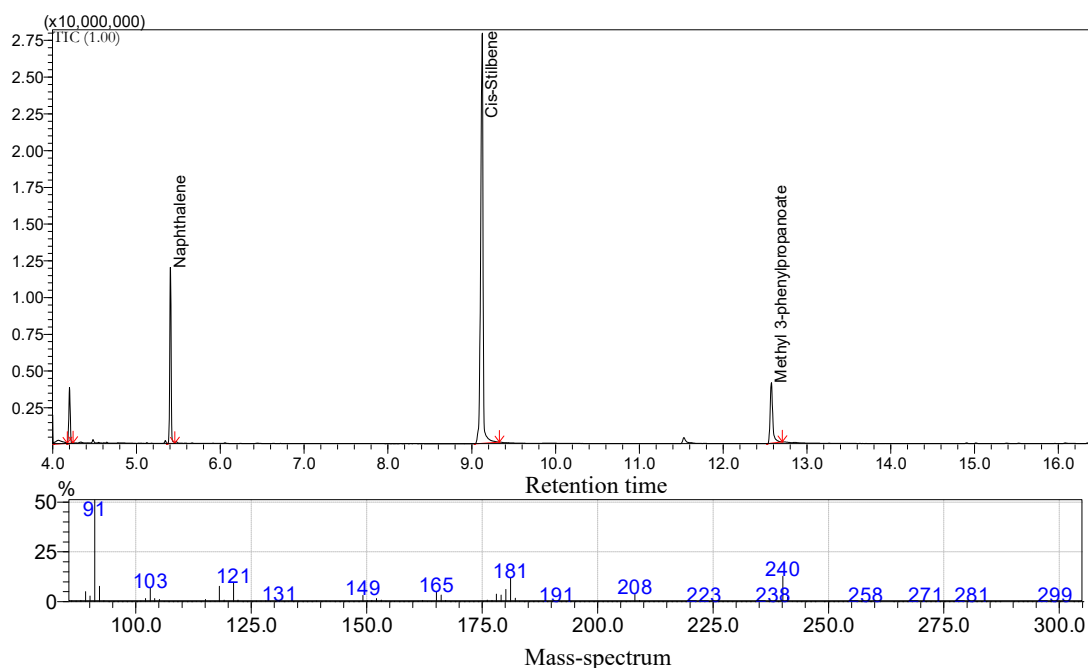


Figure 2.14 - GC-MS spectra of plasma carboxylation of *cis*-Stilbene and the mass-spectrum of Methyl 3-phenylpropanoate.

3.0 Results and Discussion

3.1 Original Research: Investigation

To begin this research, a replication of reactions conducted by Buckley's group was carried out in order to become familiar with the reaction setup. The traditional method of electrochemical reactions was taken using two-compartment cells, a salt bridge or exchange membrane to allow the electron transfer, and a sacrificial electrode which as discussed before, oxidizes providing electrons.¹⁴⁴ However the drawback of the use of sacrificial electrode is the waste oxidized material that is left after the complete process.¹⁴⁵

This experiment was carried in a single compartment cell (Figure 3.1 - Electrochemical cell setup). Styrene **22** was chosen due to known reaction mechanism, using copper cathode and aluminium anode, the reaction with carbon dioxide was carried out under atmospheric pressure at 60 mA to yield dicarboxylic acid **23**. (Scheme 17)

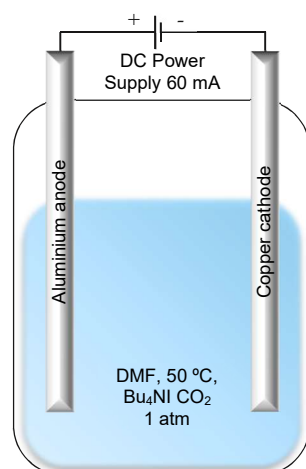


Figure 3.1 - Electrochemical cell setup

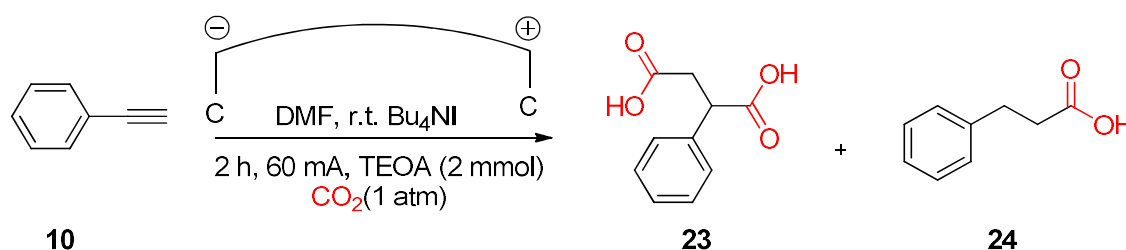
Although DMF is harmful and not environmentally friendly solvent, it is widely used in electrochemistry due to its high dielectric constant (36.7 at 25 °C), low vapour pressure (3.7 Torr at 25 °C),¹⁴⁶ high potential window, and relatively low cost.

3.1.1 Test of Reducing Agent

Following familiarization with the cell setup, I moved on the study of carboxylation

of alkynes. the need for a sacrificial electrode was removed, employing phenylacetylene **10** (1.0 mmol) under the general procedure for electrocarboxylation using a non-sacrificial electrode (section 2.2.3) in the presence of supporting electrolyte Bu₄NI (0.5 mmol), DMF (50 mL) at 60 mA and TEOA (2.0 mmol) for 2 h resulting in the formation of dicarboxylic acid **23** and monocarboxylic acid **24**.

Two experiments were carried in this test, where in one of the experiments TEOA (2.0 mmol) was added as reducing agent with carbon fiber rod anode and cathode, in the second experiment there was no addition of reducing agent, copper cathode and Al anode were selected as an electrode, all the others parameter were kept identical. (Scheme 19)



Scheme 19 - Test of carboxylation employing a reducing agent

The results of those short tests reactions are shown in Table 3.1. The results showed no variation in terms of the ratio of the product formation and once again proving that the reducing agent can successfully substitute the sacrificial electrode.

Table 3.1 - Test of carboxylation employing a reducing agent.

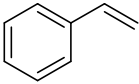
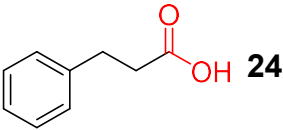
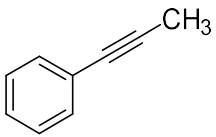
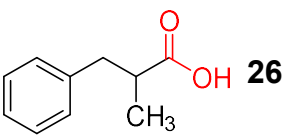
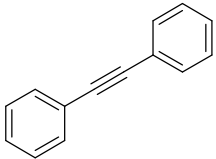
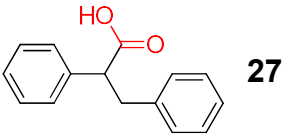
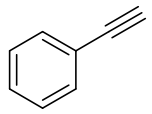
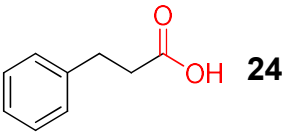
Entry	Anode (+)	Cathode (-)	Reducing Agent	Ratio dicarboxylic:mono carboxylic
1	Al	Cu	None	3:1
2	C	C	TEOA	3:1

3.1.2 Alternative Substrates.

The electrocarboxylation was successfully achieved when employing **10** where the sacrificial electrode was substituted by reducing agent TEOA, however, once this

condition was established: carbon anode/cathode connected to a single electrochemical cell, 1.0 mmol of substrate, Bu₄Ni (0.5 mmol) working as supporting electrolyte dissolved in DMF (50 mL) saturated with CO₂ along with TEOA (2.0 mmol) at 60 mA during 2 h of reaction, a range of substrate were tested (Table 3.2) under the test condition (section 2.2.3). Electrocarboxylation of **10** and **22** resulted in the formation of **24**. Carboxylation of **25** led to the formation of **26**, and, **14** to yield **27**, proving that the reducing agent is not only limited to the carboxylation of **10**.

Table 3.2 Electrocarboxylation of a range of substrate employing reducing agent

Entry	Substrate	Product	Conversion (%)
1	 22	 24	100*
2	 25	 26	10
3	 14	 27	95
4	 10	 24	100*

The product formation was identified by ¹H NMR. ¹H NMR → 100% conversion but some of the reactant could have been evaporated prior ¹H NMR.

Reaction conditions: 1 mmol substrate, 2 h reaction, 60 mA, TEOA (2 mmol), DMF (50 mL), Bu₄Ni

3.2 Electrode Properties

Some combinations of cathode and anode material were tested according to electric conductivity in the electrochemical reaction with different concentrations of Bu_4NI (tetrabutylammonium iodide) in DMF (50 mL). The idea was to evaluate how a solution with different concentrations of supporting electrolyte would impact the variation of potential applied at a constant current of 50 mA. The reason for this study is to evaluate the minimum concentration of Bu_4NI in the solution necessary to avoid high resistance, otherwise, some of the power would be dissipated in the liquid wasting the input energy in form of heat.

Seven solutions (50 mL) were prepared with different concentrations of supporting electrolyte (Bu_4NI) in DMF. Initially without Bu_4NI , then 0.5 mmol was dissolved in DMF and the electrolyte concentration was increased up to 3.0 mmol with intervals of 0.5 mmol. The electrodes chosen were carbon, nickel, and copper. The current was set in 50 mA and the power supply automatically adjust the voltage to keep the current constant.

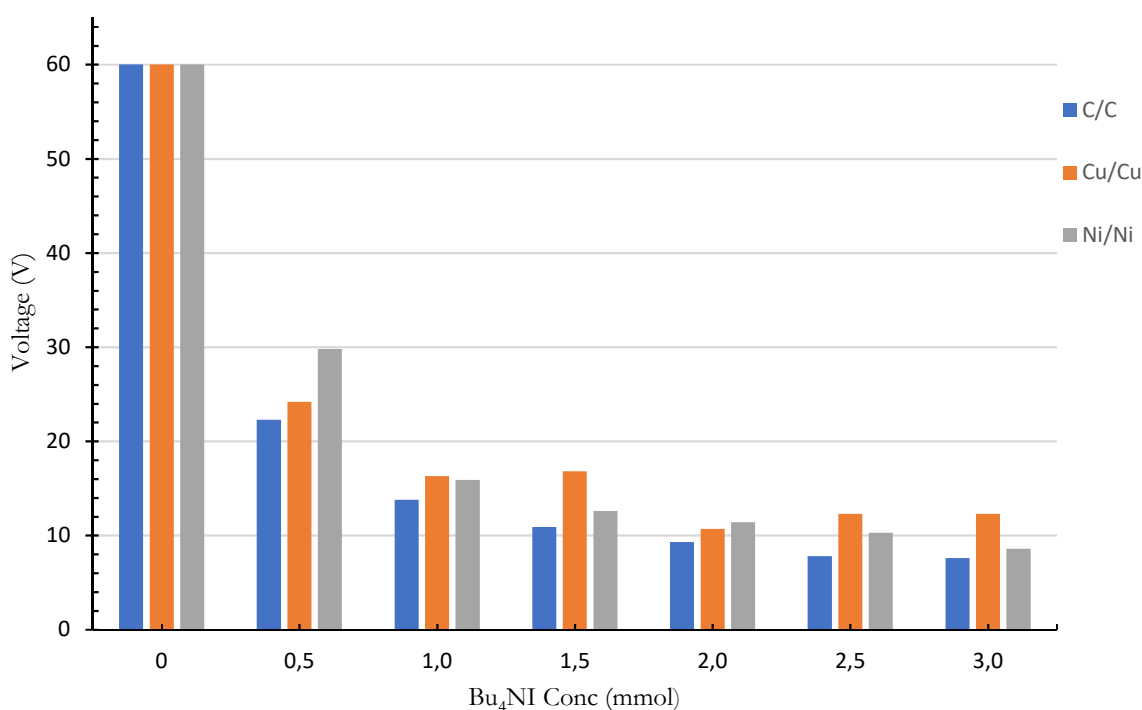


Figure 3.2 Potential applied in electrochemical reaction at different concentration of Bu_4NI to keep the current at 50 mA with different electrode material. No current was observed under zero concentration of electrolyte due to lack of ions.

Figure 3.2 represents the result of this experiment. DMF without Bu₄NI does not allow any current to flow, even increasing the potential to 60 V which is the maximum allowed by the power supply, the current measured was zero, this is due to lack of ions which are essential to the transport of electrons in liquid. With only 0.5 mmol of Bu₄NI the voltage dramatically dropped to roughly 25 V, and after that, the solution already showed almost no difference in the resistance as a function of the concentration of the electrolyte dissolved.

In general, carbon electrodes showed slightly less resistance when compared with others in this study.

3.3 Application of Cold Atmospheric Plasma in CO₂ Conversion-Initial Stages

After successfully achieving the conversion of CO₂ into valuable products through an electrochemical process, the main aim of this research was to move forward and check if the reaction could also be done employing a cold atmospheric plasma jet. Theoretically, the DC plasma jet or microplasma is the most suitable system for chemical conversion since it can be generated at low temperature (non-thermal) and pressure, microplasma jet works as a source of ions and radicals, which are necessary for activating chemical reactions. DC microplasma provides free electrons, thus, eliminating the need for a redox reaction to transfer electrons. In the experiment conducted by Richmonds and Go,¹⁴⁷ where ferricyanide was reduced to ferrocyanide, non-thermal plasma provided free electrons in a reaction scheme.

Background, chemical agents used previously in electrochemical carboxylation of diphenylacetylene **14** to form 2,3-diphenylpropanoic acid **27** was used, however, in the setup experiment, the cathode connected in the flask was replaced by a plasma jet. (Figure 3.3)

This setup experiment consists of a single compartment cell, DC power supply, high voltage anode, grounded plasma cathode and, CO₂ inlet gas bubble.

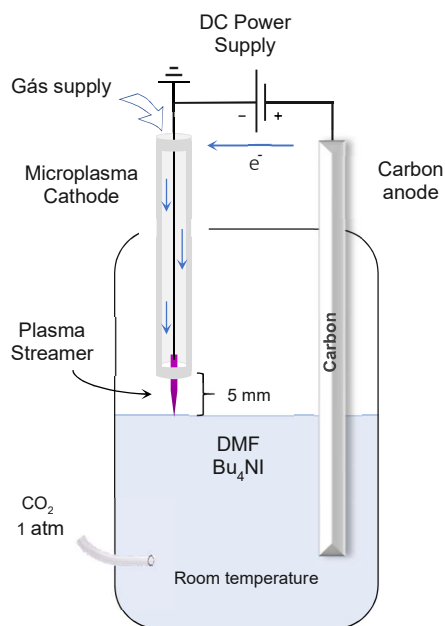


Figure 3.3 General plasma setup experiment

The reagents were added into the flask, the plasma jet cathode was connected to wire, resistors and grounded, the power supply provided high voltage to anode. Gases, supporting equipment and connections were assembled together to enable the plasma experiment (Figure 3.4). The system setup was thoroughly explained in section 2.3.2.

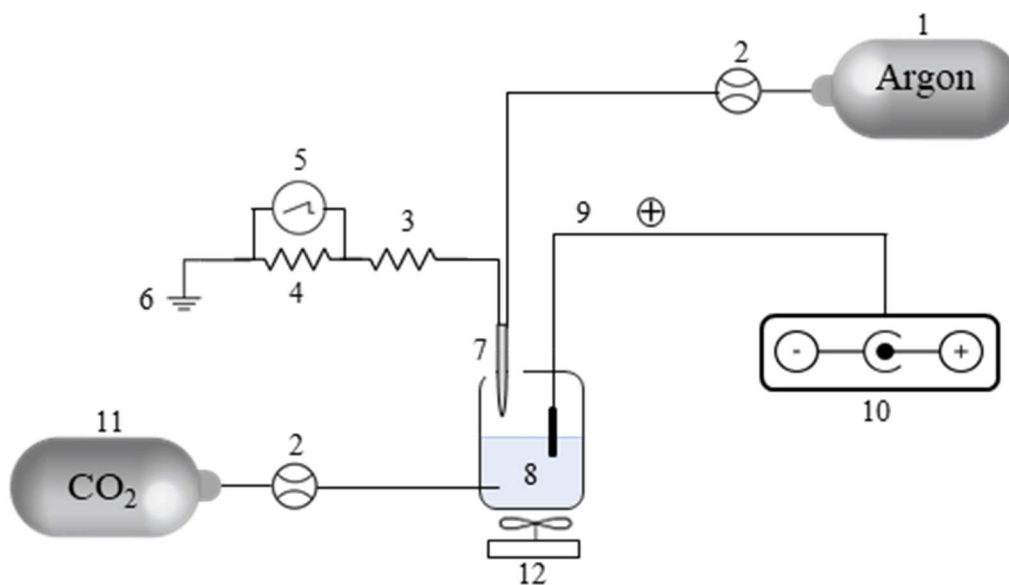


Figure 3.4 - Plasma experiment setup
 1-Argon cylinder, 2-gas flow controller, 3-surface mount resistor, 4-current measuring resistor, 5-oscilloscope, 6-grounding, 7-microplasma jet, 8- three-neck flask, 9-anode, 10- DC power supply, 11-CO₂ cylinder, 12- stirring plate.

The Flashpoint of DMF is 58 °C¹⁴⁸, in order to avoid any possibility of fire when the plasma contacts the solvent (DMF), it was dissolved in water to increase its flashpoint.

The initial attempt was conducted diluting DMF in DI water (5:1, 50 mL) where diphenylacetylene **14** (1.0 mmol), supporting electrolyte Bu₄NI (1.5 mmol) and reducing agent (TEOA, 2.0 mmol) was mixed, carbon anode and argon (1.0 SLM) plasma jet reacted for 3 h (details of plasma setup experiment was given in chapter 2.3.2). It was still unclear if free electrons would be delivered to the target for carboxylation or if it would still be necessary to add a reducing agent, so the reducing agent was kept guaranteeing that the reaction would not fail due to possible lack of a source of electrons.

On completion of the experiment, the sample was dried with magnesium sulfate so the product could be monitored by GC and extracted with diethyl ether to be analysed by ¹H NMR spectroscopy. The first results showed no detection of any traces of conversion to the desired product **27** nor the consumption of the substrate **14**. One of the reasons could be the low current. According to the Ohm's law, the current reached in this reaction was 0.8 mA using a 1.19 MΩ resistor versus 60 mA usually employed in electrochemistry, the voltage across the measuring resistor recorded was 1.74 V. It was assumed that the water present in DMF could be interfering with the reaction.

As the name suggests, a resistor limits the current in the system. Although the liquid, wire, and other components have specific resistance, the current limiting resistor is vital for the flow of the current in the system; the lower the resistance of the resistor allows the system to reach higher current at a lower voltage.

The initial resistor employed (1.19 MΩ) allowed the system to reach 0.8 mA with 1.74 V across the resistor with no conversion. After reducing the resistance of the resistor to 0.51 MΩ, the current could be increased to 1.47 mA. However, after a few minutes, the resistor burned out. It was found that the resistance is not the only important feature when deciding about which resistor to be chosen but power rating as well, which can be calculated using the formula below.

$$p = i^2 \times R \qquad \text{eq. 2.1}$$

Where p is the power in watts, i is the current in the unit of amperes and R is the resistance in ohms.

The power rating of the resistor (1.19 M Ω) was 1.0 W and the power being dissipated was 1.1 W, , the power rating of the resistor was one of the limiting parameters at this point. Thus, for the next experiment, the old resistor was replaced by a 239.9 K Ω resistor with 35 W of power rating. In respect of diluting the solvent in water to avoid fire incident, Later I found that due to the lack of oxygen during the reaction, the liquid was unlikely to catch fire, even if the temperature at the local point where the plasma touches the liquid would heat above 58 $^{\circ}\text{C}$ (Flashpoint of DMF). Therefore, I decided to use DMF without water. In addition, by working with pure DMF the preparation of GC samples would be simpler since it would not be necessary to remove water before the injection. The reaction was repeated as described in the initial attempt but at this time employing DMF ($\geq 99\%$ purity). Again, the GC-MS report still showed no formation of carboxylic acid, however, by applying the amplitude gain which exacerbates the peaks in the JEOL NMR software, it was possible to see 3 CH bonds (dd), the CH_b is also doublet of doublets but one of the peaks is overlapping with Ethyl Acetate's peaks. This splitting pattern matches with the target carboxylic acid **27**.¹⁴³ (Figure 3.5)

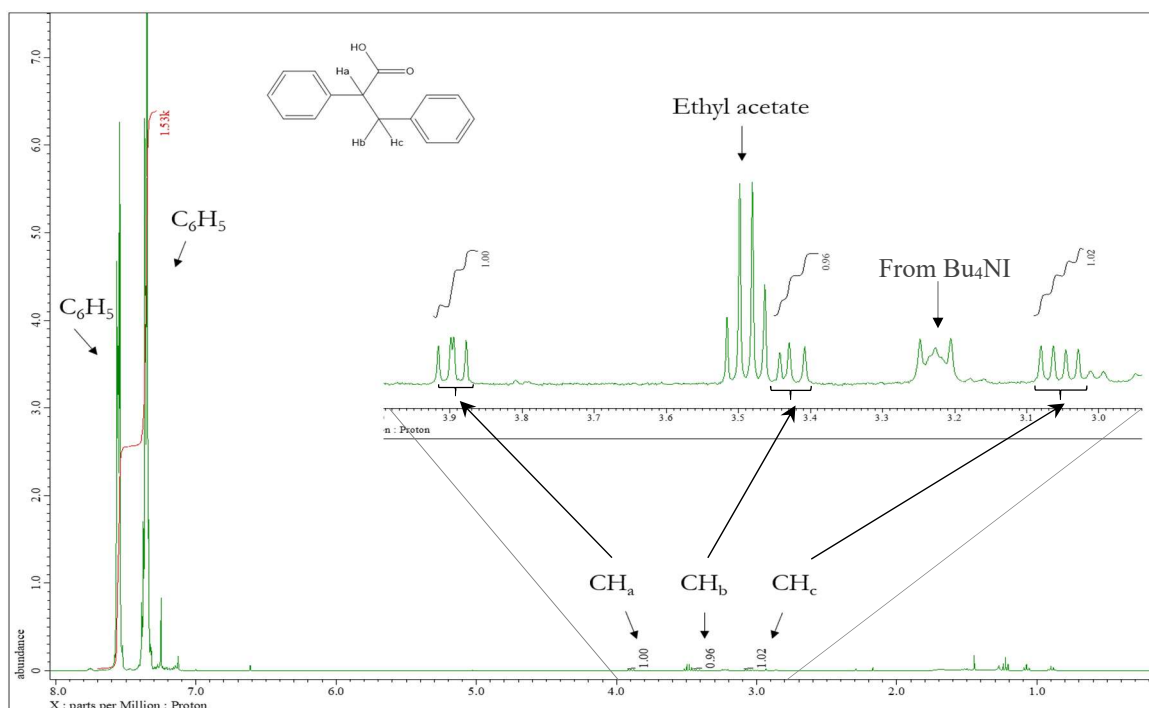


Figure 3.5 ^1H NMR spectra, the first observation of plasma carboxylation of diphenylacetylene

The carboxylic acid was identified with a conversion of 0.66% (^1H NMR integration of peaks vs aromatic H) and thus further optimization was necessary in order to increase the conversion and enhance the efficiency of the method.

3.3.1 DC Power Supply Damage

The power supply chosen to conduct these experiments is able to deliver up to a maximum of 5 mA at 5 kV, if for some reason there are an overload or short circuit a circuit breaker trips to immediately discontinue electrical flow. As soon as I found out that higher current resulted in higher conversion, I decided to continue with the optimization experiment with 4,6 mA which was still below the limit.

The power supply contains a capacitor which is a passive two-terminal electrical component that stores potential energy in an electric field known as capacitance, thus a capacitor is a component designed to add capacitance to a circuit. In power supplies, capacitors are used to smooth (filter) the pulsating DC output after rectification so that a nearly constant DC voltage is supplied to the load.¹⁴⁹

During one of the experiments, the capacitor located inside the power supply exploded and after investigation, I found out that it happened for two main reasons: First, capacitors are prone to failure if overstressed and most of the experiments were carried near to the maximum limit of current, and second is the fact that many times the power supply tripped out and this happened when the safe working limit was reached.

The repeated times that the power supply trips out summed to the overstress are the most plausible cause to explode the capacitor. After this experience, the current in the optimizing experiment was reduced to 3.6 mA and I did not observe any more issues related to the power supply.

3.3.2 Plasma Carboxylation Without the Need for a Reducing Agent

As mentioned in the literature, previous researchers have demonstrated the ability to transfer electrons and reduce species through the utilisation of a plasma reactor.¹ I wished to prove that on the contrary to electrochemical carboxylation process, there will not be a requirement for a sacrificial electrode or reducing agent

such as TEOA, where all the electrons needed in this carboxylation process would be provided by the plasma jet.

Two experiments were carried with a single plasma jet at 8.0 V, 3.7 mA at room temperature and atmospheric pressure; diphenylacetylene **14** (1.0 mmol) was mixed in DMF (50 mL), Bu₄NI (1.0 mmol) and kept under constant stirring with a stream of CO₂ (10 SCCM). In one of the experiments, TEOA (2.0 mmol) was added and in the other experiment, there was no addition of TEOA. The reaction was carried out for 3 h and the product was monitored by GC/MS, the results can be seen in Figure 3.6.

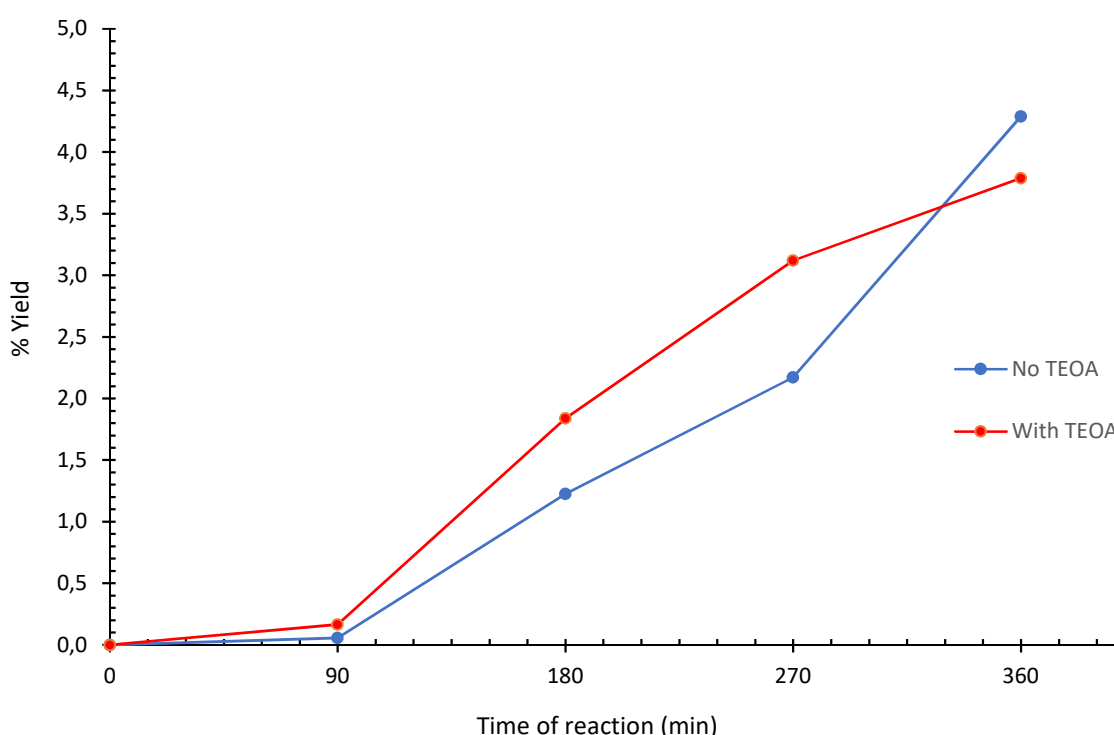


Figure 3.6 Test of plasma carboxylation of diphenylacetylene with and without reducing agent
Red line represents the experiment carried with the addition of TEOA (2.0 mmol) and blue line represents the experiment carried without the addition of TEOA. General experiment conditions are: 3.7 mA, 1.0 mmol of starting material, 50 mL of DMF, Bu₄NI (1.0 mmol) and constant CO₂ (10 SCCM). Target product monitored by GC-MS and yield calculated according to section 2.1.2.

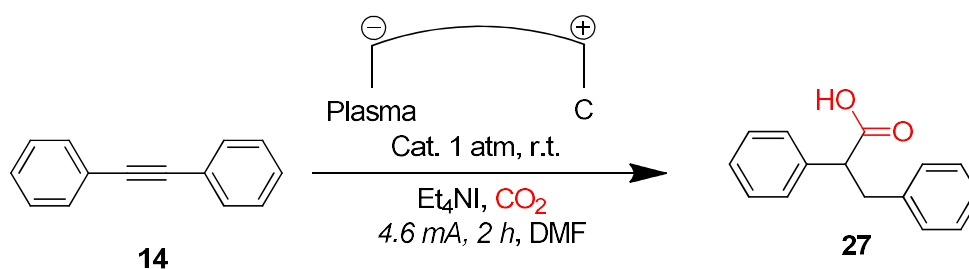
This experiment provided evidence that in the plasma carboxylation process, the reducing agent TEOA made no difference in respect of the conversion of the substrate to form the correspond carboxylic acid, therefore, the TEOA was not required as electrons were being provided by the plasma system. So, further optimization of the method would be done without a reducing agent.

3.3.3 Use of Catalyst During Plasma Carboxylation

The use of catalyst has been widely investigated and already improved numerous reaction including CO₂ reduction.^{5,85,150,151} Wang converted alkyne into carboxylic acid with 94% of isolated yield employing nickel chloride and ligand.⁸⁸

Here, the insertion of a metal catalyst was explored. In this work (Scheme 20), diphenylacetylene (0.5 mmol) was dissolved in DMF (10 mL) along with tetraethylammonium iodide (0.5 mmol) and catalyst (5% mmol). The solution was in constant stirrer under CO₂ (10 SCCM). Single plasma jet striking under argon (0.5 SLM) at 4.6 mA for 2 h.

On completion of the experiment, 500 μ L was collected, added IS (50 μ L of naphthalene 0.05 mol/L), methylated and analyzed by GC/MS. The percentage yield was calculated using the calibration curve.



Scheme 20 - Plasma carboxylation of diphenylacetylene using catalyst

The catalysts used in this experiment was plotted in Table 3.3.

Table 3.3 - Screening of catalyst used in the plasma carboxylation of diphenylacetylene to form 2,3-diphenylpropanoic acid.

Catalyst	Yield (%) ^a
No Catalyst	3.2
RuCl ₃ · 3H ₂ O	2.2
MgBr ₂	1.4
CuBr ₂	1.4
NiCl ₂ glyme	0.6
NiCl ₂ -6H ₂ O	1.9

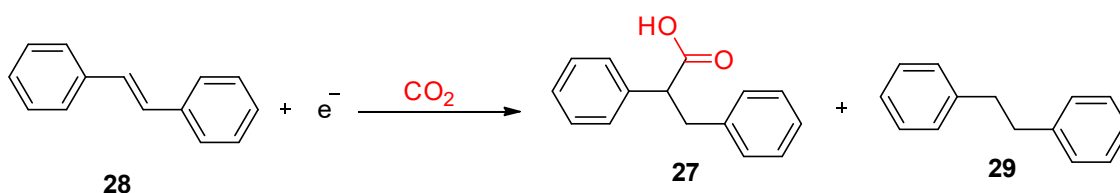
^a Yield calculated by GC/MS according to section 2.1.2

Experiment conditions: 0.5 mmol of starting material (SM), 0.5 mmol of Et₄Ni, catalyst (5% mmol), 10 mL of DMF, 2 h reaction, carbon anode, single argon plasma jet cathode, 4.6 mA, constant CO₂ at 10 SCCM.

According to table 3.3, none of the catalysts chosen presented any significant increase in the percentage yield when compared with reaction without catalyst, and in some cases the result was even worse.

3.3.4 Interesting finding

During the optimization experiments carried out with *trans*-Stilbene in plasma carboxylation, although very selective I still observed the reduction to bibenzyl **29** as one of the major side reactions (Scheme 21).



Scheme 21 - Plasma carboxylation of *trans*-Stilbene and reduction to alkane

Following a general condition setup, a range of different scenarios were modified, for instance, the initial substrate concentration, volume, and type of solvent, electrode material, and ionic salt were varied, and a common observation was the reduction of *trans*-Stilbene to bibenzyl (Figure 3.7). Consequently, interfering with the carboxylation of alkene, this occurred due to electron-withdrawing (electrons that supposed to be employed in the carboxylation but was directed to reduction of alkene to alkane) and so reducing the current efficiency.

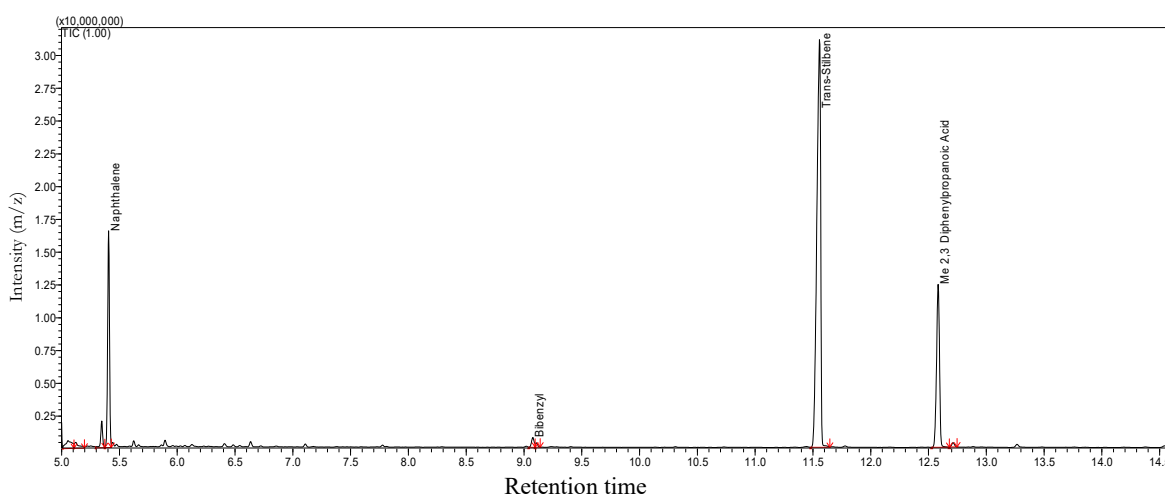


Figure 3.7 - GC-MS spectra of plasma carboxylation of *trans*-Stilbene and the side reaction of reduction to bibenzyl.

As observed in Figure 3.8, among all the experiments tested, the reduction of *trans*-Stilbene to bibenzyl ranged from 0.4% (Figure 3.9 - A) to 8.7% yield (Figure 3.9 - B), however, when employing copper(II) sulfate pentahydrate as electrolyte, the formation of bibenzyl rose to 55.1% yield (Figure 3.9 - C) dropping the conversion of carboxylic acid to 1.9%.

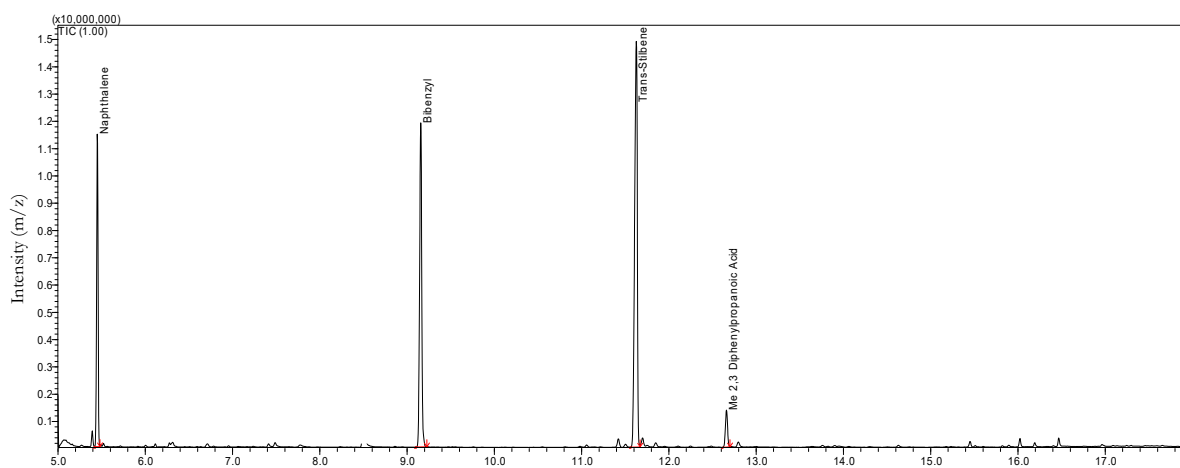


Figure 3.8 - GC-MS spectra of plasma carboxylation of *trans*-Stilbene employing $\text{CuSO}_4 \cdot 5\text{H}_2\text{O}$

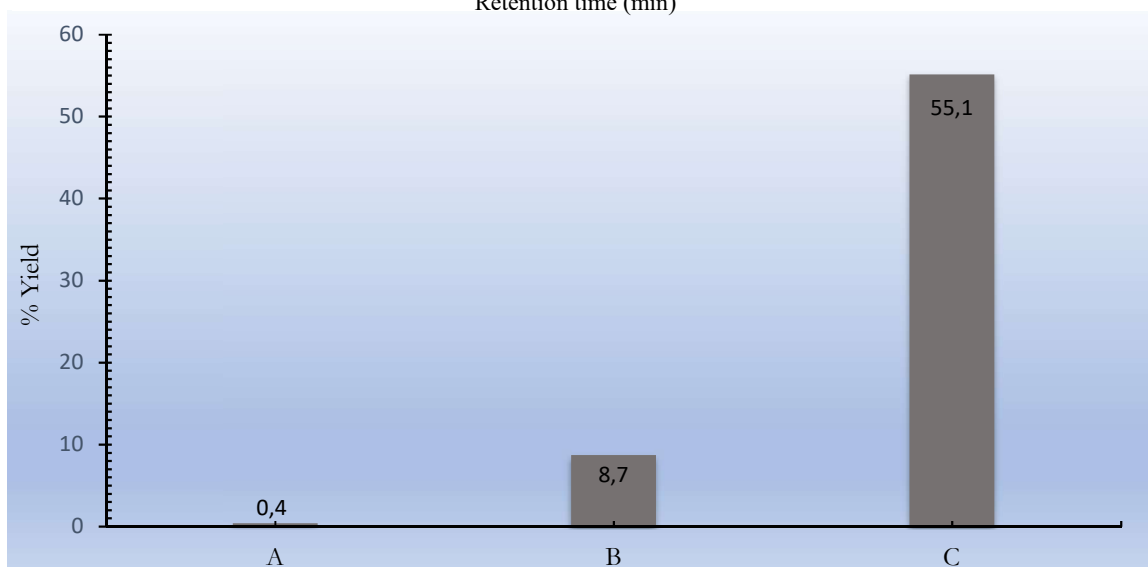
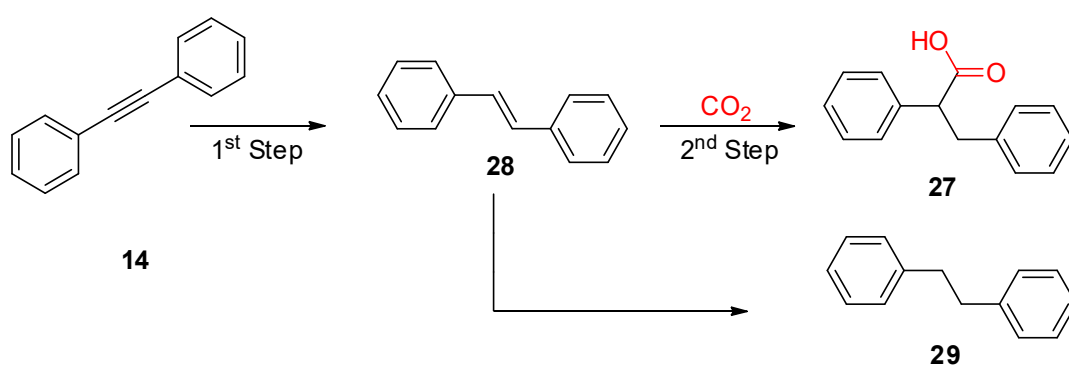


Figure 3.9 - Series of plasma experiments with the formation of bibenzyl
 Product was monitored by GC-MS and calculated according to section 3.2.1. The experiment conditions are:
 "A" 0.2 mmol of starting material (SM), 0.1 mmol of Bu_4NI , 10 mL of DMF, 1 h reaction, carbon anode, single argon plasma jet cathode, 3.6 mA, constant CO_2 at 10 SCCM.
 "B" 0.2 mmol of S.M., 0.1 mmol of Bu_4NI , 10 mL of DMF, 2 h reaction, nickel anode, triple argon plasma jet cathode, 4.6 mA, constant CO_2 at 10 SCCM.
 "C" 0.2 mmol of SM, 0.1 mmol of $\text{CuSO}_4 \cdot 5\text{H}_2\text{O}$, 10 mL of DMF, 2 h reaction, carbon anode, double argon plasma jet cathode, 4.6 mA, constant CO_2 at 10 SCCM.

Although the purpose of this project is not the optimization of formation of bibenzyl, this is evidence of a way to catalyze the reduction of an alkene to alkane.

3.3.5 Formation of 2,3-diphenylpropanoic Acid, Investigation, and Optimization.

There are a few substrates which after carboxylation can afford 2,3-diphenylpropanoic acid **27**. The investigation below demonstrates that when employing diphenylacetylene **14**, the formation of 2,3-diphenylpropanoic acid **27** can occur in 2 steps where diphenylacetylene is reduced to *trans*-Stilbene **28** which will, in turn, incorporate the CO₂ molecule to form the carboxylic acid **27**, in addition, the investigation showed traces of bibenzyl **29** as shown in the Scheme **22**.



Scheme 22 - Formation of 2,3-diphenylpropanoic acid in two steps and side reduction reaction

In this experiment diphenylacetylene **14** (0.5 mmol) was added into a solution of Et₄NI (0.5 mmol) in DMF (25 mL). The resulting solution was stirred under CO₂ (10 SCCM) and an argon plasma jet at 4.6 mA was applied for 2 h, the product and other compounds were monitored by GC/MS.

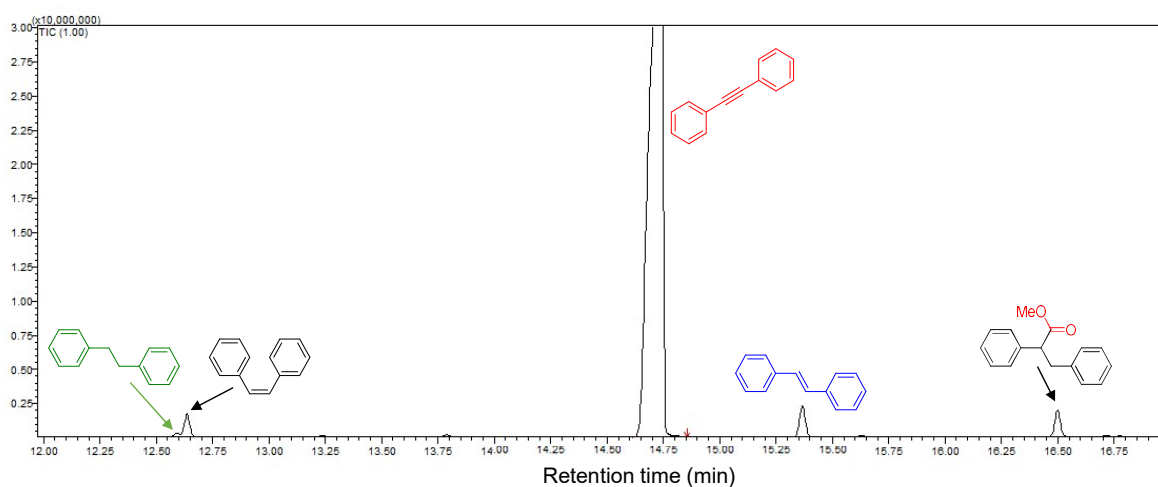


Figure 3.10 - GC/MS Spectra of carboxylation of diphenylacetylene

The GC/MS spectra showed in Figure 3.10 provides evidence of formation of Methyl-2,3-diphenylpropanoate (16.50 min) according to the injection parameters (see the experimental procedure section 2.1.2.2), however, besides the carboxylic acid formation, presence of *trans*-Stilbene **28** (15.4 min), bibenzyl **29** (12.6 min), and *cis*-Stilbene **30** (12.6 min) was observed.

Which was initially thought to be one step carboxylation, at this time the evidence shown that diphenylacetylene was first being reduced to *trans*-Stilbene and then the reduced substrate was being carboxylated with a competing reduction of *trans*-Stilbene to bibenzyl. To prove this theory, the reaction was repeated but instead of CO₂, the solution was previously saturated with helium, I expected that there would be more reduction of diphenylacetylene to *trans*-Stilbene and lack of carboxylic acid, which was confirmed in Figure 3.11.

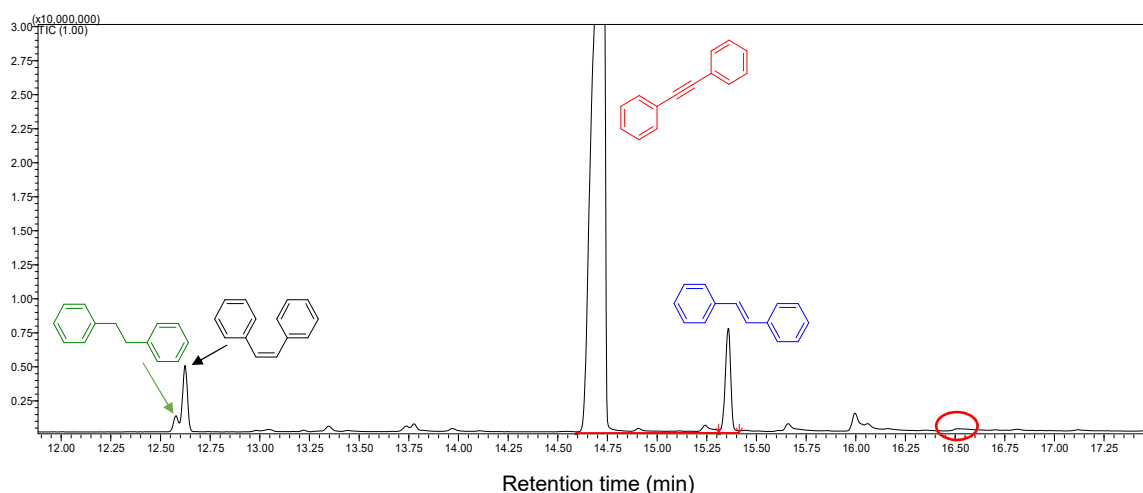


Figure 3.11 - GC/MS Spectra of the reaction of diphenylacetylene without CO₂

In the absence of CO₂, the reduction of diphenylacetylene into *trans*-Stilbene increased. The concentration of *trans*-Stilbene when the solution was saturated with CO₂ was 0.58 mmol/L but increased to 1.78 mmol/L when the solution was saturated with helium. Also, in the absence of CO₂ there was no formation of carboxylic acid, this gives evidence that instead of diphenylacetylene, *trans*-Stilbene was being carboxylated. I anticipated that *trans*-Stilbene should give a better conversion to carboxylic acid versus the alkyne as this will not require an additional step. Thus, the experiment was repeated under the same conditions as the previous experiment, and the result can be seen in Figure 3.12.

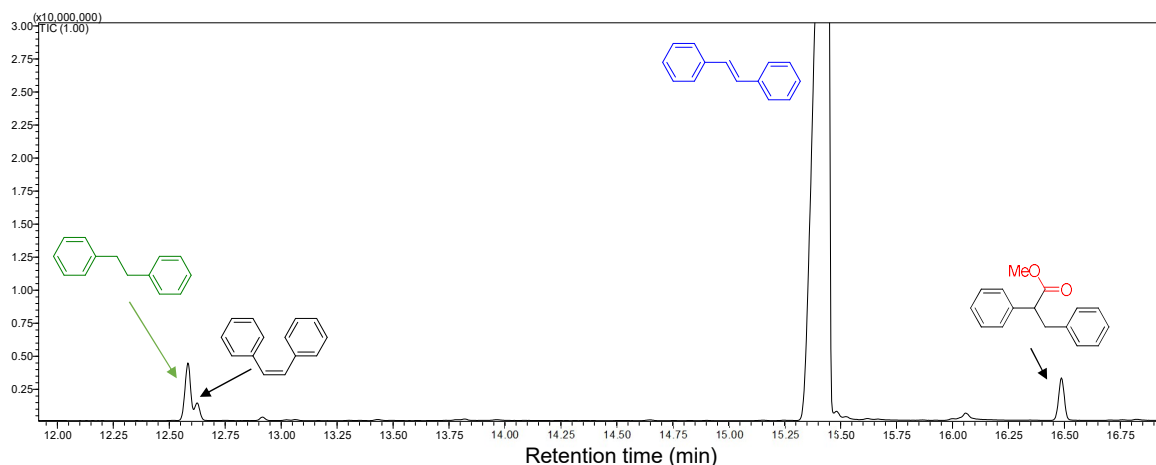


Figure 3.12 - GC/MS Spectra of carboxylation of *trans*-Stilbene

As expected, when Alkene was employed in the plasma carboxylation, the formation of the carboxylic acid increased by 83% as compared with the diphenylacetylene reaction. One of the possibility is the fact that the reduction potential of the alkyne ($E^0 = -2.11$ V) is slightly lower than alkene ($E^0 = -2.21$ V)¹⁵² therefore, the alkyne is first reduced to alkene and then it is carboxylated.

It also showed the competing reaction of reduction of *trans*-Stilbene to bibenzyl. When the alkyne was employed only 0.01 mmol/L of alkane was formed versus 0.78 mmol/L of alkane formed when alkene was employed.

3.3.6 Determination of Reaction Performance by Splitting Plasma Jet.

The electron transfer in a DC non-thermal atmospheric plasma discharge was reported by Richmonds and co-workers (as previously showed in section 1.5.4.2). However, the interaction of the electrons when in contact with liquid was not yet observed.

The proposed experiment was designed to observe if the conversion would be affected when the plasma jet is ramified into multiple jets. Importantly, a rule to allow this study to be achieved with good quality is to keep the same current and current density between all jets, keeping all the other parameters such as reaction time, the concentration of substrate, electrolyte, and volume of solvent constant, excepting the number of plasma channel that is diversified. In order to make every single channel working properly, each jet will need to have its own resistor of equal

resistance connected in parallel, consequently, the DC power input decreases as more channels are connected.

Essentially when connecting a resistor in parallel the equivalent resistance is always lower than every individual resistor, in other words, if you apply a voltage across a resistor, a certain amount of current flows but If you add another resistor in parallel with the first one, you have basically opened a new channel through which more current can flow. No matter how large the resistance of the second resistor is, the total current flowing from the power supply will be at least slightly higher than the current through the single resistor, and to keep the same total current input, the power should be adjusted. The equivalent resistance can be calculated using the formula below.

$$\frac{1}{R_{Eq}} = \frac{1}{R_1} + \frac{1}{R_2} + \frac{1}{R_3} \dots \dots \frac{1}{R_n}$$

4 Experiments were conducted according to Figure 3.13.

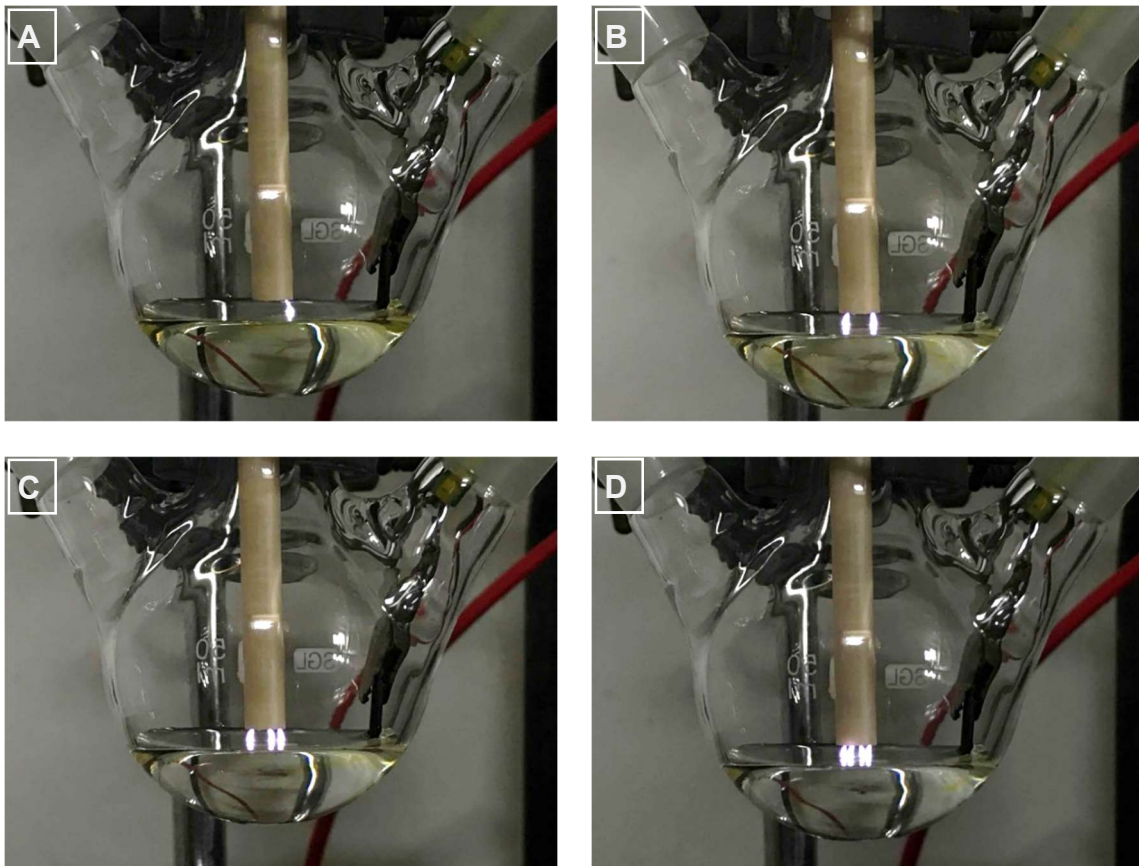


Figure 3.13 - Plasma reaction conducted with different jets configuration, “A” has one jet striking; “B” has two jets striking; “C” has three jets striking and “D” has 4 jets striking.

In this experiment *trans*-Stilbene (0.2 mmol) was employed as starting material and added into a solution of Et_4NI (0.1 mmol) in DMF (10 mL). The resulting solution was stirred under CO_2 (10 SCCM). The total current was kept at 3.6 mA for 1 h, the velocity of argon was kept at $1.9 \text{ m}\cdot\text{s}^{-1}$. A current limiting resistor (0.458 M Ω) was employed in each plasma channel in parallel and the power input was adjusted to keep the total current, as well as the flow of argon, was adjusted to keep the same velocity per channel. The reaction was monitored by GC/MS after 1 h since 1 h of reaction should be enough to observe the difference reaction rate.

Figure 3.13 shows the plasmas striking in each different configuration, each jet is 2.0 mm apart from each other, so a distance larger than that could produce different results.

The result of the experiment is plotted in Figure 3.14, the percentage of formation of the carboxylic acid in each plasma experiment configuration is compared. Working with 2 plasmas jets leads to the highest conversion reaching 8.3%, when striking one or three jets simultaneously the percentage of conversion is slightly lower and carrying the carboxylation with 4 jets resulting in 5.5% yield which is the lowest conversion of the experiment, essentially 2 jets converts 64% more acid than 4 jets.

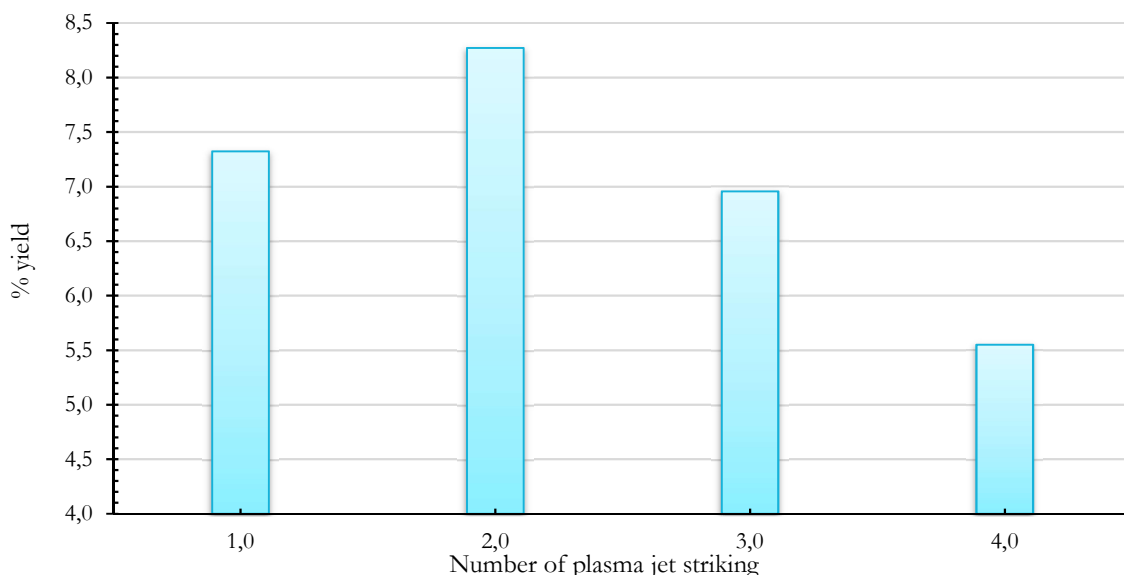


Figure 3.14 Carboxylation of *trans*-Stilbene with different numbers of plasma at the same total current. Results are shown in % yield of carboxylic acid formed, monitored by GC/MS and calculated according to section 3.1.2. Reaction conditions: Argon plasma jet, 3.6 mA, *trans*-Stilbene (0.2 mmol), DMF (10 mL), Bu_4NI (0.1 mmol), 1 h reaction.

Presumably, the possible explanation to this outcome is that on the contrary to the electrochemistry mechanism where the reaction takes place at the surface of the electrode, in plasma, besides on the surface of the electrode, the reaction also takes place at the region where the plasma touches the liquid. Depending on the voltage drop across this region, the carboxylation of the target product would increase or decrease. If this theory is true, at different current and voltage the order in this graph would also change.

One observation to support this theory is the Figure 3.15, due to the presence of iodide ions in the solution, during the reaction it is converted to iodine releasing a brown colour into the solution, in electrochemistry it only appears at the surface of electrode, however, in the plasma reaction, this behavior can also be observed in the region where the plasma touches the liquid.

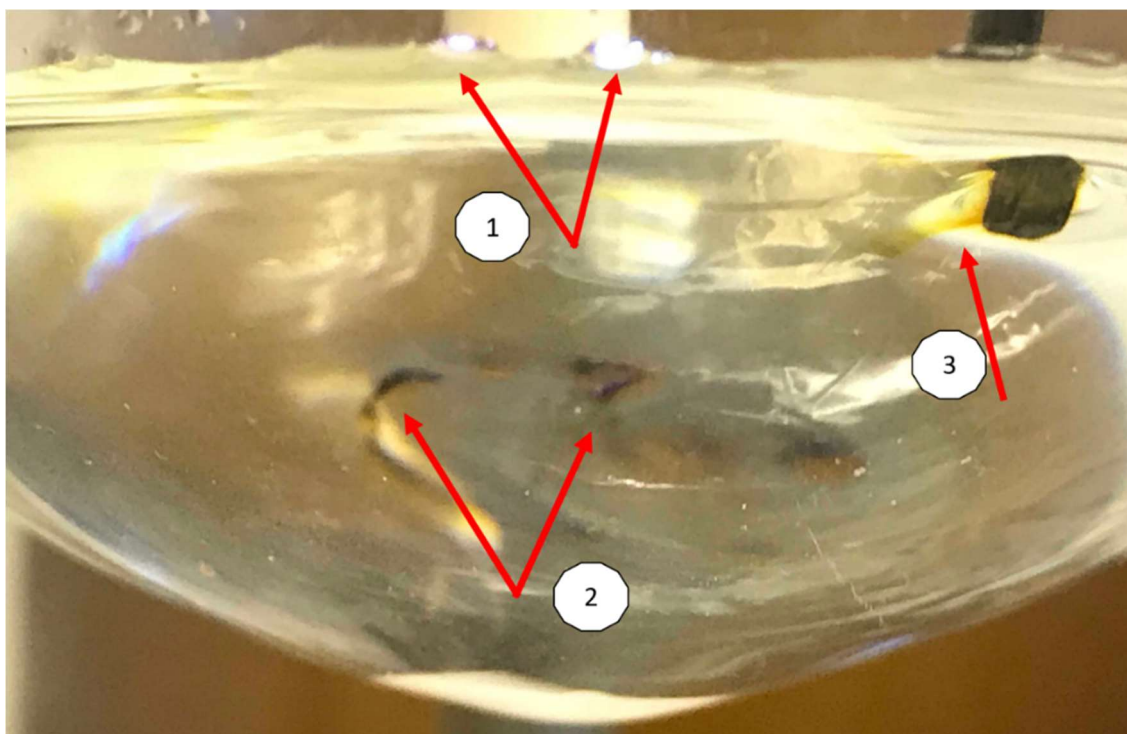


Figure 3.15 - Plasma reaction of trans-Stilbene with 2 jets - arrow 1 indicates the plasma striking, arrow 2 indicates the conversion of iodide to iodine where the plasma touches and, arrow 3 indicates the conversion at the surface of the electrode.

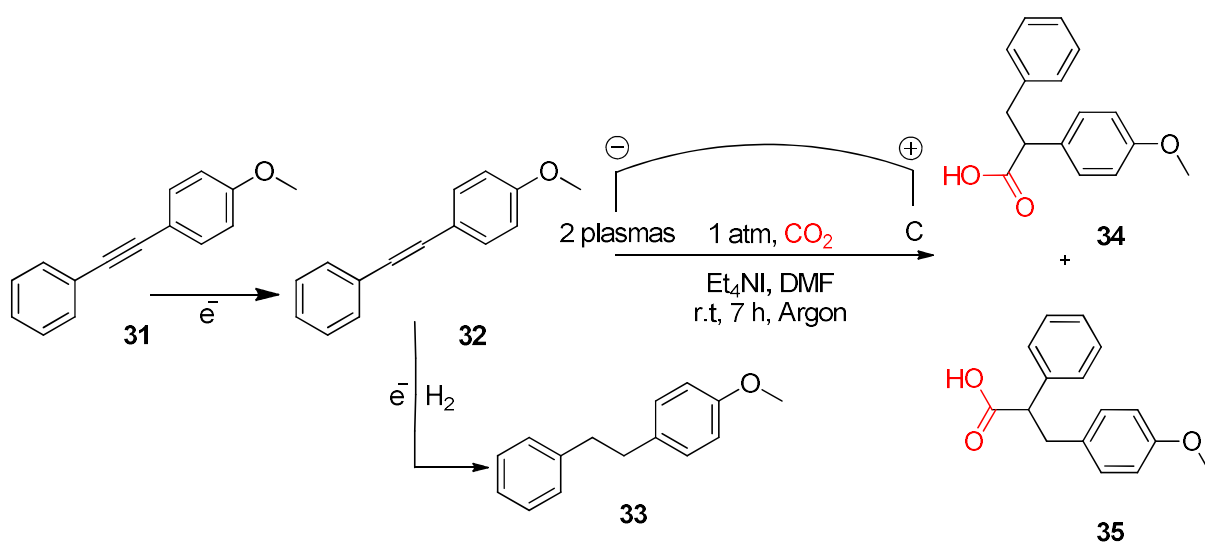
Another observation that supports the theory in which the carboxylation also takes place at the interface between the point where the plasma touches and the liquid is the current density study that will be presented in the section 3.3.9 where a large increase of the current density, increased only 4% the conversion to the desired

carboxylic acid. However, more investigation still needs to be carried out to investigate this phenomenon.

3.3.7 Carboxylation of 1-Methoxy-4-(phenylethynyl)benzene

So far, the carboxylation of alkynes provided evidence that the reaction occurs in two steps; where the alkyne is reduced to alkene, which is then carboxylated, I also assumed that there is a competing reaction between the carboxylation of alkene and the reduction to alkane.

Following this theory, 1-methoxy-4-(phenylethynyl)benzene **31** (1.0 mmol) was carboxylated (Scheme 23) employing a double argon plasma jet in DMF (10 mL) at 3.6 mA for 7 h to get 2-(4-methoxyphenyl)-3-phenylpropanoic acid **34** with 30.8% conversion and 17.8% isolated yield.



Scheme 23 - Plasma carboxylation of 1-Methoxy-4-(phenylethynyl)benzene

Besides the target carboxylic acid, it was identified 0.4% of conversion of 4-methoxystilbene **32** and 13.4% of *p*-phenethylanisole **33**. This experiment brings another evidence of the mechanism of carboxylation of alkyne where its carbon-carbon triple bond is reduced to alkene, which is further carboxylated, including a side reduction to alkane.

After further analysis of ^1H NMR spectroscopy, what was expected to be only the carboxylic acid **34**, was actually a mixture of **34** plus 3-(4-methoxyphenyl)-2-phenylpropionic acid **35**.

3.3.8 Screening of Applied Current

As observed in electrochemistry, the conversion increases as the current increases and with the plasma system I expected the same behavior. Three different experiments of plasma carboxylation of *trans*-Stilbene (1.0 mmol) to form its correspondent carboxylic acid **27** applying (12.6, 17.6 and 23.0) KV to get respectively (2.5, 3.5 and 4.6) mA was carried out. Et₄NI (0.5 mmol) was dissolved in DMF (25 mL) under CO₂ (10 SCCM). The plasma jet struck for 2 h under argon background gas, a carbon electrode (0.19 cm²) was chosen as the anode. After the completion of the experiment, the product was monitored by GC/MS.

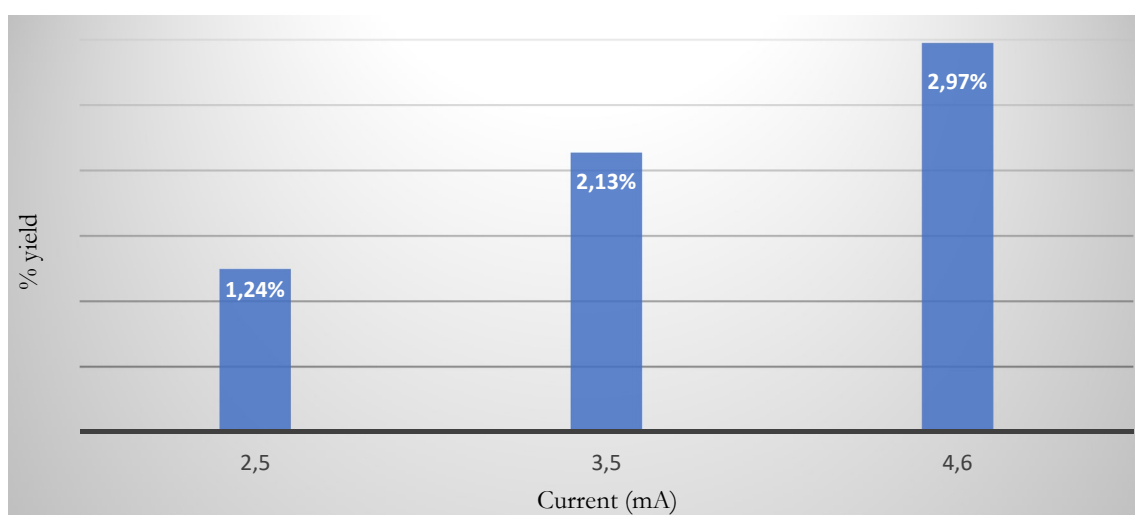


Figure 3.16 Current screening of plasma carboxylation of *trans*-Stilbene

Figure 3.16 shows a steady increase of % yield as the applied current increases, DC power supply employed here is able to deliver a maximum of 5 mA, however, is recommended to give a safety tolerance of 10% to protect the equipment which would decrease the maximum current to 4.5 mA.

3.3.9 Effect of Current Density

The increase of the current is accompanied by the increase of the number of electrons which in turn accelerates the conversion rate, in parallel, the current density is directly affected, in other words, the more electrons are provided to the system the higher the current density which results in a faster conversion rate. Some researchers have already shown a high reduction rate of CO₂ at high current

density. Tomonori and co-workers achieved very high rates at $200 \text{ mA}\cdot\text{cm}^{-2}$; ⁷ Even at $300 \text{ mA}\cdot\text{cm}^{-2}$ was successfully achieved by Gabardo.⁵⁸ The challenge of applying high current density to the electrode is that the material does not withstand these harsh condition and eventually deteriorates.

The doubt here is the fact that the result presented in the section 3.3.8 was affected by the increase of the number of electrons injected in the carboxylation reaction or it was proportional to the increase of current density?

To clarify this, a series of reactions varying the current density but keeping the same current was proposed. To carry this reaction, the size of the electrode was varied.

In this experiment, *trans*-Stilbene (0.2 mmol), in DMF (10 mL) and ET_4NI (0.1 mmol) was employed. CO_2 was constantly flushed (10 SCCM) through the system. Carbon electrode was employed in three different sizes (0.19, 0.50 and 0.97) cm^2 . The argon plasma jet was applied at the current of 3.6 mA for 1 h under constant stirring. After the duration of the experiment, the product was methylated and monitored by GC/MS and the yield was calculated using the calibration curve of the methyl-2,3-diphenylpropanoate (section 2.1.2.1).

Table 3.4 - interference of current density in the % of yield in plasma carboxylation

Surface area of the electrode (cm^2)	Current Density (mA/cm^2)	Yield (%) ^a
0.19	19.13	9.39
0.50	7.17	9.17
0.97	3.70	9.03

^a Yield was measured by GC/MS according to section 3.1.2.

Table 3.4 shows that the current density has a little impact on the conversion rate. While the current density increased 417% the yield increased by only 4%.

In electrochemistry, It is known that the reaction takes place at the surface of the cathode and the target reaction can be narrowed according to the drop voltage across the electrode which is measured by cyclic voltammetry.^{153,154} But it was not yet clear if plasma reaction would reflect similar mechanism.

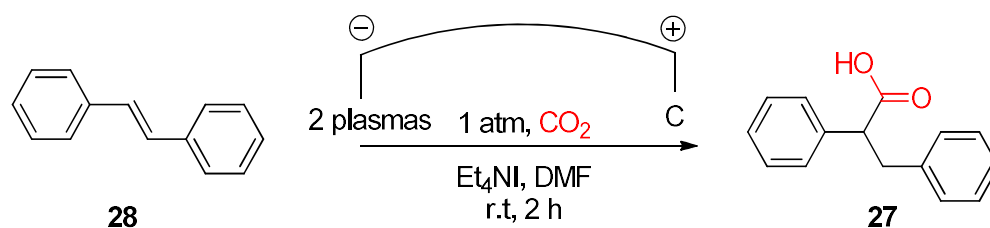
One of the possibilities of the low effect of the current density demonstrated above would be if the conversion also occurs at the interface between the plasma and the liquid, as discussed in section 3.3.6.

3.3.10 Conversion Rate and Current Efficiency Study

Optimization of current efficiency vs conversion yield was conducted aiming the best performance and giving conditions to achieve full conversion of the starting material.

The carboxylation reaction was performed with the double argon plasma jet, *trans*-Stilbene (0.2 mmol) in DMF (10 mL) employing Et₄Nl as supporting electrolyte.

Scheme 23



Scheme 24 - Plasma carboxylation of *trans*-Stilbene

Table 3.5 Optimization of % yield vs current efficiency in plasma carboxylation of *trans*-Stilbene.

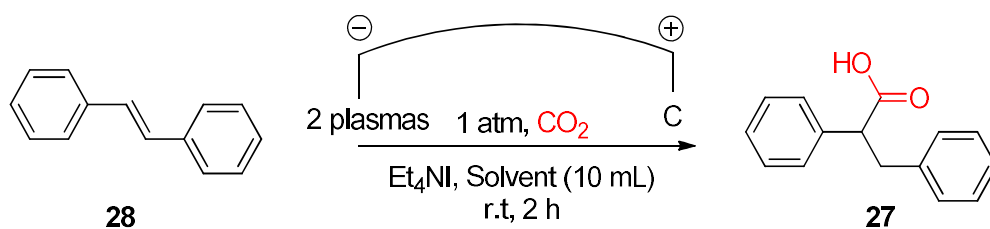
Entry	Current (mA)	Current Efficiency ^a (%)	Yield ^a (%)
1	2.8	28.6	15.0
2	3.4	29.1	18.5
3	4.0	28.8	21.6
4	4.6	26.8	23.1

^a Obtained by GC/MS analysis and calculated according to section 3.1.2.

Entry 1 to 4 of Table 3.5 revealed that the highest current efficiency was achieved at 3.4 mA and further increasing the current lead to higher yield but lower current efficiency, this could be due to side reactions, an example of this is the presence of bibenzyl 29 which comes from the reduction of 28.

3.3.11 Plasma Carboxylation - Solvent Optimization

Looking for a more environmentally friendly plasma reaction, one of my concerns was related to the solvent employed. DMF is widely used in electrochemistry and behaves very well with the plasma system, however, it is known to be a hazardous solvent and human exposure should be carefully limited.¹⁵⁵ It is classified by the IARC (International Agency for Research on Cancer) as a possible carcinogen.¹⁵⁵ Among numerous types of solvents and possible substitutes of DMF, the selection of solvents (Table 3.6) was based on low toxicity, low carcinogenicity and those shown not to bioaccumulate.



scheme 25 - Plasma carboxylation of trans-Stilbene

Table 3.6 Possible solvents replacing DMF

Entry	Solvent	Yield* (%)
1	DMF	10.4
2	DCM	≤ 0.1
3	THF	≤ 0.1
4	Cyrene	≤ 0.1
5	Methanol	≤ 0.1
6	Acetonitrile	≤ 0.1
7	DMSO	≤ 0.1
8	Propylene Carbonate	0.2
9	D-Limonene	≤ 0.1

* Obtained by GC/MS analysis and calculated according to section 3.1.2.

Special attention to Cyrene [(-)-dihydrolevoglucosenone], which among the solvents listed is claimed to be the greenest.¹⁵⁵ This is a bio-based dipolar aprotic solvent derived from cellulose.¹⁵⁵ Although it has recently been launched on industrial scale. Cyrene already has many applications such as graphene synthesis¹⁵⁶ and carbon cross-coupling reactions.^{157,158} It does not contain any chlorine, sulfur or nitrogen heteroatoms, which can present end-of-life pollution issues and create corrosive by-products if incinerated. It also has very low acute (LD50) and aquatic (EC50) toxicities biodegradable and safer to handle than many oxygenated solvents due to its flash point of 108 °C. Cyrene is stable to oxidation and (at end-of-life) upon incineration or biodegradation yields only carbon dioxide and water.¹⁵⁵ So I was very excited about replacing the current DMF by Cyrene or other less harmful solvent.

Solvents such as DCM, THF, methanol, and acetonitrile were evaporating after the exposition to plasma, nevertheless, to stop the loss of solvent by evaporation a conventional condenser with a chiller running water at 2 °C was connected, however, it still didn't stop the evaporation. In the end the "Graham" condenser which has a coiled inner tube (Figure 3.17) was utilised. Under these conditions, the evaporation of the solvent was ceased.

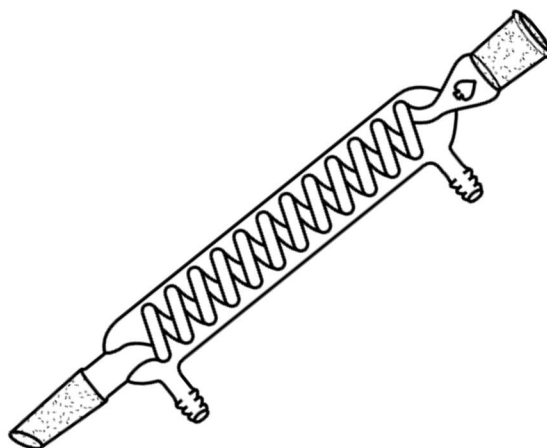


Figure 3.17 - Condenser type "Graham"

The substrate **28** is not soluble in THF and methanol, thus 10% of DMF was initially used to dissolve the starting material and then completed with the solvent to be tested. In order to do the reaction in D-Limonene, the electrolytic salt was dissolved in acetone 1:9 and *cis*-Stilbene was employed due to its greater solubility.

3.3.12 Study of Gas Ionization Efficiency

A study to determine the efficiency of ionization of helium, neon, and argon was reported by Filip Smith in 1930.¹⁵⁹ Essentially this study determined the number of new electrons produced by ionization per unit path at a specific gas pressure by an electron of given energy and measured the total number of positive charges produced per electron.¹⁵⁹

Figure 3.18 draws the efficiency of these gases as a function of the accelerating potential of the electrons up to 4500 V.

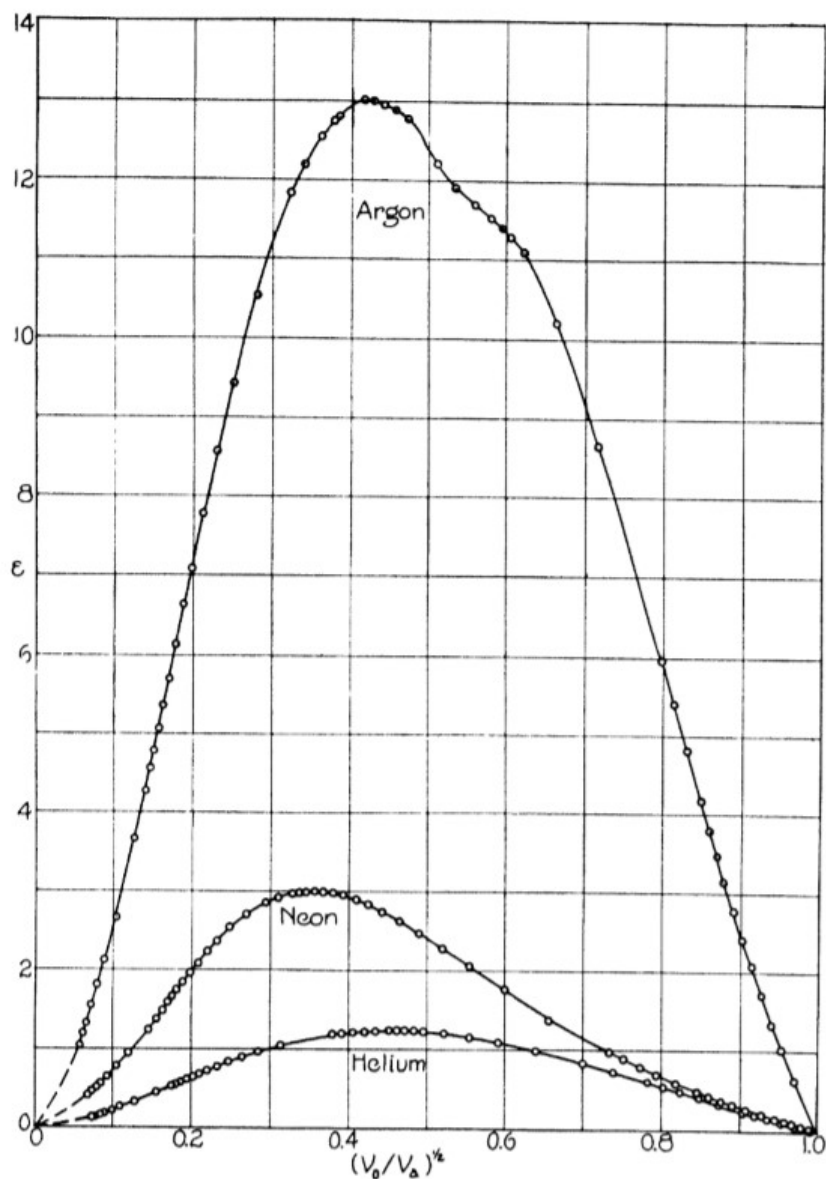


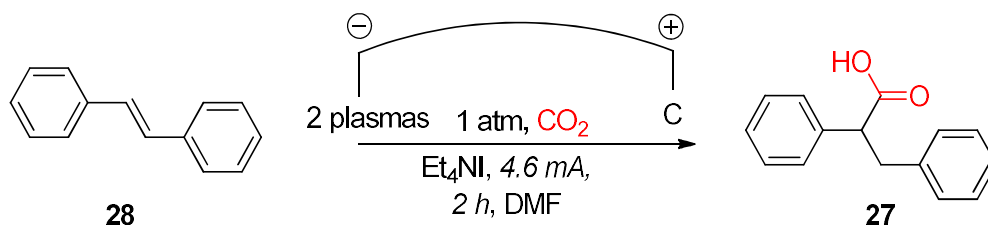
Figure 3.18 - The efficiency of ionization of He, Ne and Argon as a function of $(V_0/V_a)^{1/2}$, reduced to 1mm pressure at 0 °C. Reproduced from "The Ionization of Helium, Neon, and Argon by Electron Impact".¹⁵⁹

The efficiency is shown as a function of $(V_0/V_a)^{1/2}$ where V_0 is the ionization potential of the gas and V_a is the accelerating potential of the electrons which varied according to the electric field and distance that the particle travels.

The ionization potential of helium was assumed to be 24.5 V¹⁶⁰, neon equal to 21.5 V and that of argon 15.6 V¹⁶¹

At a certain point, the efficiency of ionization is a linear function of the energy of the impacting electrons however at high speed the efficiency is inversely proportional to the energy, it is believed that at high velocities, not all the electrons produce positive charge resulting in lower efficiency.

The behavior of plasmas in gas phases is somewhat already well investigated, however, its interaction with liquids is still obscure.¹⁰⁹ This was particularly interesting and opened a new possibility of investigating the plasma carboxylation in different type of gases. This initial test was carried out using substrate **28** (1.0 mmol) added into a solution of Et₄Ni (0.5 mmol) in DMF (25 mL) under CO₂ (10 SCCM). Scheme **26**. The experiment was carried out for 2 h which should be enough time to observe the difference of results between helium and argon at 4.6 mA, analyzed by GC-MS to calculate the percentage yield and current efficiency according to section 2.1.2.



Scheme 26 - Plasma carboxylation of trans-Stilbene

Figure **3.19** represents the result of the experiment described above, both experiments where helium was employed, the carboxylation of starting material resulted in current efficiency in the range of 10% to 14% (average of 12%) while employing argon, the conversion was in the range of 31% to 34% (average of 32.5). The same trend was observed in the percentage yield, helium plasma resulted in 1.7% to 2.4% (average of 2.1%) yield of the carboxylic acid **27** whereas employing argon, the result was in the range of 5.3% to 5.8% (average of 5.6%).

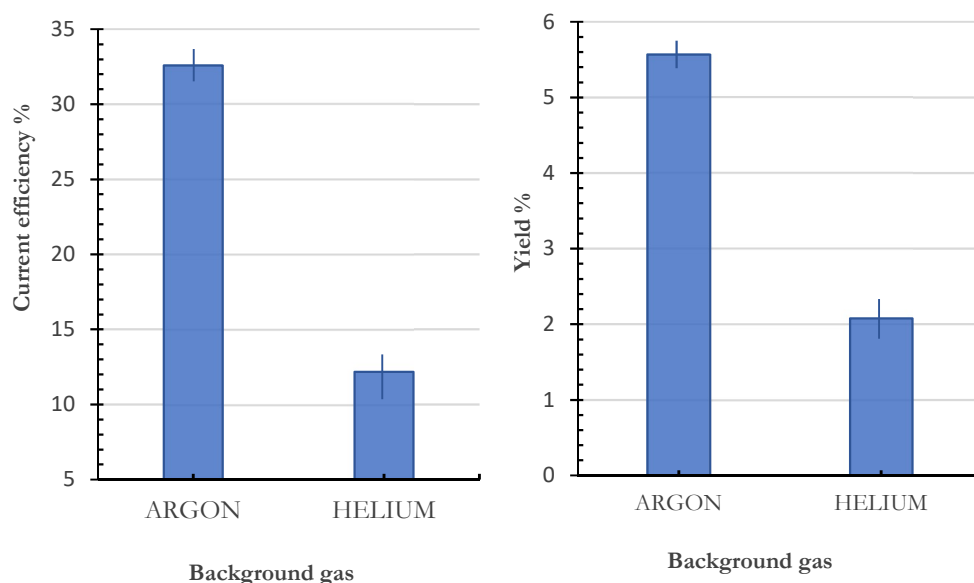
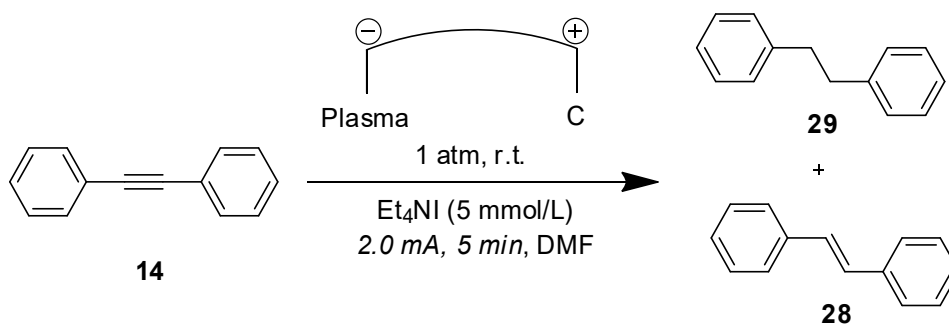


Figure 3.19 - Study of plasma carboxylation employing helium and argon

These results follow the same observations reported by Smith¹⁵⁹, where the efficiency of ionization is greater in argon than helium, here, it directly reflects the interaction of plasma in liquids and chemical activation.

Researchers from our group conducted a similar experiment where 2.5 mL of a mixture of diphenylacetylene **14** (5 mmol/L) in DMF containing Et₄NI (5 mmol/L) were treated with argon and helium plasma at 2 mA for 5 min (Scheme 25). The result of this experiment is shown in Figure 3.20.



Scheme 27 - Reduction of diphenylacetylene under plasma treatment

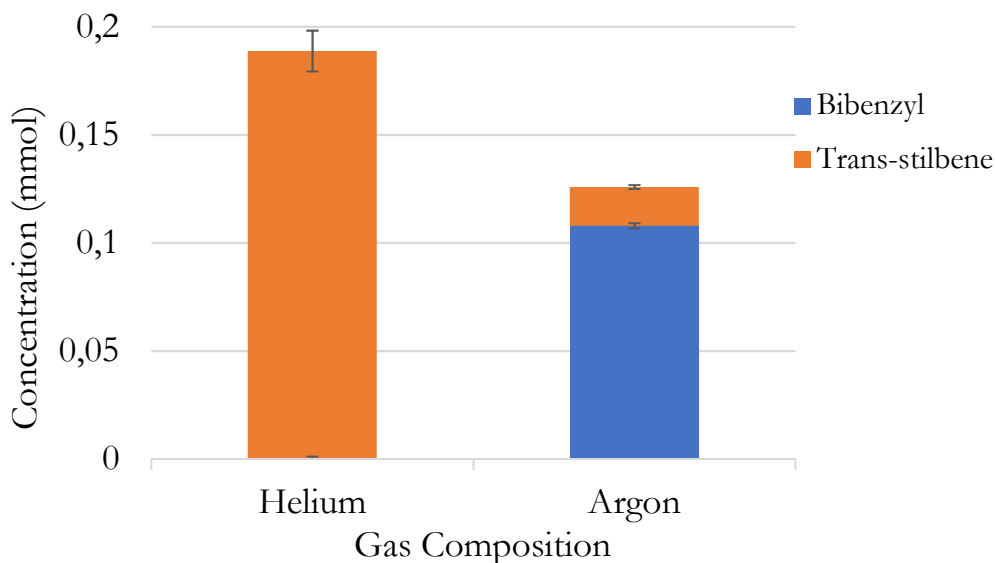
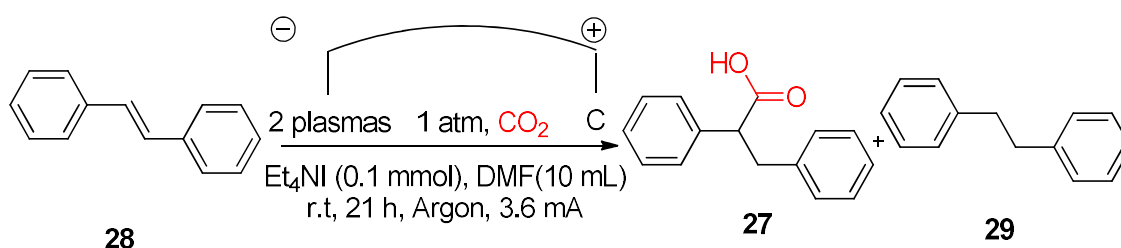


Figure 3.20 Argon and helium plasma treatment of diphenylacetylene with the formation of bibenzyl and trans-Stilbene

After the treatment with helium, 3.95% of **14** was reduced to **28**. By treating with argon plasma, 3.75% of **14** was initially reduced to **28** of which 85% of *trans*-Stilbene was further reduced to **29** requiring twice more electrons.

3.3.13 Complete Reaction Conversion

After finding the optimized system parameters, in order to demonstrate the practical utility of this approach, I decided to run plasma carboxylation reactions until all the substrate is converted that's why I named this reaction as "Complete Reaction Conversion". Scheme **28**



Scheme 28 - Plasma carboxylation of *trans*-stilbene

The substrate *trans*-Stilbene **28** (0.2 mmol) was added into a mixture containing Et₄NI (0.1 mmol) in DMF (10 mL) where CO₂ was bubbled (5.0 SCCM) at constant flow rate during the whole process. Double argon (0.2 SLM each channel) plasma jet striking at 3.6 mA until all the substrate is converted. The reaction was monitored by GC/MS. Figure **3.21**

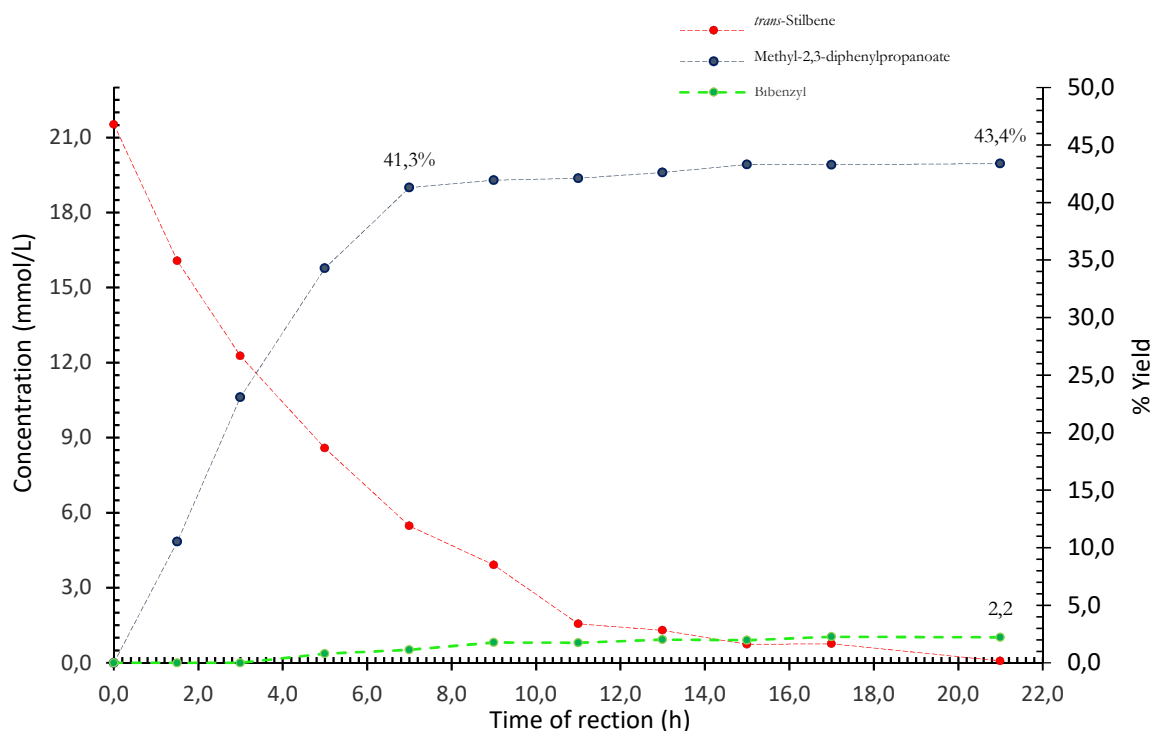


Figure 3.21 Plasma Carboxylation of *trans*-Stilbene.

Experiment conditions: 10 mL of DMF, 0.1 mmol Et_4NI , 3.6 mA

The substrate is represented by the red dashes and its concentration is shown on left axes along with bibenzyl concentration in green.

Formation of the product (% yield) is shown on the right axes represented by the blue dashes.

Figure 3.21 shows the results of the experiment explained above, after 7 h of plasma reaction, the rate of formation of the target product **27** reached a plateau, even despite the fact that there was still roughly 25% of the substrate remaining. In electrocarboxylation, sources of hydrogen atoms remain highly speculative and once this source is ceased or reduced, it becomes more difficult to continue the conversion to the desired product (Figure 3.22), so this could be one of the possibilities of this behavior. Knowing what the source of the hydrogen atom is, would give a better understanding of the mechanism and allow further optimization of this reaction. Interestingly, there is a constant reduction of the substrate **28** into bibenzyl **29** which also requires sources of hydrogen atom proposing a second mechanism for this reaction (Figure 3.23).

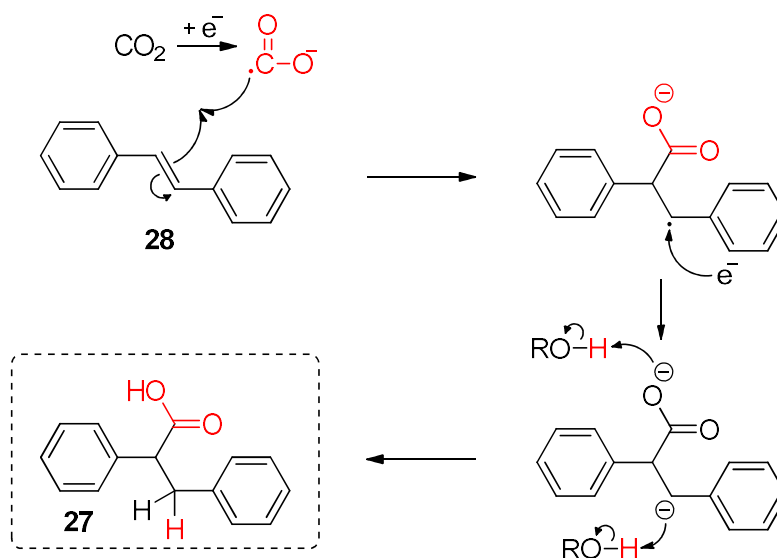


Figure 3.22 Plausible mechanism of carboxylation of alkene

In the mechanism shown in Figure 3.22, CO₂ is dissociated with $\ll 1$ eV free electrons¹⁶² which is provided by plasma, it is then bonded to α position of the benzene ring of the molecule forming a functional group. In the presence of sources of hydrogen atom, it is pulled by the lone electrons forming the carboxylic acid.

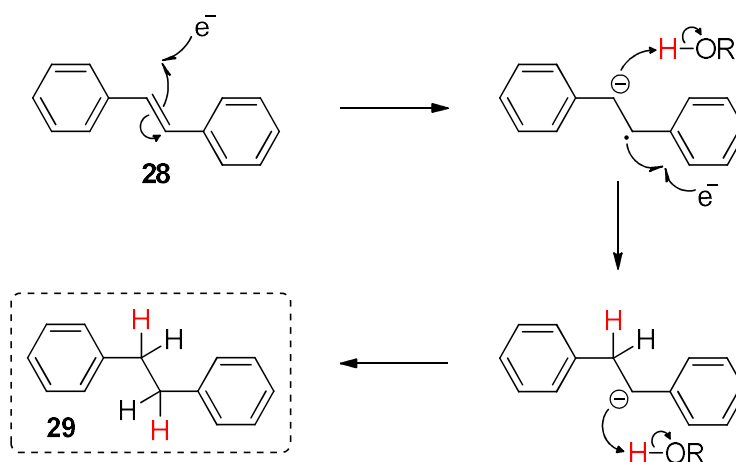


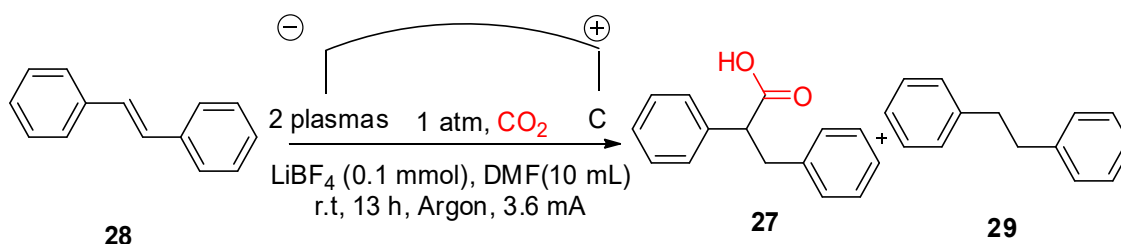
Figure 3.23 Plausible mechanism for the reduction of the alkene to alkane

In this mechanism (Figure 3.23), the electrons break the double bond of alkene, in the presence of hydrogen atom, the lone electron at α and β position pull the hydrogen atom available forming an alkane.

The reaction is coordinated according to the reduction potential of alkene and CO₂, being the lowest reduction potential more likely to happen. The reduction potential of CO₂ ($E^0 = -1.90$ V)¹⁶³ which is slightly lower than the reduction potential of alkene

($E^0 = -2.21 \text{ V}$)¹⁵². The reduction potential could explain the preliminary observation showing a competing reaction with the majority of electron driving the formation of carboxylic acid but still some traces of reduction to alkane.

One of the possible sources of the hydrogen atom is the electrolyte employed in this experiment (Et_4NI) which contains 20 molecules of hydrogen per mol of salt, and to find out if the salt provided the hydrogen atom in the carboxylation reaction, a second experiment was conducted exchanging Et_4NI by LiBF_4 which is an electrolyte without hydrogen atom (Scheme 29), (Figure 3.24 reaction "B").



Scheme 29 - Plasma carboxylation of *trans*-stilbene employing LiBF_4

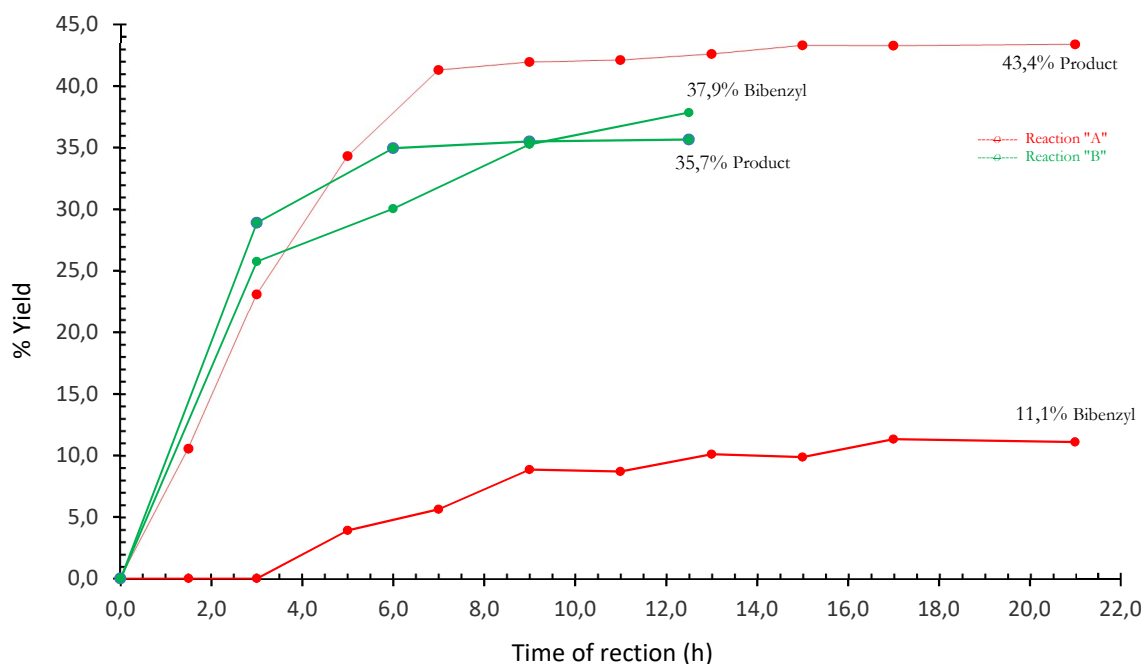


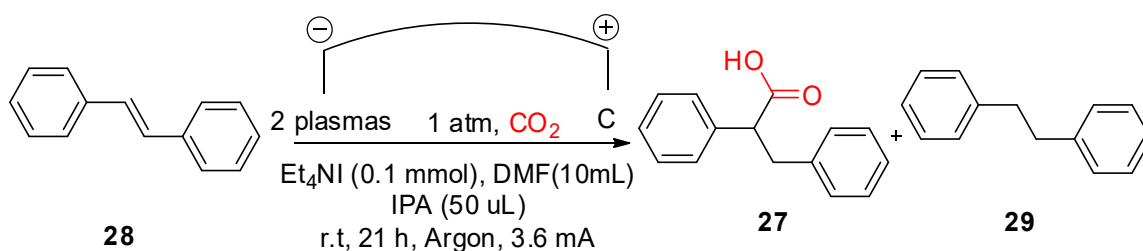
Figure 3.24 Carboxylation of *trans*-Stilbene under different scenarios showing the formation of methyl 2,3-diphenylpropanoate as a product and bibenzyl as a by-product. The reaction stops when all the starting material is consumed.

Reaction "A" *trans*-Stilbene 0.2 mmol, 10 mL of DMF, 0.1 mmol of Et_4NI , 3.6 mA, argon double plasma jet 0.4 SLM.

Reaction "B" *trans*-Stilbene 0.2 mmol, 10 mL of DMF, 0.1 mmol of LiBF_4 , 3.6 mA, argon double plasma jet 0.4 SLM.

In the reaction employing an electrolyte without hydrogen (Figure 3.25 reaction "B"), the carboxylation began at faster conversion rate if compared with reaction employing Et₄NI (Figure 3.26 reaction "A"), however, after 13 h of reaction, all of the substrates were converted either into carboxylic acid **27** or reduced to bibenzyl **29** but still the formation of carboxylic acid didn't show any improvement. This result provides evidence that this reaction was being fed with unknown source hydrogen atom and that was not from the electrolyte Et₄NI.

Taking into the consideration that lack of hydrogen atoms is limiting this reaction, I decided to start a new plasma carboxylation reaction adding a known amount of hydrogen atoms ensuring that the conversion of the substrate into carboxylic acid would not be interrupted for this reason. In the next experiment, 50 μL of IPA (2-propanol) was mixed with DMF (9.95 mL), LiBF₄ was employed as electrolyte and all other parameters were kept the same as the previous experiment. Scheme 30



Scheme 30 - Complete carboxylation of *trans*-Stilbene employing 2-propanol as a source of hydrogen atoms

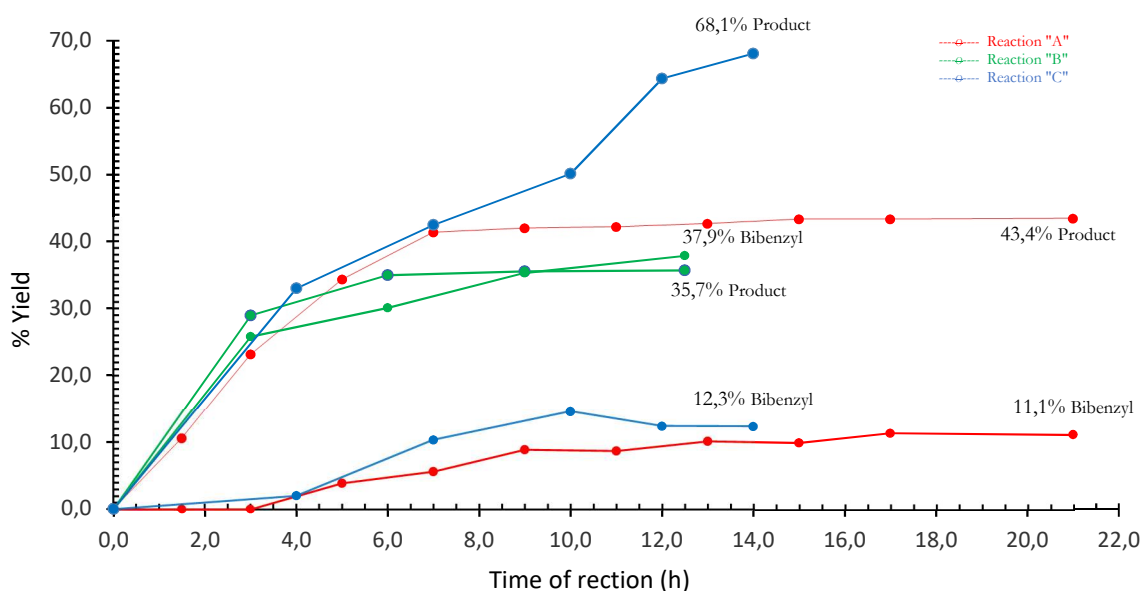


Figure 3.27 Carboxylation of *trans*-Stilbene under different scenarios showing the formation of methyl 2,3-diphenylpropanoate as a product and bibenzyl as by-product. The reaction stops when all the starting material of each reaction is consumed.

Reaction "A" *trans*-Stilbene 0.2 mmol, 10 mL of DMF, 0.1 mmol of Et₄Nl, 3.6 mA, argon double plasma jet 0.4 SLM.

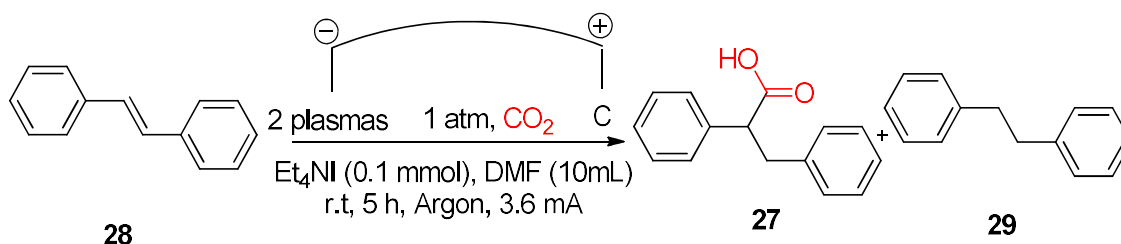
Reaction "B" *trans*-Stilbene 0.2 mmol, 10 mL of DMF, 0.1 mmol of LiBF₄, 3.6 mA, argon double plasma jet 0.4 SLM.

Reaction "C" *trans*-Stilbene 0.2 mmol, 10 mL of DMF, 0.1 mmol of LiBF₄, 50 μL of IPA, 3.6 mA, argon double plasma jet 0.4 SLM.

Figure 3.27 shows the comparison of experiments where the substrate is completely consumed, by adding IPA as a source of hydrogen atom (reaction "C"), clearly increased the formation of carboxylic acid but the reduction of the **28** into bibenzyl **29** was still observed.

At this point, the source of hydrogen atom was still a mystery and I was engaged to find out about it. The other possible source could be that moisture was being introduced from the CO₂ or Argon line supply, although the gases used were as pure as 99.995%. To check this possibility, another experiment was carried in a dry system. Without IPA, DMF was dried with activated molecular sieves 3Å, all the glassware was dried in the oven, both line gases were connected into drying column with molecular sieves (CO₂ column) and silica gel (argon column), so any trace of water should be removed. Scheme 29

If all the apparatus, gas and solvent was properly dried and if the concept of the external source of hydrogen atoms confirmed, there shouldn't be any conversion to the carboxylic acid or reduction to bibenzyl.



Scheme 31 - Carboxylation of trans-Stilbene in a dry system

Figure 3.28 contains the result of the experiment under dry conditions (reaction "D") and compare it against the other experiments. Dry conditions showed the highest conversion rate where after just 5 h there was only 4% of the initial substrate **28** unreacted, moreover, the reduction to bibenzyl **29** also presented in high conversion rate.

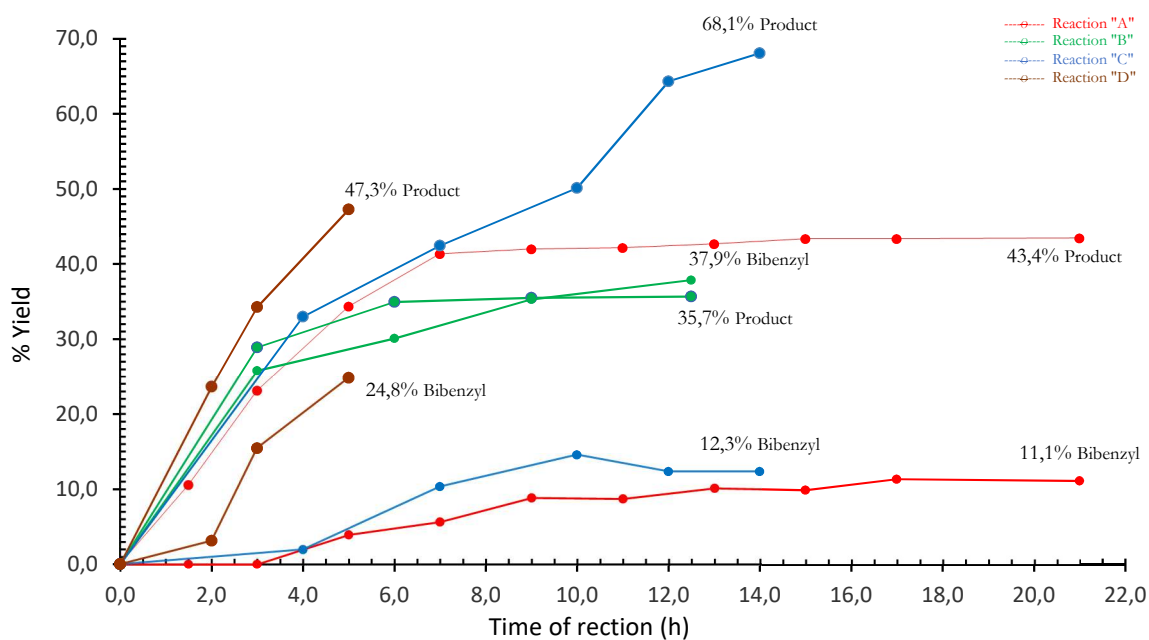


Figure 3.28 Carboxylation of *trans*-Stilbene under different scenarios showing the formation of methyl 2,3-diphenylpropanoate as a product and bibenzyl as a by-product.

The reaction stops when all the starting material of each reaction is consumed, besides the reaction "D" which stopped when there was still 4% of starting material.

Reaction "A" *trans*-Stilbene 0.2 mmol, 10 mL of DMF, 0.1 mmol of Et₄Ni, 3.6 mA, argon double plasma jet 0.4 SLM.

Reaction "B" *trans*-Stilbene 0.2 mmol, 10 mL of DMF, 0.1 mmol of LiBF₄, 3.6 mA, argon double plasma jet 0.4 SLM.

Reaction "C" *trans*-Stilbene 0.2 mmol, 10 mL of DMF, 0.1 mmol of LiBF₄, 50 μL of IPA, 3.6 mA, argon double plasma jet 0.4 SLM.

Reaction "D" *trans*-Stilbene 0.2 mmol, 10 mL of dry DMF, 0.1 mmol of LiBF₄, 3.6 mA, argon double plasma jet 0.4 SLM, flask, all the glassware was dried in the oven before the initiation of experiment.

Although I was very carefully drying all the apparatus, solvents and gases, on 22nd of November / 2018 (the date of the experiment) the humidity in Loughborough was of 99%, so it is very unlikely to keep everything completely dry during the 5 h of the reaction, however I should run this experiment in drier conditions to be able to confirm this result.

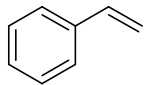
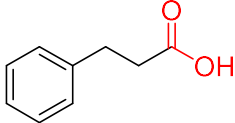
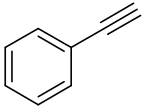
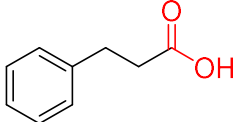
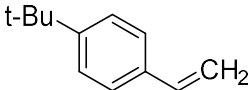
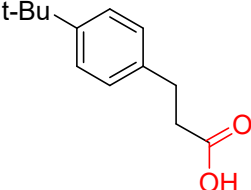
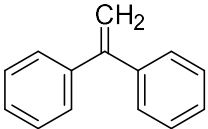
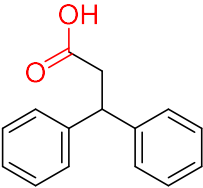
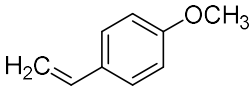
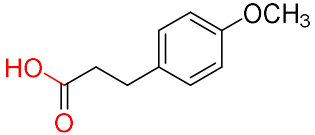
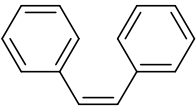
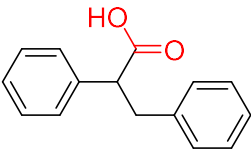
There should be a tipping point where the humidity is beneficial to this carboxylation reaction and when an excess of humidity would hydrolyze the water withdrawing some of the energy injected in the system, energy of which could be used to carboxylate the substrate.

3.3.14 Alternative Substrates

Once configured the optimum reaction conditions for the optimization process. 0.2 mmol of reactant, 0.1 mmol LiBF₄ dissolved in dry DMF (10 mL), argon at 0.4

SLM, bubbling CO₂ at 5 SCCM, carbon electrode with 0.19 cm², the plasma carboxylation at 3.6 mA and the addition of IPA as source of hydrogen atoms, a range of alkene and alkynes were tested in order to determine the scope of the reaction conditions (Table 3.7).

Table 3.7 – Plasma Carboxylation of alkene and alkyne

Entry	Substrate		Product		GC/MS Yield (%)
1		22		24^a	3.1
2		10		24^a	3.9
3		38		39^a	6.4
4		36		37^a	7.0
5		40		41^a	6.6
6		30		27^a	5.9

^a Identification of methyl ester of the carboxylic acid

Reaction conditions: 0.2 mmol of reactant, 0.1 mmol LiBF₄, DMF (9.95 mL), IPA (0.05 mL), argon double plasma jet (0.4 SLM), constant CO₂ (5 SCCM), carbon anode (0.19 cm²), 3.6 mA, 1 h reaction.

The purpose of the test listed in Table **3.7** is merely to certify that the employability of plasma jet in carboxylation reaction is not limited to *trans*-Stilbene and therefore can also be extended to other substrates and for this reason, they were tested under plasma carboxylation setup for only 1 h. Each product was methylated according to the procedure stated in section 3.2.1. and identified according to each molecular weight of their methyl ester in GC/MS.

4.0 Conclusions and Recommendation for Future Works

4.1 Conclusions

This work has shown the successful approach of a cold atmospheric pressure plasma devices employed to selectively carboxylate alkenes and alkynes, under the optimal conditions: Substrate (0.2 mmol) dissolved in dry DMF (9.95 mL) along with LiBF₄ (0.1 mmol) as supporting electrolyte and IPA (50 μ L) to guarantee a source of hydrogen atoms. The plasma was formed using double jet under argon (0.4 SLM) with 3.6 mA of current with continuous atmospheric CO₂ at a flow rate of 5.0 SCCM, employing carbon fiber rod anode. Besides the successful conversion of alkenes and alkynes into a carboxylic acid, when compared with electrochemistry, plasma proved to be significantly more selective.

Before the electrochemical experiments were conducted, a range of concentrations of Bu₄NI as supporting electrolyte in DMF were tested with different electrode materials configuration, where with only 0.5 mmol of salt in 50 mL of solvent was enough to allow the electrons to move freely, reducing drastically the resistance, in addition, the combination of carbon fiber electrode offered slightly less resistance compared with copper and nickel.

The conditions of the plasma carboxylation experiment changed substantially during this research. By replacing the carbon cathode by argon (1.0 SLM) plasma jet, initial tests employed diphenylacetylene **14** (1.0 mmol) as a substrate to yield 2,3-diphenylpropanoic acid **27**. 0.66% conversion was achieved when applying 0.8 mA direct current for 3 h. TEOA (2.0 mmol) was used in this experiment, however, later it was found that in this plasma reaction, the electrons are provided by plasma itself, thus the reducing agent does not play a role and could be disregarded for future experiments.

Investigations revealed that the alkyne is not directly carboxylated, but instead, it is reduced to alkene which is then carboxylated. Two alkynes showed the same pattern, diphenylacetylene **14** was reduced to *trans*-Stilbene **29** and 1-Methoxy-4-

phenylethynyl-benzene **31** was reduced to 4-Methoxystilbene **32**, moreover, in both cases, there was evidence of reduction of the alkene into the alkane. When employing alkene in the plasma carboxylation, the formation of carboxylic acid increased by 83% as compared to carboxylation of alkyne.

The current applied in the plasma jet is directly related to the conversion rate, for example, the carboxylation of *trans*-Stilbene **28**, at currents of (2.5, 3.5 and 4.6) mA were tested for 1 h showing a steady increase of conversion up to a maximum of 3.0%. The maximum current was limited by the power supply.

Current density over the carbon fiber anode did not represent significant correlation with the conversion rate, in the test employing *trans*-Stilbene **28**, the reduction of the surface of the electrode from 2.50 cm² to 0.18 cm² increased only 4% of the conversion applying the same current.

Studies showed the formation of the target carboxylic acid under different plasma configurations. In the test of plasma carboxylation of *trans*-Stilbene **28**, at 3.6 mA, the plasma was branched in up to 4 different jets. This test showed the highest conversion when striking two jets simultaneously and the conversion decreased as the number of jets was further increased. The use of supporting electrolyte containing iodine is dissociated and it is released into the solution in form of iodide, which releases a brown colour or yellow when in low concentration, this colour change was observed on the electrode surface and at the point where the plasma touches the liquid. This evidence brings the most plausible reason of the statement above which is the fact that the selectivity of the target formation relies on the drop voltage across the interface of the plasma and the liquid more than the drop voltage at the electrode surface.

The efficiency of conversion was also demonstrated to be influenced by the nature of the gas employed in the plasma formation, here argon and helium as background gas to carboxylate *trans*-Stilbene **28** was explored. The ionization takes place at a different voltage and so the impact of electrons is also changed. In this experiment, the percentage yield of target carboxylic acid was in the average of 2.1% when helium was used and 5.6% for argon in 2 h of reaction at 4.6 mA.

When carrying out the reaction until all the substrate is completely converted, after 7 h, the conversion to target carboxylic acid reached a plateau, however, reduction of alkene to alkane still carried on without reduction of the concentration of product formed. The possible interferences were thought to be the source of hydrogen in the formation of a carboxylic acid which could be from moisture or salt. LiBF_4 was then employed accelerating the conversion of the reaction, parallelly, the reduction of alkene into alkane. However, when adding IPA as a source of hydrogen, the reaction reached its highest conversion to 68.1% after 14 h under 3.6 mA with low reduction of alkene to alkane.

The availability of hydrogen is essential in the carboxylation reaction of alkene and alkyne, and although none of the chemicals used in this experiment contains free source of hydrogen and it is difficult to keep the whole experiment completely dry, it is safe to say that moisture could be providing it, which could be being delivered along with gases (CO_2 or argon), air, containing in the solvent or any other source, as it is, therefore, the addition of IPA supported the conversion when employed with dry solvent.

DMF is harmful and not environmentally friendly solvent, as one of the purposes of this research is for environmental reasons, it would make sense to do so employing an environmentally friendly solvent. Over 9 different solvents were tested and besides DMF, propylene carbonate reached the highest conversion, however still significantly lower than DMF.

Although only a few catalysts were tested, none were effective for this reaction, over 5 different catalysts were tested including NiCl_2 -glyme successfully employed in the electrocarboxylation of alkyne⁸⁸ but did not produce any result here.

Overall, the results presented in this research provides essential information for future carboxylation research involving plasma process, first is the evidence of applicability of such technology without the need of sacrificial electrode or reducing agent, turning the carboxylation process an environmental and cost-effective alternative for carbon dioxide utilisation, also the fact that the conversion is influenced by the number of plasma channels interacting with liquids opens a new possibility of energy efficiency optimization.

4.2 Recommendations for Future Work

In this research there are enough evidence that in plasma carboxylation, the conversion takes place mainly at the interface between the plasma and the liquid relying on the drop voltage at this point, therefore important future work would be the development of a technique able to measure the drop voltage at this interface and, by doing this, a cyclic voltammetry study could be carried out narrowing the voltage window in which the reaction is more selective. With this information, the number of plasma jets could be increased optimizing the setup experiment and scaling it up.

I also presented how different gases ionize at different voltages and how the electron impact influences the carboxylation efficiency, however, only two different gases were studied in this research. There are other gases and a mixture of gases which could be explored. For instance, carbon dioxide could be in the mixture with the background gas to form the plasma.

According to the results, the most plausible source of hydrogen in this experiment is moisture, however, it is still necessary to confirm this possibility and if so, if the moisture is being carried with gas, liquid or something else. Also, with the possibility of moisture being the source of hydrogen, at which concentration it is still supporting the reaction and when moisture becomes a problem, are future important investigations.

The investigation of an environmentally friendly solvent for plasma carboxylation still needs to be carried out, there could be a relation with the availability of hydrogen in the solvent or the dielectric properties which are so far unexplored. Ideally in H₂O.

A catalyst is also an investigation that could be more explored, which would benefit not only plasma carboxylation but also the investigation of plasma chemistry. The catalyst speeds up the reaction improving energy efficiency and reducing the time of conversion, this could be interesting in terms of economics and brings more attention to industry.

Besides the reaction occurred due to free electrons interaction, there should be an investigation of active species formed at the interface of plasma and liquid and its interference with reaction.

5.0 References

- 1 P. Rumbach, M. Witzke, R. M. Sankaran and D. B. Go, *Journal of the American Chemical Society*, 2013, **135**, 16264–16267.
- 2 C. Richmonds, M. Witzke, B. Bartling, S. W. Lee, J. Wainright, C. C. Liu and R. M. Sankaran, *Journal of the American Chemical Society*, 2011, **133**, 17582–17585.
- 3 J. Bringmann and E. Dinjus, *Applied Organometallic Chemistry*, 2001, **15**, 135–140.
- 4 C. H. Li, G. Q. Yuan, X. C. Ji, X. J. Wang, J. S. Ye and H. F. Jiang, *Electrochimica Acta*, 2011, **56**, 1529–1534.
- 5 H. S. Jeon, S. Kunze, F. Scholten and B. Roldan Cuenya, *ACS Catalysis*, 2018, **8**, 531–535.
- 6 B. R. Buckley, A. P. Patel and K. G. U. Wijayantha, *Chemical Communications*, 2011, **47**, 11888.
- 7 T. Saeki, K. Hashimoto, N. Kimura, K. Omata and A. Fujishima, *Journal of Electroanalytical Chemistry*, 1996, **404**, 299–302.
- 8 D. Simonsson, *Chemical Society Reviews*, 1997, **26**, 181.
- 9 (IEA) International Energy Agency, *Key World Energy Statistics 2017*, OECD, Paris, 2017.
- 10 C. Song, *CO2 Conversion and Utilization*, 2002, **809**, 1–2.
- 11 Global Carbon Project, *Supplemental data of Global Carbon Budget 2018 (Version 1.0) [Data set]*, 2018, vol. 10.
- 12 C. Marchetti, *Climatic Change*, 1977, **1**, 59–68.
- 13 WMO website | World Meteorological Organization, https://public.wmo.int/en/our-mandate/climate/causes_of_climate_change.php, (accessed 31 March 2016).
- 14 In *United Nations, Department of Economic and Social Affairs, Population*

- Division*, New York, 2017, pp. 1–30.
- 15 J. J. . Olivier, G. J. Maenhout, M. Muntean and A. H. . Peters, Jeroen, *PBL Netherlands Environmental Assessment Agency*, 2014, **217**, 227–238.
 - 16 IPCC, *Climate Change 2007: Synthesis Report. Contribution of working groups I, II and III to the fourth assessment*, Geneva, Switzerland, 2007.
 - 17 T. Stocker, D. Qin, G.-K. Plattner, M. Tignor, S. Allen, J. Boschung, A. Nauels, Y. Xia, V. Bex and P. Midgley, *Climate Change 2013 - The Physical Sciences Basis*, 2013.
 - 18 World Meteorological Organization, WMO climate statement: past 4 years warmest on record, <https://public.wmo.int/en/media/press-release/wmo-climate-statement-past-4-years-warmest-record>, (accessed 13 June 2019).
 - 19 M. Denchak, Consequences and Effects of Global Warming, <https://www.nrdc.org/stories/are-effects-global-warming-really-bad>, (accessed 4 April 2016).
 - 20 U. L. Ins, B. Bag and S. July, *Science*, 2014, **294**, 1379–1388.
 - 21 M. E. Mann and L. R. Kump, *Dire Predictions: Understanding Climate Change*, DK Publishing, New York, 2nd edn., 2015.
 - 22 How do we know global warming is not a natural cycle?, http://www.climatecentral.org/library/faqs/how_do_we_know_it_is_not_a_natural_cycle, (accessed 6 November 2018).
 - 23 B. Henley and N. Abram, The three-minute story of 800,000 years of climate change, <https://theconversation.com/the-three-minute-story-of-800-000-years-of-climate-change-with-a-sting-in-the-tail-73368>, (accessed 15 June 2019).
 - 24 The National Academy of Sciences and The Royal Society, *Climate Change, Evidence and Causes*, National Academy of Press, Washington, DC, 2014.
 - 25 P. Friedlingstein, J. L. Dufresne, P. M. Cox and P. Rayner, *Tellus, Series B: Chemical and Physical Meteorology*, 2003, **55**, 692–700.
 - 26 How does sea ice affect global climate?, <https://oceanservice.noaa.gov/facts/sea-ice-climate.html>, (accessed 6

- November 2018).
- 27 Climate Change: Vital Signs of the Planet: Engage: Warming Arctic, https://climate.nasa.gov/resources/education/pbs_modules/lesson2Engage/, (accessed 13 June 2018).
 - 28 The Runaway Greenhouse Effect, <https://www.earthintransition.org/2010/07/the-runaway-greenhouse-effect/>, (accessed 6 November 2018).
 - 29 H. Riebeek, The Ocean's Carbon Balance: Feature Articles, <https://earthobservatory.nasa.gov/Features/OceanCarbon/>, (accessed 13 June 2018).
 - 30 S. P. Xie, C. Deser, G. A. Vecchi, J. Ma, H. Teng and A. T. Wittenberg, *Journal of Climate*, 2010, **23**, 966–986.
 - 31 Products made from petroleum, <https://www.ranken-energy.com/index.php/products-made-from-petroleum/>, (accessed 6 November 2018).
 - 32 M. M. Sydney, How good was the Australian peak oil report BITRE 117 (peaky leaks part 4), <http://crudeoilpeak.info/how-good-was-the-australian-peak-oil-report-bitre-117>, (accessed 6 November 2018).
 - 33 D. B. Botkin and E. A. K. Keller, *Environmental Science: Earth as a Living Planet*, JOHN WILEY & SONS, INC., United States, 8th edn., 2010.
 - 34 K. Langin, *Science*, , DOI:10.1126/science.aat0811.
 - 35 P. W. Boyd, *Marine Ecology Progress Series*, 2008, **364**, 213–218.
 - 36 J. Cullen and P. Boyd, *Marine Ecology Progress Series*, 2008, **364**, 295–301.
 - 37 C. G. Trick, B. D. Bill, W. P. Cochlan, M. L. Wells, V. L. Trainer and L. D. Pickell, *Proceedings of the National Academy of Sciences*, 2010, **107**, 5887–5892.
 - 38 CCSA, What is CCS? – The Carbon Capture & Storage Association (CCSA), <http://www.ccsassociation.org/what-is-ccs/>, (accessed 19 June 2018).
 - 39 Enhanced Hydrocarbon Recovery, <http://www.ccsassociation.org/what-is-ccs/storage/enhanced-hydrocarbon-recovery/>, (accessed 6 November 2018).

- 40 Carbon Dioxide Utilisation The CO₂Chem Network, <http://co2chem.co.uk/>, (accessed 6 November 2018).
- 41 US EPA, Global Greenhouse Gas Emissions Data. Greenhouse Gas (GHG) Emissions, <https://www.epa.gov/ghgemissions/global-greenhouse-gas-emissions-data>, (accessed 13 October 2018).
- 42 B. P. Spigarelli and S. K. Kawatra, *Journal of CO₂ Utilization*, 2013, **1**, 69–87.
- 43 H. Naims, *Environmental Science and Pollution Research*, 2016, **23**, 22226–22241.
- 44 B. Metz, O. Davidson, H. de Coninck, M. Loos and L. Meyer, *Carbon Dioxide Capture and Storage*, Cambridge University Press for the Intergovernmental Panel on Climate Change, 2010, vol. 49.
- 45 The Royal Society, *The potential and limitations of using carbon dioxide. Policy briefing.*, London, 2017.
- 46 A. Demirbaş, *Energy Sources*, 2004, **26**, 715–730.
- 47 T. Inui, *Effective Conversion of CO₂ to Valuable Compounds by Using Multifunctional Catalysts*, American Chemical Society, 2009.
- 48 R. D. Richardson, E. J. Holland and B. K. Carpenter, *Nature Chemistry*, 2011, **3**, 301–303.
- 49 B. Hu, C. Guild and S. L. Suib, *Journal of CO₂ Utilization*, 2013, **1**, 18–27.
- 50 Q. Liu, L. Wu, R. Jackstell and M. Beller, *Nature Communications*, 2015, **6**, 5933.
- 51 R. M. Cuéllar-Franca and A. Azapagic, *Journal of CO₂ Utilization*, 2015, **9**, 82–102.
- 52 S. P. Cuellar-Bermudez, J. S. Garcia-Perez, B. E. Rittmann and R. Parra-Saldivar, *Journal of Cleaner Production*, 2015, **98**, 53–65.
- 53 L. Yanqun, H. Mark, W. Nan, L. C. Q and D.-C. Nathalie, *Biotechnology Progress*, 2008, **24**, 815–820.
- 54 M. Calvin and N. G. Pon, *Carboxylations and Decarboxylations*, University of

- California, Berkeley, CA, 1959.
- 55 Global Climate Change and Vital Signs of the Planet, The relentless rise of carbon dioxide, https://climate.nasa.gov/climate_resources/24/graphic-the-relentless-rise-of-carbon-dioxide/, (accessed 13 October 2018).
- 56 A. P. Patel, PhD Thesis, Loughborough University, 2013.
- 57 X. B. Lu, Y. J. Zhang, B. Liang, X. Li and H. Wang, *Journal of Molecular Catalysis A: Chemical*, 2004, **210**, 31–34.
- 58 C. M. Gabardo, A. Seifitokaldani, J. P. Edwards, C.-T. Dinh, T. Burdyny, G. Kibria, C. P. O. Brien and E. H. Sargent, *Energy & Environmental Science*, , DOI:10.1039/C6EE00811A.
- 59 N. W. Krase and V. L. Gaddy, *Industrial and Engineering Chemistry*, 1922, **14**, 611–615.
- 60 T. Iijima and T. Yamaguchi, *Applied Catalysis A: General*, 2008, **345**, 12–17.
- 61 Y. Fan, M. Tiffner, J. Schörgenhuber, R. Robiette, M. Waser and S. R. Kass, *The Journal of Organic Chemistry*, 2018, **83**, 9991–10000.
- 62 C. Martín, G. Fiorani and A. W. Kleij, *ACS Catalysis*, 2015, **5**, 1353–1370.
- 63 G. L. Gregory, PhD Thesis, University of Bath, 2017.
- 64 X.-H. Ji, N.-N. Zhu, J.-G. Ma and P. Cheng, *Dalton Transactions*, 2018, **47**, 1768–1771.
- 65 A. Coletti, C. J. Whiteoak, V. Conte and A. W. Kleij, *ChemCatChem*, 2012, **4**, 1190–1196.
- 66 D. C. Webster, *Progress in Organic Coatings*, 2003, **47**, 77–86.
- 67 M. Pérez-Fortes, J. C. Schöneberger, A. Boulamanti and E. Tzimas, *Applied Energy*, 2016, **161**, 718–732.
- 68 M. Jacquemin, A. Beuls and P. Ruiz, *Catalysis Today*, 2010, **157**, 462–466.
- 69 Electrochemical Reaction, <http://www.britannica.com.ezproxy.psz.utm.my/EBchecked/topic/183010/electrochemical-reaction>, (accessed 3 August 2018).

- 70 P. M. S. Monk, *Physical Chemistry: Understanding our Chemical World*, John Wiley & Sons Ltd, Manchester, 2008.
- 71 L. Vinet and A. Zhedanov, *A 'missing' family of classical orthogonal polynomials*, John Wiley & Sons, Inc, Pennington, NJ, 2nd edn., 2011, vol. 44.
- 72 L. Vinet and A. Zhedanov, in *Journal of Physics A: Mathematical and Theoretical*, Butterworth-Heinemann, 2011, vol. 44, pp. 87–151.
- 73 G. Centi and S. Perathoner, *Catalysis Today*, 2009, **148**, 191–205.
- 74 H. Wang, G. Zhang, Y. Liu, Y. Luo and J. Lu, *Electrochemistry Communications*, 2007, **9**, 2235–2239.
- 75 N. Asao, T. Sudo and Y. Yamamoto, *The Journal of Organic Chemistry*, 2002, **62**, 5656–5656.
- 76 S. F. Zhao, H. Wang, Y. C. Lan, X. Liu, J. X. Lu and J. Zhang, *Journal of Electroanalytical Chemistry*, 2012, **664**, 105–110.
- 77 R. Matthessen, J. Fransaer, K. Binnemans and D. E. De Vos, *Beilstein Journal of Organic Chemistry*, 2014, **10**, 2484–2500.
- 78 L. J. Bellamy, in *The Infrared Spectra of Complex Molecules*, John Wright & Sons Ltd, New York, 2nd edn., 1980, pp. 183–202.
- 79 Carboxylic Acids Market- Global Industry Analysis Forecast 2015-2023, <https://www.transparencymarketresearch.com/carboxylic-acids-market.html>, (accessed 17 October 2018).
- 80 G. Silvestri, S. Gambino and G. Filardo, *Acta Chemica Scandinavica*, 1991, **45**, 987–992.
- 81 G. Silvestri, S. Gambino, G. Filardo and A. Gulotta, *Angewandte Chemie International Edition in English*, 1984, **23**, 979–980.
- 82 H. Senboku and A. Katayama, *Current Opinion in Green and Sustainable Chemistry*, 2017, **3**, 50–54.
- 83 R. Matthessen, J. Fransaer, K. Binnemans and D. E. De Vos, *ChemElectroChem*, 2015, **2**, 73–76.

- 84 C. Li, G. Yuan and H. Jiang, *Chinese Journal of Chemistry*, 2010, **28**, 1685–1689.
- 85 S. N. Steinmann, C. Michel, R. Schwiedernoch, M. Wu and P. Sautet, *Journal of Catalysis*, 2016, **343**, 240–247.
- 86 E. Duñach, S. Dérien and J. Périchon, *Journal of Organometallic Chemistry*, 1989, **364**, C33–C36.
- 87 S. Dérien, E. Duñach and J. Périchon, *Journal of Organometallic Chemistry*, 1990, **385**, C43–C46.
- 88 X. Wang, M. Nakajima and R. Martin, *Journal of American Chemical Society*, 2015, **137**, 8924–8927.
- 89 K. Müller, K. Brooks and T. Autrey, *Energy & Fuels*, 2017, **31**, 12603–12611.
- 90 X. Zhang, Y. Zhao, S. Hu, M. E. Gliege, Y. Liu, R. Liu, L. Scudiero, Y. Hu and S. Ha, *Electrochimica Acta*, 2017, **247**, 281–287.
- 91 A. A. Isse and A. Gennaro, *Chemical Communications*, 2002, 2798–2799.
- 92 G. I. Shul'zhenko and Y. B. Vasil'ev, *Bulletin of the Academy of Sciences of the USSR Division of Chemical Science*, 1991, **40**, 1217–1220.
- 93 V. S. González, PhD Thesis, Loughborough University, 2015.
- 94 R. Xu and Y. Xu, *Modern inorganic synthetic chemistry*, Elsevier B.V. All, 2nd edn., 2017.
- 95 C. C. Yang, Y. H. Yu, B. Van Der Linden, J. C. S. Wu and G. Mul, *Journal of the American Chemical Society*, 2010, **132**, 8398–8406.
- 96 T. Yui, A. Kan, C. Saitoh, K. Koike, T. Ibusuki and O. Ishitani, *ACS Applied Materials and Interfaces*, 2011, **3**, 2594–2600.
- 97 Get out of your element! Convert CO₂ into molecules to power bio-manufacturing in space., <https://www.co2conversionchallenge.org/>, (accessed 11 November 2018).
- 98 M. A. Lieberman and A. J. Lichtenberg, *Principles of Plasma Discharges and Materials Processing*, John Wiley & Sons, Inc., 2nd edn., 2005.

- 99 F. Alexander, *Plasma Chemistry*, Cambridge University Press, Philadelphia, 1st edn., 2008, vol. 1.
- 100 Y. Yang, Y. I. Cho and A. Fridman, *Plasma Discharge in Liquid*, Taylor and Francis, Boca Raton, 1st edn., 2017.
- 101 R. A. M. Carvalho, A. T. Carvalho, M. L. P. da Silva, N. R. Demarquette and O. B. G. Assis, *Química Nova*, 2005, **28**, 1006–1009.
- 102 Y. Liu, A. Z. Fire, S. Boyd and R. A. Olshen, *Journal of the American Chemical Society*, 2014, **135**, 16264–16267.
- 103 P. L. Vasile I. Parvulescu, Monica Magureanu, *Plasma Chemistry and Catalysis in Gases and Liquids*, Wiley-VCH, 1 edition., 2012.
- 104 A. Peschot, N. Bonifaci, O. Lesaint, C. Valadares and C. Poulain, *Applied Physics Letters*, 2014, **105**, 123109.
- 105 G. Aday, P. Guillot, J. Galy and H. Brunet, *Journal of Applied Physics*, 1998, **83**, 5917–5921.
- 106 N. M. Bhat, L. M. Lee, R. F. Van Vollenhoven, N. N. H. Teng and M. M. Bieber, *Annu. Rev. Food Sci. Technol*, 2011, **29**, 2114–2121.
- 107 H. Cavendish, *Philosophical Transactions of the Royal Society*, 1785, **75**, 372–384.
- 108 A. Starikovskiy, Y. Yang, Y. I. Cho and A. Fridman, *Plasma Sources Science and Technology*, 2011, **20**, 024003.
- 109 P. Bruggeman and C. Leys, *Journal of Physics D: Applied Physics*, 2009, **42**, 053001.
- 110 S. Hofmann, A. F. H. Van Gessel, T. Verreycken and P. Bruggeman, *Plasma Sources Science and Technology*, 2011, **20**, 065010.
- 111 Special issue on Plasma and Liquids, <https://iopscience.iop.org/journal/0022-3727/page/PlasmaandLiquids>, (accessed 8 August 2018).
- 112 P. Sunka, V. Babický, M. Clupek, P. Lukes, M. Simek, J. Schmidt and M. Cernák, *Plasma Sources Science and Technology*, 1999, **8**, 258–265.

- 113 V. A. Kolikov, V. E. Kurochkin, L. K. Panina and A. F. G. Rutberg, 2005, **403**, 561–563.
- 114 Water sanitation and health, http://www.who.int/water_sanitation_health/en/, (accessed 21 June 2018).
- 115 A. F. Smith, *Food and drink in American history: A 'full course' encyclopedia*, ABC-Clio, Santa Barbara, 1st edn., 2013.
- 116 B. R. Locke, M. Sato, P. Sunka, M. R. Hoffmann and J. S. Chang, *Industrial and Engineering Chemistry Research*, 2006, **45**, 882–905.
- 117 T. Viraraghavan and F. De Maria Alfaro, *Journal of Hazardous Materials*, 1998, **57**, 59–70.
- 118 B. Sun, M. Sato and J. S. Clements, *Environmental Science and Technology*, 2000, **34**, 509–513.
- 119 A. A. Joshi, B. R. Locke, P. Arce and W. C. Finney, *Journal of Hazardous Materials*, 1995, **41**, 3–30.
- 120 B. Sun, M. Sato and J. S. Clements, *Journal of Physics D: Applied Physics*, 1999, **32**, 1908–1915.
- 121 F. L. Rosario-Ortiz, S. P. Mezyk, D. F. R. Doud and S. A. Snyder, *Environmental Science & Technology*, 2008, **42**, 5924–5930.
- 122 G. Fridman, G. Friedman, A. Gutsol, A. B. Shekhter, V. N. Vasilets and A. Fridman, *Plasma Processes and Polymers*, 2008, **5**, 503–533.
- 123 P. Lukes, E. Dolezalova, I. Sisrova and M. Clupek, *Plasma Sources Science and Technology*, 2014, **23**, 015019.
- 124 W. Siemens, *Annalen der Physik und Chemie*, 1857, **178**, 66–122.
- 125 B. Eliasson, M. Hirth and U. Kogelschatz, *Journal of Physics D: Applied Physics*, 1987, **20**, 1421–1437.
- 126 J. Warnatz, R. W. Dibble and U. Maas, *Combustion*, Springer, Berlin, 4th edn., 1996.
- 127 A. J. Bard and L. R. Faulkner, *Electrochemical Methods: Fundamentals and*

- Applications*, John Wiley & Sons, INC., Austin, 2nd edn., 2001.
- 128 C. Liu and A. J. Bard, *Nature Materials*, 2008, **7**, 505–509.
- 129 K. Harada and S. Suzuki, *Nature*, 1977, **266**, 275–276.
- 130 X. T. Deng, J. J. Shi and M. G. Kong, *Journal of Applied Physics*, 2007, **101**, 074701.
- 131 M. G. Kong, G. Kroesen, G. Morfill, T. Nosenko, T. Shimizu, J. Van Dijk and J. L. Zimmermann, *New Journal of Physics*, 2009, **11**, 115012.
- 132 G. Fridman, H. Ayan, A. Fridman, M. Balasubramanian, A. Gutsol, A. Brooks and M. Peddinghaus, *Plasma Chem Plasma Process*, 2006, **26**, 425–442.
- 133 S. U. Kalghatgi, G. Fridman, M. Cooper, G. Nagaraj, M. Peddinghaus, M. Balasubramanian, V. N. Vasilets, A. F. Gutsol, A. Fridman and G. Friedman, *IEEE Transactions on Plasma Science*, 2007, **35**, 1559–1566.
- 134 G. E. Morfill, T. Shimizu, B. Steffes and H. U. Schmidt, *New Journal of Physics*, 2009, **11**, 115019.
- 135 E. Stoffels, I. E. Kieft, R. E. J. Sladek, L. J. M. van den Bedem, E. P. van der Laan and M. Steinbuch, *Plasma Sources Science and Technology*, 2006, **15**, S169–S180.
- 136 A. F. Gaisin, *High Temperature*, 2005, **43**, 680–687.
- 137 M. Hoľub, *International Journal of Applied Electromagnetics and Mechanics*, 2012, **39**, 81–87.
- 138 T. Cserfalvi and P. Mezei, *Analytical and bioanalytical chemistry*, 1996, **355**, 813–9.
- 139 A. C. Fisher-Cripps, *The electronics companion*, Institute of Physics Publishing, Boca Raton, 1st edn., 2013, vol. 42.
- 140 P. Bruggeman, E. Ribižl, A. Maslani, J. Degroote, A. Malesevic, R. Rego, J. Vierendeels and C. Leys, *Plasma Sources Science and Technology*, 2008, **17**, 025012.
- 141 A. Presser and A. Hufner, *Monatshefte fur Chemie/Chemical Monthly*, 2004,

- 135**, 1015–1022.
- 142 J. L. Walsh and M. G. Kong, *Applied Physics Letters*, , DOI:10.1063/1.2982497.
- 143 S.-F. Zhu, Y.-B. Yu, S. Li, L.-X. Wang and Q.-L. Zhou, *Angewandte Chemie International Edition*, 2012, **51**, 8872–8875.
- 144 D. Aurbach, Y. Talyosef, B. Markovsky, E. Markevich, E. Zinigrad, L. Asraf, J. S. Gnanaraj and H. J. Kim, *Electrochimica Acta*, 2004, **50**, 247–254.
- 145 C. Gabelle, F. Baraud, L. Biree, S. Gouali, H. Hamdoun, C. Rousseau, E. van Veen and L. Leleyter, *Applied Geochemistry*, 2012, **27**, 2088–2095.
- 146 L. F. Silvester and P. A. Rock, *Journal of The Electrochemical Society*, 1974, **121**, 518.
- 147 C. Richmonds, M. Witzke, B. Bartling, S. Whan Lee, J. Wainright, C.-C. Liu and R. M. Sankaran, *Journal of the American Chemical Society*, 2011, **133**, 17582–17585.
- 148 Sigma Aldrich, N,N-Dimethylformamide, anhydrous, 99.8%, <https://www.sigmaaldrich.com/catalog/product/sial/227056?lang=en®ion=GB>, (accessed 27 March 2019).
- 149 Capacitors and capacitance, <https://www.khanacademy.org/science/physics/circuits-topic/circuits-with-capacitors/v/capacitors-and-capacitance>, (accessed 3 January 2019).
- 150 Z. He, Z. Hou, Y. Zhang, T. Wang, Y. Dilixiati and W. Eli, *Catalysis Today*, 2015, **247**, 147–154.
- 151 R. Pappo, D. S. Allen, R. U. Lemieux and W. S. Johnson, *Journal of the American Chemical Society*, 1956, **21**, 478–479.
- 152 M. Szostak, M. Spain and D. J. Procter, *Journal of Organic Chemistry*, 2014, **79**, 2522–2537.
- 153 J. L. Olloqui-Sariego, V. M. Molina, D. González-Arjona, E. Roldán and M. Domínguez, *Journal of The Electrochemical Society*, 2010, **157**, E64.
- 154 N. S. Murcia and D. G. Peters, *Journal of Electroanalytical Chemistry*, 1992,

- 326**, 69–79.
- 155 J. Sherwood, M. De Bruyn, A. Constantinou, L. Moity, C. R. McElroy, T. J. Farmer, T. Duncan, W. Raverty, A. J. Hunt and J. H. Clark, *Chemical Communications*, 2014, **50**, 9650–9652.
- 156 H. J. Salavagione, J. Sherwood, M. De bruyn, V. L. Budarin, G. J. Ellis, J. H. Clark and P. S. Shuttleworth, *Green Chemistry*, 2017, **19**, 2550–2560.
- 157 K. Wilson, J. Murray, C. Jamieson and A. Watson, *Synlett*, 2018, **29**, 650–654.
- 158 K. L. Wilson, A. R. Kennedy, J. Murray, B. Greatrex, C. Jamieson and A. J. B. Watson, *Beilstein Journal of Organic Chemistry*, 2016, **12**, 2005–2011.
- 159 P. Smith, *Physical Review*, 1930, **36**, 1293–1302.
- 160 C. A. Gearhart, *Studies in History and Philosophy of Science Part B: Studies in History and Philosophy of Modern Physics*, 2017, **60**, 95–109.
- 161 C. G. Found, *Physical Review*, 1920, **16**, 41–53.
- 162 G. Chen, L. Wang, T. Godfroid and R. Snyders, in *Plasma Chemistry and Gas Conversion*, InTech, 2018.
- 163 J. Wu, Y. Huang, W. Ye and Y. Li, *Advanced Science*, 2017, **4**, 1700194.